Hydrolysable DMAEA and DMAEMA Copolymers For dsRNA Protection in Soil: Influence of Composition and Architecture

Fannie Burgevin

A thesis submitted in partial fulfilment of the requirements for the degree of

Doctor of Philosophy in Chemistry

Department of Chemistry

University of Warwick

April 2021

Table of content

List of figures

List of tables

List of schemes

Abbreviations

AA	Acrylic acid
AEA	Aminoethyl acrylate
AEMA	2-(Aminoethyl) methacrylate
AFM	Atomic Force Microscopy
AGO	Argonaute
APM	3-Aminopropylmethacrylamide
ASNP	Amine functionalised silica nanoparticles
ATRP	Atom transfer radical polymerisation
BA	Butyl acrylate
BAPC	Branched amphiphilic peptide capsules
bp	Base pair
CFIA	Canadian food inspection agency
CL	Crosslinker
Conv.	Conversion
CPAETC	(4-Cyano pentanoic acid)yl ethyl trithiocarbonate
CQD	Carbon quantum dots
CTA	Chain transfer agent
Đ	Dispersity
DHMA	2-Hydroxymethyl acrylate
DLS	Dynamic light scattering
DMAE	*N*,*N*'-Dimethylaminoethanol
DMAEA	2-Dimethylaminoethyl acrylate
DMAEMA	2-Dimethylaminoethyl methacrylate
DMEM	Dulbecco's Modified Eagle's Medium
DMAPA	2-(Dimethylamino)propyl acrylate

DMF	*N*,*N*-Dimethyl formamide
DNA	Deoxyribose nucleic acid
DP	Degree of polymerisation
DRBD	DsRNA binding domain
dsRNA	Double stranded ribose nucleic acid
EDTA	Ethylenediaminetetraacetic acid
EPA	Environmental protection agency
EtBr	Ethidium bromide
FBS	Foetal bovine serum
FNP	Fluorescent nanoparticle
GFP	Green Fluorescent Protein
GMO	Genetically modified organisms
GPC	Gel permeation chromatography
GUMA	Guanylated methacrylate
HEA	Hydroxyethylacrylate
IR	Infra red
LS	Light scattering
M	Monomer
mCTA	Macromolecular chain transfer agent
M_n	Number average molecular weight
mRNA	Messenger ribose nucleic acids
MW	Molecular weight
Mw	Weight average molecular weight
NAM	*N*-Acrylmorpholine
N_{arm}	Number of arms per stars
NMP	Nitroxide mediated polymerisation
NMR	Nuclear magnetic resonance

NPs	Nanoparticles
PAA	Poly(acrylic acid)
PABTC	(Propanoic acid)yl butyl trithiocarbonate
PDI	Polydispersity Index
pDMAEA	Poly(2-dimethylaminoethyl acrylate)
pDMAEAq	Quaternised poly(2-dimethylaminoethyl acrylate)
pDMAEMA	Poly(2-dimethylaminoethyl methacrylate)
pDMAPA	poly(2-(dimethylamino)propyl acrylate)
PDMAPAAm	Poly(N,N-dimethylaminopropyl acrylamide)
pDNA	Plasmid DNA
PEI	Poly(ethyleneimine)
PEO	Poly(ethylene oxide)
pGPMA	Poly[*N*-(3-guanidinopropyl)methacrylamide]
PLL	Poly(L-Lysine)
PMMA	Poly(methyl methacrylate)
PS	Polystyrene
PTD	Peptide transduction domain
PVS	Polyvinylsulfonate
RAFT	Reversible addition fragmentation chain transfer
RDRP	Reversible deactivation radical polymerisation
Rg	Radius of gyration
R_H	Hydrodynamic radius
RI	Refractive index
RISC	RNA-induced silencing complex
RNA	Ribose nucleic acid
RNAi	RNA interference
SARA	Supplemental activator and reducing agent

SAXS	Small Angle Neutron Scattering
SEM	Scanning electron microscopy
SET-LRP	Single electron transfer living radical polymerisation
SID-1	Systemic RNA interference-deficient
SIL	Systemic RNA interference-deficient-1-like
siRNA	small interfering RNA
ssRNA	Single-stranded RNA
TBE	Tris-Borate-EDTA buffer
TEM	Transmission electron microscopy
UV	Ultra violet
XTT	2,3-Bis-(2-Methoxy-4-Nitro-5-Sulfophenyl)-2H-Tetrazolium-5-Carboxanilide
η	Viscosity

Acknowledgements

This is the part I waited so long to write as I think it is probably the most important one. I am so grateful to have shared these three and a half years with so many amazing people. A PhD is a full experience with not only successful results (and "failures" or repeats) but also so many memories shared inside and outside the lab. We all change considerably during this process, we learn how to be better scientists but also better person. This is why I want to properly thank all the people who contributed to my work but also to my personal life.

First, I would like to thank my supervisor, Pr. Sébastien Perrier for giving me the opportunity to join his group at Warwick. I would not have thought I would be doing a PhD in England (and even less a postdoc now!), thanks for convincing me. Your trust, guidance and support have allowed me to become an independent researcher.

I would like to thank Drs. Annette Christie, Chris Lindsay, Marta Omedes-Pujol and Vanessa Rose-Loczensky from Syngenta for their contribution to this project and positive encouragements. It was a pleasure to work with you. I also want to thank the Syngenta team in Ghent for welcoming me, just before it was too late in January 2020. It was very interesting to see the project from a bigger perspective.

Many thanks to the Perrier group in general, past and present. I will always remember my first day and weeks and how you welcomed me. Tammie showing me around, Sean crying over his dead cells at the pub, Joji driving me back home or Alex showing me the joy of this project and working with DMAEA. Thank you to Guillaume Moriceau, Tammie Barlow, Joji Tanaka, Pratik Gurnani, Andrew Lunn, Raoul Peltier, Edward Mansfield, Carlos Sanchez-Cano, Caroline Bray, Majda Akrach, Tomos Morgan for all your great advices and even if it was just for few months, it was great to spend this time with you in the group. I particularly want to thank Alexander Cook for teaching me how to work with RNA, run gels… And I would also like to thank especially Julia Rho who was always here for scientific and non-scientific advices, thank you for all the chats, for taking care about so many thing, organising socials, the tea/coffee breaks, all your cakes, and also for cooking in my own kitchen… Good luck with your new project back in the group. Agnès Kuroki,

thank you for the year and half we spent together, thank you for all the conversations, your help, your Frenchness, the day trips, your enthusiasm and not killing us on the road in Ireland. If the woman from the B&B in Galway won't remember us, Tom will. I would also like to thank Lucas Al-Shok, it was great spending my first 6 months with you in the office, thanks for all the Shins, the day trips and week-ends to explore more of England/Wales (let's not do that to Cardiff). Good luck with the rest of your PhD on the other side of the corridor. I am looking forward to more amazing food reviews. Also, thank you to Steve Hall for your help with SAXS fitting, your ideas and being such a great neighbour of fume hood. I would like to thank Qiao Song for being not just an amazing chemist but also for your nice presence in the office and for almost all my PhD, as you arrived just before me, you were always happy to help and talk. Good luck with your new position! Thank you also to Jie Yang, it was a pleasure to spend these years with you in the group, and the trip in Ireland. I would also like to thank Andrew Kerr for his presence and help with AFM. Sean, thank you for your constant joy, your laugh, your Frenchness, all the chats and complains and for making me discover more about our (kind of) French islands in the middle of the ocean. I am happy we survived the cows in Scotland, thank you for these trips (Lake District, Highlands). Hope you enjoy Paris and be ready for us when things get better…

Now to all the newest members of the group, I am particularly grateful to Alexia Hapeshi who was amazing at managing the labs in life sciences and for all the help with my project. Thank you for all the discussions and proofreading so efficiently my thesis. Many thanks to Ji Song as well, for showing me around in life sciences, for your help throughout my PhD with my project and particularly for the transfection experiments. Sophie Hill, thank you for always being happy to help, to chat and share your views, thank you for your support. I am sure your PhD will be great and you will be great too, you have everything you need already. Maria Kariuki, thank you so much for being so you, inspiring woman and always supportive, even if you have sometimes questionable music taste. I am happy you discovered the joys of hiking during our trip to Scotland. Ramon Garcia-Maset, thank you for always being so supportive, for your interesting ideas and taking SEM pictures for me even at 6pm on a Friday (I won't forget the beer). I hope we can go back to Scotland soon for a little trip or somewhere else (like Spain...?), but definitely in Bath at least. Vito, even if we haven't spent much time together as you were hiding in the medical school, thank you for your enthusiasm,

it was really nice having you around. Thank you to Hannah Burnage, Cathy/Zihe Zheng, Taki/Zihe Cheng, Maryam Obaid, all the best for the rest of your PhD. Of course, I won't forget all the students and in particular Ting Koh, you did a good job even if it was not always easy. I learned a lot with you as well and I really wish you to find what you want. Thank you as well to James Coe, for his work. And to Leila Vicker, Manisha Pandey among others, thank you for your work and your energy. I have a special thought for Gabbrielle Han, I will always remember you, you were always so enthusiastic and positive, I am really grateful to have met you. Manpreet Kaur, thank you for raising more attention on sustainability in our labs, and congratulations for your work in the group, it was a really weird situation. All the best for your future. Also thank you to the visitors, Enrique Folgado, sorry it was such a bad timing last time but great to have you around. Jiajia, it was a pleasure meeting you, I know you enjoyed your year with us. Xiujun Cao, I hope you will enjoy as much your time in the group. And of course, I would like to thank Sophie Laroque, the "last" "French" of the group after I leave, so nice to have you around, you came back to start your PhD at a weird time, we didn't think you would have left again that soon when we welcomed you back at the airport last year. I am looking forward to do more social things soon and see you in Bath. Magdalena Przybyla, I am very grateful you decided to come back in the group for your PhD, we are lucky to have you. Thank you for the nice chats in the morning and all the best for your PhD.

Finally, I want to particularly thank Thomas Floyd, Robert Ridchardson and Satu Häkkinen who I shared my whole PhD with. We went through these three and something years together, good and less good times, some conferences and in particular San Diego for the ACS; I remember our breakfast at the airport, that crazy night as well (Thank you Robert for following me back to the hostel… and Satu for taking care of me with water). But also the YRMs, we went through the pandemic in our last year... So I am very thankful I could always count on you. First to finish your PhD was you Robert, we were not surprised, congratulations again for your great work and your position in Liverpool. I have to say I really enjoyed watching you open your viva presents for 30 minutes, you were so happy. Thank you for all your help and your company. Tom, thank you for sharing with me all the joys of cationic polymers and complexation, for trusting me (a bit) with your car, for all your help in the lab, all the chats, the barbecues, for being a regular to all socials… I wish you the best for your

future carrier, I hope I can come and visit wherever you are (ideally somewhere outside of the UK, if they allow you…!). And Satu, I can't tell you how grateful I am to have shared all this with you. Like you said it probably would not have been the same if you would not have been sitting next to me in the office (before we were separated by a pandemic, but it was too late to separate us), all the random chats, your constant and amazing support and encouragements, thank you so much. You even found me a job! Thank you so much for sharing this with me, I admit when you sent it, I did not think I would actually want this job and get this job. I am honoured you chose to share all these things with me and I think we both learned a lot from each other. All the best for the end of this journey, and remember you are enough. I am sure wherever you go next; you will be as great as you have always been and in particular during these three and a half years.

I also want to thank the people I met outside of the group, in the department or in life sciences. Thank you Christophe Atkins for the French breaks from the other side of the corridor. And I will finish this chemistry related part with Marjolaine Thomas. I remember that day at the YRM in Kent (such a sexy location), when Satu told me there was this French girl she had known from Helsinki she should present me (again thank you). We started talking and we have never stopped. And I think having our rooms in front of each other was definitely a sign. You showed me your love for mushrooms and wine straight away. Thank you for your fun and high energy (as Nello would say) with your Sud-Ouest accent and most of all thank you for all your support and listening to me. I think I never had so much French food in this country since I know you, when we are together we switch to full French, so thank you for all the raclettes, crepes, ravioles, cheeses, pates, rillettes, confits and your great garbure. I am looking forward to more weekends and maybe holidays with you anywhere. In the end, you will be the one abandoning me in this country… But can't wait to come and visit you.

I should also thank all my housemates from Earlsdon Avenue North, for being so diversified, you were very important, it was always nice to come back home and share a bit of my life with you. Te-Anne, Chrisa who I shared my first year with you in 2018, thank you both. Chrisa I will always remember your Greek food and all the olive oil. Christine, I really enjoyed living with you, our chats, our Sunday dinners with Lorenzo who was also great to live with for half of the week, talking French,

talking politics. I will particularly remember living with Nello and Mar in the hard times of 2020, we were more than housemates at this point. I could not have wish for better housemates for this moment, thank you for all the fun, the movie nights, the shared (gluten free) meals. Thank you Mar for your high energy, your crazy stories, the Spanish music and food. I will remember that day we went to buy a swimming pool and the flowers. Finally, Beatrice, it was truly a pleasure having you in this house, standing up to Nello, thank you for the great chats. Good luck with your PhD. Nello don't worry, I promised you your own paragraph:

Thank you so much for all the fun and high energy you brought into this house. Thank you for your patience with me sometimes and for not judging me too much about different things if not citing the Moon. And thank you for correcting the first part of my thesis so well, for all your help in general and most of all for being so good at listening. I will miss watching Topchef with you or watching you trying to cook like them. I hope we will find some time to go to Paris soon and go eat at Adrien's new restaurant and maybe Justine! I hope you will find your guide.

My experience during these years would not have been the same without some breaks and broadening my horizons with my travels around the world (Mongolia, Ireland, California, Scotland, France…). I went to Mongolia with strangers who quickly became my friends. Thank you to Les Mongoles de la Yourt, Delphine, Marine, Tiphaine, Diane and Delphine and I hope we will soon come back together!

And I cannot thank enough my friends Mathilde and Audrey for being always there, for the countless Skypes and phone calls, for our weekends or holidays, not always easy to organise. Thank you for your visits and I know I said I would try to find a job between you two… but instead you can come and visit Bath! Thank you for your constant support, I remember that weekend in Paris, I arrived announcing I finally made stars showing you my GPC graph. Thank you for listening, for sharing all those moments with me. I also want to thank my friends Chloe and Laura for their support even if I don't see you often but also Laurie, Josephine, Marion, Andrea and Sarah.

Finally, I want to finish by thanking my family starting with my parents for always supporting me, it is thanks to them that I am here. MERCI. Thank you to my sister, Claire for being here and you will be a doctor soon too, but not before I am! Good luck. And to my brother Valentin thank you for your support. And without going

into details not to make even longer these way too long acknowledgements (I know!) because my family is way too big, thank you to all my family for always supporting each other, for being so strong and being a part of me. Je voudrais spécialement remercier ma grand-mère de Normandie pour son énergie et son soutien mais aussi mon grand-père qui je suis sûre serais fier. Et à Grannie puis Pacha (de la part de ta chimiste préférée), merci pour tout ce que vous nous avez transmis à travers cette grande famille, toutes ces valeurs qui m'ont permis de faire tout ça.

Declaration

Experimental work contained in this thesis is original research carried out by the author, in the Department of Chemistry at the University of Warwick between October 2017 and February 2021. No material contained here has been submitted for any other degree, or at any other institution.

Results from other others are references throughout the text in the usual manner.

The work presented was carried out by the author with the following exceptions:

Chapter 4: SAXS analysis was performed by Steven Huband and processed by Steven Hall (University of Warwick). AFM analysis was performed by Andrew Kerr (University of Warwick).

Chapter 5: The XTT assay with HEK293T cells by Alexia Hapeshi (University of Warwick, School of Life Sciences). The GFP plasmid transfection were performed by Ji Song (University of Warwick, School of Life Sciences). TEM was acquired by Alexia Hapeshi (University of Warwick, School of Life Sciences). SEM was acquired by Ramon Garcia-Maset (University of Warwick).

Abstract

RNAi has shown great potential for applications in crop protection. However, double stranded RNA (dsRNA) is quickly degraded in the environment and particularly in soil. Cationic polymers can be used as vectors to transport and efficiently protect the nucleic acids. The aim of this thesis was to synthesise well-defined cationic 2-dimethylaminoethyl acrylate (DMAEA)-based copolymers using RAFT polymerisation to improve the protection and delay the release of the dsRNA in soil.

Firstly, four pDMAEA 4-arm stars were synthesised by RAFT polymerisation to compare them to previously reported pDMAEA stars, synthesized by Cu(0)-RDRP, and further study their potential as dsRNA vectors for soil stability and study the effect of the molecular weight. But results showed no prolonged protection of dsRNA in soil and only little effect of the polymer molecular weight on the complexation.

The influence of the composition on the hydrolysis of pDMAEA and time for the release of dsRNA was investigated by incorporating 2-dimethylaminoethyl methacrylate (DMAEMA) as a non-hydrolysable co-monomer. The DMAEMA content was increased by up to 50% leading to slower and lower hydrolysis of the DMAEA side chains and slower dsRNA release (with 20% DMAEMA, the dsRNA was release in about 15 days). However, the binding was not strong enough to give an efficient protection of the dsRNA in the presence of nucleases or in soil conditions, although good complexation was observed with linear copolymers in water.

The successful chain extension of p(DMAEA$_{80}$-*stat*-DMAEMA$_{20}$) with acrylamide monomers allowed the preparation of stars by the arm-first approach to investigate the influence of the architecture on the complexation of dsRNA. Soluble stars with a high number of well-defined arms ($N_{arm} \sim 55 – 100$) were obtained with the introduction of non-cationic *N*-acrylmorpholine (NAM) prior to the crosslinking step. The influence of the architecture on the hydrolysis was studied, with only small differences observed compared to the corresponding arm. The binding of the dsRNA with the stars was weaker than with the linear copolymer as the dsRNA interacts only at the surface of multiple dense stars. Therefore, these architectures were not able to extend the stability of the dsRNA in soil.

Chapter 1: Introduction

1.1. RNAi for pest control

Every year, an estimate of 20 to 40% of crops are lost, mainly due to pathogens, weed and insect pests.[1, 2] Insect pests represent a significant part of this damage, affecting crop yield and quality. Currently, the main approach to solve this problem is the use of broad-spectrum chemical pesticides as they are easily available, reliable and fast acting. However, in recent years there has been a rise in pest resistance to existing chemical pesticides, as well as a need to address societal concerns about the impact of pesticides on the environment and non-target organisms.[3-5] Therefore, to balance the needs of farmers, consumers and the environment, it is vital to find novel and effective alternative approaches with increasing pest specificity that manage resistance and reduce residues.

RNA interference (RNAi) has been shown to have great potential as an alternative to chemical pesticides because of its high specificity. It was first demonstrated in *Caenorhabditis elegans* in 1998 by Fire, Mello, and co-workers, where by introducing double stranded-RNA (dsRNA), it was able to specifically silence genes.[6] By selectively targeting, using dsRNA, the expression of an essential gene or a group of similar genes in one particular species can be silenced. Depending on the gene targeted, RNAi can lead to pest mortality while leaving other non-target organisms unaffected.[7, 8] A proof of concept study was published in 2007 by Baum et al.[9] It showed transgenic corn crop expressing dsRNA against Western corn rootworm *Diabrotica virgifera virgifera* V-ATPase gene ingestion resulted in larval stunting and death.

In recent years, further work has been done on design, synthesis and delivery of dsRNA for plant protection[10] and therapeutics.[11] Its use in pest control can be done in two ways; either induction of the dsRNA expression in the plant itself or directly apply it like conventional pesticides.[3] Oral delivery of dsRNA from the environment has shown to have the greatest potential, as it is probably the easiest and most efficient delivery method for application.[12] However, further investigation is needed on the

practical application due to the instability of dsRNA, especially in the gut lumen of insects. This may explain the differing efficiency of RNAi among various insect species.[13] While Orthopteran (grasshopper and locusts), Blattodean (cockroaches and termites) and most Coleopteran[8, 14] (beetles) species are generally responsive to environmentally delivered dsRNA, Hemipteran[15-17] organisms (aphids, leafhoppers, psyllid, whiteflies) have very variable responses and Lepidopteran[8, 18] (butterflies and moths) and dipteran[19] (flies) species are more refractory to RNAi. Many factors are responsible for this variation, thus no single method can be applied. As the stability of the dsRNA is a critical parameter to obtain successful silencing, nanoparticles (NPs) can be a useful tool to help protect the nucleic acids from degradation as well as facilitating cellular uptake.[20] Application of RNAi-based technologies is rapidly expanding, but there are still some knowledge gaps. Notably, not many papers are reporting on delivery vectors like cationic polymers, which are able to complex dsRNA. These vectors have been extensively studied on mammalian cells but not as much for pest management applications.[11, 21]

In this chapter, the mechanism of RNAi after dsRNA introduction is first presented, followed by its use as pest management with limitations ouside and inside the insect. Finally, novel strategies to overcome these obstacles and improve stability and uptake of dsRNA are discussed.

1.1.1. RNA Interference

RNAi is a natural mechanism conserved in the vast majority of eukaryotic organisms. It is an important tool in the defence against invasive nucleic acids, such as viruses, as well as, for regulation of endogenous gene expression. This mechanism is able to silence almost any gene and studies have shown that this technique can be used in agrochemical applications as a new generation of pesticide targeting specific harmful insects with very high specificity.[3]

DsRNA can be applied by spraying the plant crop or via different delivery methods such as trunk injection and root soaking.[3] When ingested, the nucleic acids must be transported into the gut lumen to reach gut epithelial cells.[12] Once the dsRNA is inside the cell, it is then processed by the enzyme DICER to give fragments (20-30 nucleotides long) known as small interfering RNA (siRNA). The siRNA can then be incorporated into the RNA-induced silencing complex (RISC), a protein complex. The

protein unwinds the two strands of siRNA, and the sense strand is cleaved, this gives the activated RISC. The single strand now functions as a template that allows interaction with the complementary target messenger RNA (mRNA), leading to its degradation, thus preventing expression of a specific gene (Figure 1.1).[22] RNAi pathways have been identified in all insect orders.[3] However, the mechanism has been particularly studied in-depth in the model organism; *Drosophila melanogaster*.

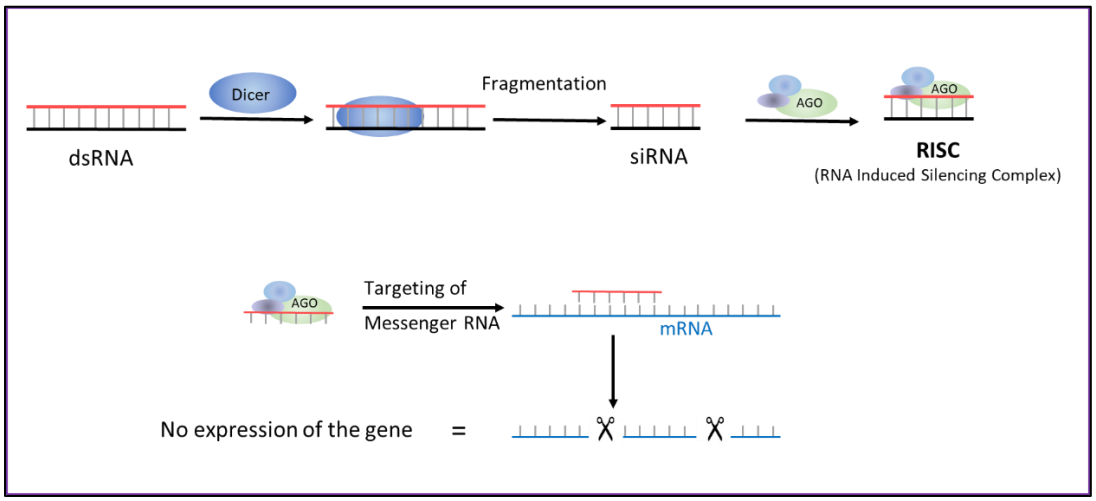

Figure 1.1: RNA interference mechanism inside cell processing dsRNA. When dsRNA enter the cell, it is fragmented by DICER. The resultant siRNA is loaded into proteins members of the ARGONAUTE (AGO) family to generate the RNA induced silencing complex (RISC). The sense strand is then cleaved to obtain the activated RISC. This complex is then able to target a specific messenger RNA (mRNA) leading to its degradation.

1.1.2. Use of RNAi for pest management

The use of RNAi to create a new generations of pesticide holds great promise due to its high specificity. Choosing the best method to deliver the dsRNA for each case is crucial to obtain good results. The practical and economic aspects are also very important and need to be taken into consideration. Moreover, the method needs to be accessible to farmers at a field scale.

In the laboratory, a commonly used technique is microinjection directly into hemolymph. This is a good approach as a proof of concept, to study the response to one dsRNA without the issues related to oral ingestion (instability in the gut mainly),[7, 23-25] however, in practice for application in fields, injection is not possible. Therfore, oral delivery seems to be the most efficient approach in most cases. Nevertheless,

insects have different feeding behaviour, feeding on the plant leaves, stem, phloem sap or roots. Hence adapting the delivery method is crucial.[26]

1.1.2.1. Transgenic and transplastomic crop plants

A common way to deliver dsRNA orally to insects is with the use of transgenic plants, where the plant is expressing the dsRNA. It is a promising approach as shown by multiple studies investigating genetically modified crops resistant to pests, including western corn rootworm,[9] aphids,[27] *Leptinotarsa decemlineata*,[28] among others. In 2016, SmartStax, a transgenic corn, was approved by the Canadian food inspection agency (CFIA) and in 2017 by the US environmental protection agency (EPA). In this product the action of a dsRNA (*DvSnf7*) is combined with the action of two insecticidal proteins to minimise root injury by corn rootworms.[29] However, the development of dsRNA-transgenic plants is limited as the RNAi response is dependent on the dsRNA dose and dsRNA length.[3, 23] Since the plant possesses its own RNAi machinery, in most cases the dsRNA is processed into short siRNA before it is ingested by insects.[20, 30] Short dsRNA and siRNA are known to be less efficient to induce a good RNAi response.[3] Yet, a way to overcome these difficulties is by expressing dsRNA in chloroplasts. These organelles are lacking RNAi machinery so dsRNA stay intact and a higher dose of dsRNA can be delivered to the target insect. For instance, chloroplast-expressed dsRNA in potato plants induced 100% mortality in Colorado potato beetles, whereas no response was observed with conventional transgenic plants where the dsRNA is not contained in the chloropast.[31] Transgenic plants could be an attractive method to deliver dsRNA to phloem-feeding insects as shown with *Nilaparvata lugens* by Zha *et al.*.[32]

Public opposition to GMOs (Genetically Modified Organisms) limits the broader use of transgenic crops, particularly in Europe. Moreover, the generation of the genetically modified plant is a long and expensive process, therefore, delaying the release and use of such products. An alternative is the use of non-transformative approaches by directly applying synthesised dsRNA onto the crop plant.

1.1.2.2. Direct applications

1.1.2.2.1. Foliar spray and artificial diet

San Miguel *et al*. showed naked dsRNA was stable enough to be used as foliar application under greenhouse conditions.[33] In these conditions, the dsRNA on the leaves was preserved in an active state for at least 28 days against Colorado potato beetles. Once dried on the potato leaves, it is not readily removed with water. Under UV exposure, dsRNA seems to be more stable on leaf surfaces than on glass surfaces, with it being retained for two weeks and degrading in less than two hours, respectively. However, it is important to note, that UV light intensity in the study was 44% of that of the outdoors. Additional studies need to be carried out to determine the half-life of dsRNA *in situ* field conditions with different key plant species. A main concern is that farmers may not want to apply the dsRNA extensively to keep their crop protected. Formulations with the use of nanoparticles (NPs) might be essential in most cases to mitigate the degradation of the pest control agent.[34]

dsRNA can be formulated into sprayable forms, or artificial diets (bait) to induce RNAi in a variety of species such as Colorado potato beetle,[35] *S. Exigua*[36], H. heros,[37] *B. Germanica*[38] among others. However, in most cases, naked dsRNA has very low silencing efficiency due to degradation in the insect digestive tract.[12] To overcome this obstacle, carriers are essential to protect and deliver the dsRNA into the cells.[14, 19, 39] Transdermal delivery for gene silencing has proved to be efficient as well. This is an interesting approach for phloem feeders, such as aphids, because they ingest very low amounts of plant tissue compared to chewing insects. It has been demonstrated that topically applied dsRNA formulation could penetrate the cuticles of the insects to induce gene silencing and mortality.[15, 16] Both studies with different dsRNA-carrier systems showed around 80% decrease of aphid population. However, the ability of dsRNA to penetrate into the body is different among insects and is not an efficient delivery method for all insect pests. On the other hand, aerosols have shown some promise with Thairu *et al*. introducing siRNA-NP complexes into aphids successfully.[40]

1.1.2.2.2. Irrigation and soil

For pests feeding on roots, like corn rootworms, dsRNA can be applied in soil. The dsRNA is either ingested directly from the wet soil or through the roots.[20] This method has shown to be able to trigger RNAi in hemipteran insects by root drenching.[41] The dsRNA could be detected in the Citrus plants for 7 weeks after a single exposure of 2 g of dsRNA in 15 L of water. With these methods, other insects, such as those feeding on phloem, could be targeted as the dsRNA can move through the vascular system of the plant. The irrigation method or soil drenching is a simple method in practice. However, its application is limited due to the instability of the dsRNA, which has a half-life in soil of less than 30 hours regardless of its concentration.[42, 43] Dubelman *et al*. studied the degradation of DvSnf7 dsRNA in 3 representative agriculture soils (loamy sand, silt loam and clay loam). These types of soil differ in their physicochemical properties such as percentages of sand, silt and clay, USDA textural class, bulk density, percentage of organic matter, pH, cation exchange capacity, field moisture capacity and a number of chemical elements and nucleases. Only small differences of degradation were observed between the different types of soil, with time for 50% degradation to occur between 15 hours to 27 hours. Interestingly, there is always an initial period with very low degradation (less than 10 hours), corresponding to an acclimation phase, followed by rapid degradation. These results were assessed by loss of biological activity (mortality of the target organism). This suggests that the resident soil microbial community and RNases rapidly interact with the dsRNA and degrade it. Advances in formulations with regards to improving life-time of dsRNA in soil is key to the success of these delivery strategies.[44]

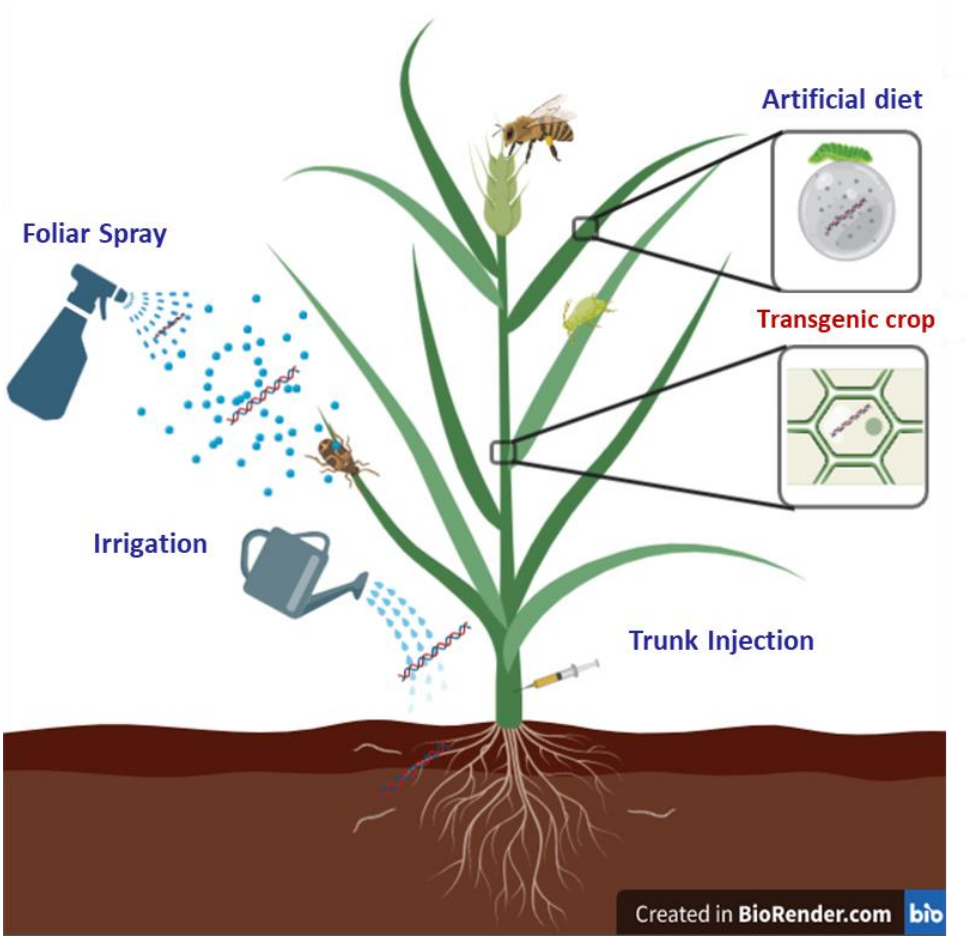

Figure 1.2: Delivery methods for RNAi-mediated insect pest control. All these strategies have their own advantages depending on the condtions and targets.

1.1.3. From ingestion to RNAi in the cells: DsRNA inside the insect environment

After the application of dsRNA to the crop, the orally ingested dsRNA has to go through the insect gut (Figure 1.3). This is the biggest barrier for the dsRNA due to differring environments found in the digestive tract of insects.[45] Nucleases are present in the saliva, the hemolymph but especially in the different parts of the gut where their activity is the highest.[7, 46, 47] And in some insects extreme shifts in pH occur causing denaturation of the dsRNA.[36, 47]

1.1.3.1. Digestive nucleases

Different types of enzymes, essential for digestion, can be found throughout the insect gut. Nucleases (DNases and RNases) play an important part in processing the nucleic acids that are naturally present in most species' diet. These nucleases are the predominate reason for the poor RNAi response after oral administration as evidenced by the observation that a better RNAi efficiency was obervered after knocking out the gene encoding for dsRNase in the gut.[7, 46] The different RNAi responses among insects might suggest the activity or ability to degrade the dsRNA by these digestive nucleases vary among insects as well. Peng *et al*. studied dsRNases activity in four different insect species from different orders (*Spodoptera litura* (Lepidoptera), *Locusta migratoria* (Orthoptera), *Periplaneta Americana* (Blattaria) and *zophobas atratus* (Coleoptera)). The structure and quantities of RNAses vary between insects.[12] The nucleases activity for all insects was higher in alkaline environment (above pH 9.0) and at optimal Mg^{2+} ion concentrations.[47] However, these optimal conditions and kinetic parameters differ among insect species as well as their physiological conditions. Moreover, chemical environment within the different areas of the gut, such as foregut, midgut, hindgut, fluctuate. These nucleases are also present in saliva, with some madibulate insects spreading saliva onto leaves when feeding.[48] Hence, some degradation can occur before it is even ingested.[17, 12]

To enhance the stability of dsRNA, NPs can again be the key to the RNAi success.[3, 28] Another method is to use Ethylenediaminetetraacetic acid (EDTA) as chelating agent. The presence of EDTA in addition to a liposome carrier, improved the stability of the dsRNA as shown by the higher mortality of the target insects. The chelating agent acts as a protein inhibitor to the nucleases as it binds to divalent cations such as Mg^{2+}.[37] This is in agreement with other reported studies on degradation in the hemolymph plasma of *M. Sexta*[49] and midgut of *C. puncticollis*.[50]

Even if the activity of the nucleases in the different species can be used as an indicator to estimate RNAi sensitivity, many factors have to be taken into consideration. Only *in vivo* assays will confirm the preliminary *ex vivo* tests such as degradation in gut juice or saliva assays.

1.1.3.2. Gut pH

RNA is more stable in acidic conditions. Single-stranded RNA (ssRNA) can be degraded via a two-step reaction: a transesterification (concomitant cleavage of the RNA strand) followed by hydrolysis. Although, the alkaline hydrolysis of dsRNA has not yet been investigated in detail, it is believed that by the presence of the double helix it can be limited to some degree. [12] Hence, the pH in the gut acts twofold against RNAi; optimising nucleases for cleavage and through alkaline hydrolysis. Moreover, it can strongly vary in the different areas of the gut and among species depending on the physiology. For example, Lepidoptera very often have highly alkaline pH (pH 10 to 11). Associating the dsRNA with NPs such as cationic polymers could be of use to improve stability. However, the electrostatic interaction between the two needs to withstand decomplexation at high pH to prolong the stability of the dsRNA long enough so it can enter the cells. A strong basic group, with high pKa, such as a guanidine group (pKa 13.6), is required so the polymer stay protonated at alkaline pH.[36, 51]

1.1.3.3. Peritrophic matrix

For most insects, when in the gut lumen, the dsRNA passes through the peritrophic matrix, which separates food particles, digestive enzymes and pathogens from epithelial cells (Figure 1.3).[52] It protects against mechanical damage and is also a biochemical barrier to inactivate ingested toxins. This membrane is composed mostly of chitin and glycoproteins and this is another obstacle for the dsRNA to reach the gut epithelial cells. Proteoglycans present in the peritrophic matrix are negatively charged, thus it may create a repulsive force against the negative charge of the dsRNA. Shielding the negative charges with NPs can improve the efficiency of the transport through the matrix. When *Drosophila* were fed with dsRNA complexed with cationic core-shell fluorescent NPs, the dsRNA crossed the membrane more efficiently than the naked dsRNA.[39] However, the pore size of this membrane needs to be taken into consideration to design the NP carriers. The size of the apertures range from 7 nm to 36 nm and can change throughout the day depending on ingested meal.[53] The current literature on the peritrophic matrix is limited and cannot really provide enough insight

on how the pore size could affect dsRNA transport.[12] More studies are necessary to understand the role of this membrane and the way it interacts with dsRNA.

1.1.3.4. Uptake of dsRNA

Once it passes the peritrophic matrix, the dsRNA needs to enter the gut epithelial cells. Two main pathways are reported for the dsRNA uptake from the environment: the transmembrane channel protein-mediated uptake pathway and the endocytic pathway (Figure 1.3).[54] A family of genes encoding for proteins involved in the transmembrane channel pathway named SID-1-like (systemic RNA interference-deficient-1-like) or SIL has been identified in some insect species but not all.[3, 12, 55, 56] The involvement of this pathway was demonstrated by looking at the expression level of SIL genes that are increasing after exposure to dsRNA through feeding. These proteins are also important for cell-to-cell movement of dsRNA, thus a local administration of dsRNA can lead to an RNAi response into different tissues of the insect body.[5, 16] However, this systemic spread has also shown to be triggered in insects lacking SIL proteins suggesting that other mechanisms are involved for dsRNA uptake and spread. Clathrin-dependent receptor mediated endocytosis has also been reported to mediate dsRNA uptake in different insect species.[57-59] Studies showed that inhibiting this endocytic pathway leads to a decrease of dsRNA uptake. After endocytosis, the dsRNA has to escape the endosome to reach the RNAi machinery into the cytosol. Accumulation of dsRNA in endosomes due to inefficient endosomal escape and subsequent degradation, could be one of the major factors explaining moderate gene silencing effects in lepidopteran insects.[59] If the dsRNA is not able to move inside the cell and enter the cytosol, the access to the RNAi machinery is limited and almost no siRNA can be produced. This is what was demonstrated by Shukla *et al*., with no siRNA being detected in *S. frugiperda's* (Lepidopteran) cells even after dsRNA was taken up.[8] The association with NPs can help avoid degradation in these endocytic vesicles. The escape with the help of amine-based polymers or peptides is assumed to occur via 'proton sponge' effect. With the acidification of the organelle, the tertiary amine groups become more protonated. To restore neutrality, Cl^- counter ions are pumped into the endosome and through osmosis, an excess of water enters, causing membrane rupture.[12, 60] Although, the exact mechanism is not fully understood and the process is considered controversial in the literature.[61, 62]

It is still unclear if these two uptake pathways can operate simultaneously and what are their relative contributions to the dsRNA uptake process.[56] More work still needs to be carried out to understand fully all mechanisms involved in dsRNA uptake, RNAi machinery and systemic spread. This will provide better insight to develop more efficient strategies to optimise RNAi-based technologies for insect pest control.[22]

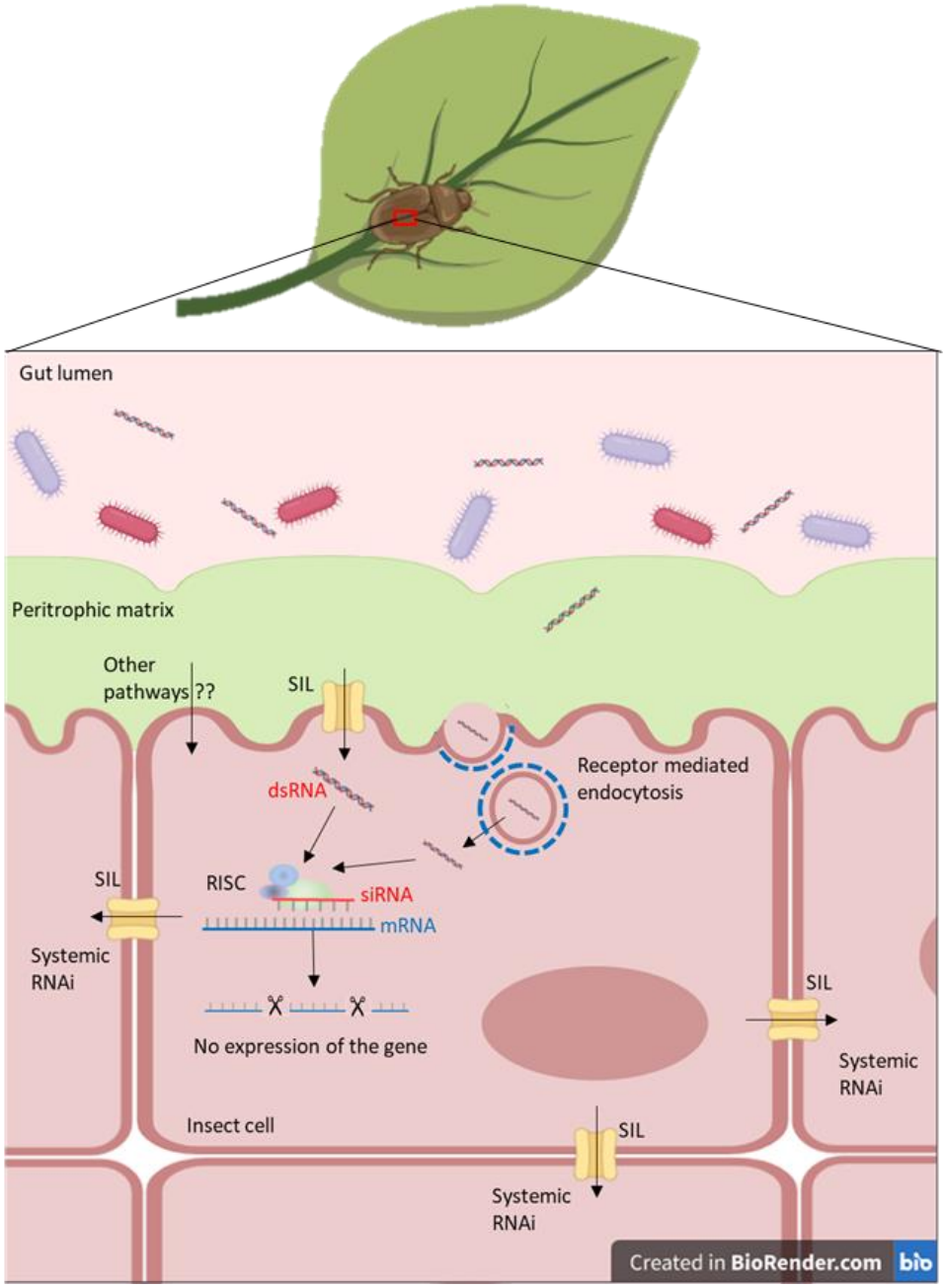

Figure 1.3: Schematic representation of the dsRNA way from the environment to RNAi machinery inside the insect cell. After ingestion by the insect pest, the dsRNA enters the gut lumen. It will have to cross the peritrophic matrix to enter the epithelial cell. The uptake is essentially accomplished by clathrin-dependent receptor-mediated endocytosis (RME) (Clathrin coat is represented by the blue dotted lines) and by SID-1-like (SIL) proteins. Once the dsRNA entered the cell, it can be processed by the RNAi machinery leading to target gene silencing.

1.1.3.5. Others factors impacting the stability of the dsRNA

Great variations of RNAi efficiency can be observed among insect orders. For some species, an excess of dsRNA is required to obtain small results.[41] The instability of the dsRNA in the gut is a factor contributing to this small response. Another factor that is not well studied is the potential effect of the microbiota in the gut. The microbiome of the insect gut influences the pH, while some bacteria also secrete nucleases. This could have an impact on dsRNA stability and cellular uptake.[12]

The developmental stage can have an influence as well on the efficiency of external administration of dsRNA.[63, 64] Again, it seems that the differences in stability of the dsRNA in the gut is the main reason for these observed variations between adult and larvae. Albeit, another factor is their rate of food consumption.[12] Even intraspecies variations of sensitivity have been observed. Sugahara *et al*. showed these variations with different populations of *Locusta migratoria* (orthopteran).[65] This supports the idea that resistance could become a problem with this method as well. But further research on the mechanisms causing the development of resistance is required in order to provide insight and possible strategies to counteract this.[5] Consequently, due to the variability between insect pests, there are no clear rules that govern the sensitivity of a particular species towards RNAi.

1.1.4. New strategies to improve stability and uptake

The variability in RNAi efficiency is particularly dependent on dsRNA stability inside the insect body. The dsRNA can be degraded by nucleases in the saliva, the gut fluids and in hemolymph or even before ingestion in the field (UV light, rain or enzymes in soil).[7, 33, 36] In order to deliver intact dsRNA into the cells, the use of formulation is essential. Delivery vectors can be used to reduce dsRNA degradation, to increase the cellular uptake but also to promote translocation of dsRNA across the peritrophic matrix and insect cuticle.[12, 15, 16, 20] DsRNA can be carried by viral or non-viral vectors. Viral systems provide positive results for transfection but because of safety concerns, such as potential mutation, applications are limited.[5] Non-viral NP vectors such as cationic polymers, peptides, lipids, sugars or metals have attracted more and more attention because their physical and chemical properties can be tuned (**Table 1.1**). The NPs are usually positively charged to interact electrostatically with the negatively charged phosphate group of the dsRNA and form a complex. The

NPs/dsRNA complex is overall positively charged and this net positive charge can facilitate the interaction with negatively charged cell membrane surface and help with the transit through the peritrophic matrix.

Table 1.1: Overview of cationic polymers, liposomes and peptides used as delivery vectors and their effect on RNAi efficiency.

Nanoparticle	**Insect pest**	**dsRNA**	**Delivery method**	**effect**	**Ref.**
Chitosan	A.gambiae A.aegypti (Dipteran)	dsCHS1 dsCHS2	Artificial diet	34% knockdown 40-60% knockdown	Zhang 2010[66] Zhang 2015[67]
Chitosan	A.aegypti (Dipteran)	siRNA sema1a	Artificial diet	Disruption of olfactory system development.	Mysore 2013[68]
Cationic core-shell fluorescent nanoparticles (FNP)	O.furnacalis (Dipteran)	CHT10-dsRNA	Artificial diet	High gene delivery. Effect on larval development	He 2013[39]
Chitosan	A.aegypti (Dipteran)	dsAaSNF7 dsAaSRC	Artificial diet	Mortality up to 47%	Das 2015[19]
PEI coated Carbon quantum dot	A.aegypti (Dipteran)	dsAaSNF7 dsAaSRC	Artificial diet	Mortality up to 75%	Das 2015[19]
Amine functionalised silica	A.aegypti (Dipteran)	dsAaSNF7 dsAaSRC	Artificial diet	No mortality	Das 2015[19]
Guanidinium functionalised polymer	S.frugiperda (Lepidopteran)	dsvATPase	Oral delivery	>80% gene knockdown Protection against degradation at high pH Moderate larval death after 29 days (30%)	Parson 2018[51]

Nanoparticle	Insect pest	dsRNA	Delivery method	effect	Ref.
Guanylated and DMAEMA copolymers	S.exigua (Lepidopteran)	dsCHSB	Spray for oral delivery	Strong protection against nucleolytic degradation at pH 11 Enhanced cellular uptake Increased mortality to 53%	Christiaens 2018[36]
Cationic dendrimer (fluorescent perylene diimide core and peripheral amino acid arms) formulated with detergent	A.glycines (adults) (Hemipteran)	dsHem	Transdermal delivery (spray)	High knockdown effect (95.4%) and 80% mortality	Zheng 2019[16]
pDMAEMA 4-arm stars formulated with detergent	A.glycines (adults) (Hemipteran)	dsATPD dsATPE dsCHS1	Transdermal delivery (spray)	High mortality (82%) with combination of dsRNA	Yan 2019[15]
pDMAEMA star polycation	A.ypsilon (Lepidopteran)	dsV-ATPase	Oral feeding	70% gene knockdown Reduced larvae body length	Li 2019[69]
Ribonucleoprotein particle (RNP)	A.grandis (adults) (Lepidopteran)	dsCHS2	Oral delivery	Improved dsRNA stability 80% knockdown but no mortality	Gillet 2017[14]
Branched amphiphilic peptide capsules (BAPC)	T.castaneum (Coleopteran) A.pisum (Hemipteran)	BiP-dsRNA Armet-dsRNA	Solid artificial diet Liquid artificial diet	75% larvae death Faster premature death Successful delivery of dsRNA to knockdown the genes	Avila 2018[70]
Lipofectamine 2000	D.melanogaster D.pseudoobsurra D.sechellia D.yacuba (Dipteran)	Gus-dsRNA	Soaking	GUS gene knockdown (52%) Species-specific mortality (30-65%)	Whyard 2009[71]

Nanoparticle	Insect pest	dsRNA	Delivery method	effect	Ref.
Lipofectamine 2000	D.suzukii (Dipteran)	dsVha26 dsrps13	Artificial diet	Significant silencing and mortality. 22-42% mortality after 5h exposure	Taning 2016[63]
GenJet lipoplex	B.germanica (Blattodean)	dsTub	Oral delivery	12h protection against nucleases 60% mortality after 16 days of continuous feeding	Lin 2017[38]
Lipofectamine 2000 formulated with EDTA	E.heros (Hemipteran)	dsvATPase	Artificial diet	Longer protection in saliva Increased mortality (51%)	Castellanos 2019[37]

1.1.4.1. Cationic polymers

Cationic polymers have been proven to transport and protect nucleic acids for therapeutic applications and pest control. They are usually protonated, positively-charged amine-based polymers. The “gold standard” for gene delivery in therapeutics is polyethylenimine (PEI) as it is a inexpensive and commercially available material. It proved to be an efficient delivery vector in multiple studies, however, its application is currently limited due to high cationic charge density causing high cytotoxicity.[72, 73] Other polymers such as chitosan, poly(2-dimethylamino ethyl methacrylate) (PDMAEMA), poly-l-lysine (PLL) and poly(*N*,*N*-dimethylaminopropyl acrylamide) (PDMAPAAm) are frequently used (**Scheme 1.1**).

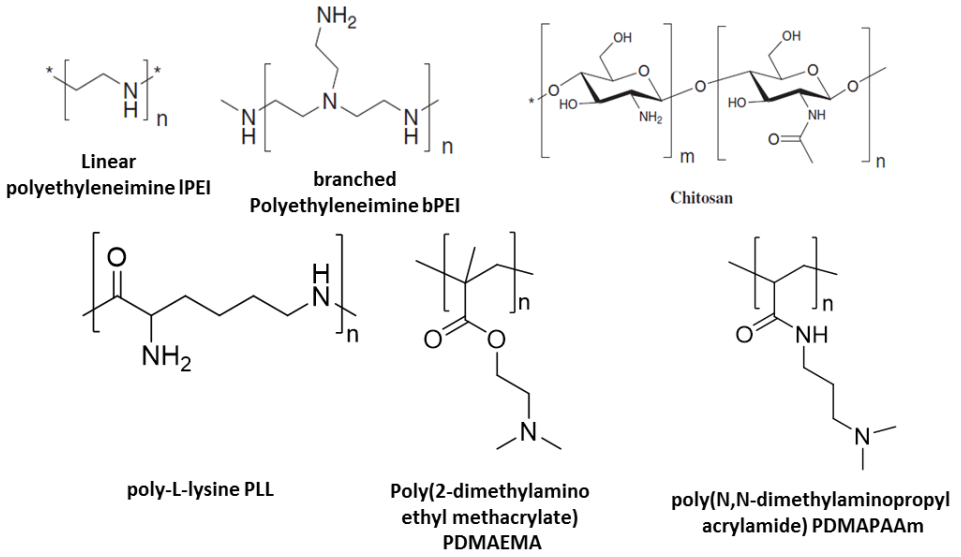

Scheme 1.1: Cationic polymers commonly used for nucleic acids complexation in the litterature.

Although cationic polymers have been widely studied in human medicine, this is not the case for pest control applications with literature being more limited. Proof of concept was reported in 2010 by Zhang *et al*., where chitosan was used to complex dsRNA, improving the RNAi efficiency in mosquitoes. In this study, the authors were able to reduce chitin synthase genes by up to 60% by feeding the larvae with agarose gel-coated mixture with dsRNA entrapped in chitosan-based nanoparticles. Even though this did not lead to mortality, this study proved the ingestion of protected dsRNA could induce gene knockdown.[66] Other studies are also suggesting that chitosan could be a good candidate to complex dsRNA[67] or siRNA[68] in order to trigger RNAi more efficiently in dipteran insects. Comparative studies have started being done directly comparing the chitosan vector to PEI-coated carbon quantum dots (CQD) and amine functionalised silica nanoparticles (ASNP). They evaluated the ability of the systems to increase stability of dsRNA and to facilitate its uptake and endosomal release in order to trigger an efficient silencing of target genes in dipteran insect pest. All the nanoparticles were able to complex the dsRNA but the stability of these complexes varied. In gut conditions, the pH can go from acidic to alkaline, therefore the complex needs to remain stable in a large pH range. Only the PEI-coated CQD complex was stable at pH 10, 7 and 4, while the chitosan complex was stable only at pH 4 and 7 and ASNP vector was only stable at pH 7. This stability in a range of pHs is one factor explaining why the oral administartion of ASNP/dsRNA

complexes did not lead to mortality compared to chitosan and PEI-coated CQD complexes led to a 47% and 75% increase in mortality, respectively. It is interesting to note the small size of the PEI-coated CQD complexes (3.7 nm) compared to the two other systems (both 15.5 nm).[53] The small size of the particles could help with the passage through the peritrophic matrix. He *et al*. followed on from this work targeting genes responsible for chitin synthesis, studying the effect of oral feeding on dipteran larvae. Here, the authors complexed the dsRNA with a cationic core-shell fluorescent nanoparticle (FNP). The cationic shell composed of primary amine polymers was able to complex, protect the dsRNA and improve the uptake efficiently to knock down key developmental gene expressions and kill the insect pests. The fluorescent property of the core enabled them to monitor the ability of the particles to cross the cell membrane. The results showed that by increasing the FNP concentration it was possible to accelerate the uptake of the complex.[39] In another study, a similar fluorescent structure was used to deliver transdermally dsRNA to the aphid *A. glycines*. The cationic arms were composed of peripheral amino acid groups which were able to complex the dsRNA. As aphids are sap-sucking insect pests, they developed a formulation that is able to deliver the dsRNA by soaking the insects. By combining the dendritic polymer with a detergent, the surface tension of the hydrophilic complex droplets was reduced, thus helping it adhere quickly to the oily surface of the aphids and infiltrate the body wall (in an hour). The dsRNA was then systematically delivered throughout the aphids as shown by the high fluorescence detected in various tissues across the body. It resulted in a 95% decrease of the target gene and 80% population suppression.[16] In a second paper, the group investigated the efficiency of a cheaper nanocarrier, a 4-arms star pDMAEMA polymer, to reduce the economic cost. The star polymers ($M_{n,GPC}$=18300 g/mol, $Đ$=1.07) were synthesised by atom transfer radical polymerisation (ATRP) and the star-shaped structure had a high density of functional group to efficiently condense the dsRNA. This system as well as the previous dendrimer structure led to a high RNAi efficiency. Up to 82% mortality of the aphid population was obtained with a combination of two dsRNA molecules through topical application (drop of formulation directly applied to the aphid body) and 78.5% lethal effect through spray method.[15] In another study, they investigated the use of this inexpensive pDMAEMA 4-arm star nanocarrier for lepidopteran *A. ypsilon* larvae. Oral feeding was used as the delivery method and visible effects were observed after 4 days on body length.[69] Overall, these results show dendrimeric/star architectures are

suitable as effective gene carrier for dsRNA delivery. As previously mentioned, soil and leaves are environments to be considered as well. The ability of this type of architecture to complex dsRNA and to protect it in soil was investigated by Whitfield *et al*. According to this report, the use of pDMAEA 4-arms star polymers to complex dsRNA improved the stability of the nucleic acid in soil to up to two weeks. The hydrolysis of the DMAEA side chains in this polymer plays an important role in this work, as the system was designed to be able to release the dsRNA in soil over time and make naked dsRNA available for ingestion by worms. The star structure was also compared to a linear polymer equivalent. The latter did not improve performance compared to the star configuration. No differences in speed of hydrolysis was observed which could have explained this difference in protection efficiency.[74] However, weaker binding between the linear polymer and the dsRNA was reported, as a higher N/P ratio (the ratio of positive charges on the nitrogen of the polymer to negative charges on the phosphorus of the dsRNA) was required to fully complex the dsRNA. Moreover, simulation of binding showed star polymers were bending and wrapping nucleic acid more efficiently and were forming a more compact complex compared to the linear equivalent.[75] DMAEA-based branched polymer systems have also been studied for soil stability of dsRNA. Better stability was observed (up to 7 days) compared to linear equivalent. However, the structure is not well controlled compared to the star polymers. Again, the structure does not seem to have an impact on the hydrolysis rate but the incorporation of non-hydrolysable co-monomer was able to slow down the hydrolysis and the release of dsRNA.[76, 77] This supports the idea that the architecture of the polymer has an impact on the binding and stability of the dsRNA. Nevertheless, more results would be necessary to determine if the rate of hydrolysis has an effect on protection and release of dsRNA in soil as well as RNAi response in insects.

Most polymer complexes that are commonly used to improve stability of the nucleic acid are not stable at the high pH found in the gut of some species, typically lepidopteran.[19] Yet, guanylated polymers, with their high pKa (12.5-13.5), are potential candidates to withstand decomplexation even at high pH as shown by Parson *et al*.[51] and Christiaens *et al*.[36] In both works, they used guanylated based polymers, poly[*N*-(3-guanidinopropyl)methacrylamide] (pGPMA) synthesised by aqueous radical addition-fragmentation chain transfer (RAFT) polymerisation ($M_{n,GPC}$=20,000

g/mol, $Đ$=1.09)[51] and poly[(guanylated methacrylate)$_{0.87}$-*co*-(2-(aminoethyl) methacrylate)$_{0.13}$] (pGUMA$_{0.87}$-*co*-AEMA$_{0.13}$) made by free radical polymerisation ($M_{n,GPC}$=45,000 g/mol, $Đ$=1.41). Both polymers were able to increase protection at alkaline pH (pH 10 or 11) but high content of guanylated functions is required to preserve the interaction for more than 30 hours.[36] Moreover, guanidinium functionalised polymers can facilitate uptake of nucleic acids through endocytosis mechanism.[78] Better gene suppression was observed in the RNAi refractory cell line with pGPMA/dsRNA complexes than with naked dsRNA. The ingestion of the complex by the *S. frugiperda* larvae led to high gene knockdown and moderate mortality.[51] Similarly, ingestion of pGUMA$_{0.87}$-*co*-AEMA$_{0.13}$/dsRNA 90% silencing efficiency was obtained leading to 50% decrease of *S. exigua* population.[36]

1.1.4.2. Liposomes

Liposomes have also been reported as good protective vectors for oral ingestion of dsRNA in insects.[41, 71] They are typically composed of a positively charged hydrophilic head that can interact with the dsRNA and a hydrophobic tail.[53, 79] Because of the ease of synthesis, their non-toxicity and biodegradability properties, it makes them very attractive as delivery vectors.[80] Different liposomes are now available on the market and some are already used in drug formulation.[81] Successful encapsulation of dsRNA was demonstrated for species of *Drosophila*. The larvae fed with encapsulated dsRNA in Lipofectamine 2000 liposome suffered high mortalities after ingestion while larvae fed with naked dsRNA did not show any response.[71] DsRNA combined with Lipofectamine 2000 also showed better results than naked dsRNA on *D. suzukii*[63] or with GenJet lipoplex on *B. Germanica*.[38] More recently, Castellanos *et al*. showed that Lipofectamine 2000 combined with EDTA has great potential to protect the dsRNA against degradation by enzymes. The chelating agent inhibit the metal-dependent enzyme responsible for the degradation as shown by the saliva assays. The presence of EDTA in addition to the liposome prolong the stability and stronger RNAi effects are observed.[37]

1.1.4.3. Peptides

The use of cell-penetrating peptides as delivery systems for dsRNA is also an interesting approach to enhance silencing activity. As well as being able to provide

protection, they facilitate cellular uptake. By combining peptide transduction domain (PTD), to promote endosomal escape, with dsRNA binding domain (DRBD) to complex the dsRNA, Gillet *et al*. were able to improve the knockdown of chitin synthase II compared to naked dsRNA. The dsRNA stability is higher in gut conditions and the silencing efficiency is enhanced significantly (80%) compared to naked dsRNA (30%).[14] Amphiphilic peptide capsules (BAPCs) have also been reported as efficient nanocarriers to facilitate uptake of dsRNA in two different diet mediums with *T. castaneum* and *A. pisum* feeding on a solid flour diet and an artificial liquid diet, respectively. Delivery of dsRNA is observed as transcript levels and population dramatically decreased. As this approach proved its efficiency in both Coleopteran, *T. castaneum* and Hemipteran, *A. pisum*, it suggests that it could be widely applicable to other insects.[70] Cell-penetrating peptides represent a wide diversity of possible potential nanocarriers for oral dsRNA delivery.

1.1.5. Summary

These recent results on combination of dsRNA with cationic vectors are highlighting the importance of formulation to develop successful RNAi-based pest control. Cationic polymers are particularly attractive due to their variety, ease of synthesis and cost. Composition, functions and architecture can be easily adjusted to optimise the system in each desired target. A good carrier needs to be able to protect the dsRNA in various conditions from the field to the insect's cells through the gut, to deliver it to knockdown the target gene. The complexation needs to be able to withstand the binding in all of these conditions. First assessing the good binding in ideal conditions (water) is necessary, without the presence of any competing and degrading species. The ability of the polymer to efficiently protect the dsRNA can be assessed by putting the polyplex in presence of nucleases or competing species (for example Heparin) and also in more real conditions *ex vivo* (gut juice assay, soil assay…) before doing bio assays *in vivo* by applying the formulation on the plant or in the soil so the target insect are in contact to the dsRNA. An important aspect to take into consideration are the toxicity of the cationic polymer for the target pest, the plant but also non-target insects and animals without forgetting the fate of the polymers in the field. Concerns can be made about accumulation in soil, presence in the food chain…

RNAi used for pest management using direct application is believed to soon reach the market as more and more progress are made in this area of research. Moreover, the cost of dsRNA production has decreased in recent years.[26] The patents landscape is still very limited for nontransgenic plants in terms of formulations, with some examples of chitosan polymers to complex and protect dsRNA.[82-84] But a large number of patents can be found on the RNAi field in general (Figure 1.4) focusing more on specific dsRNA to target pest or use for GMOs.[85]

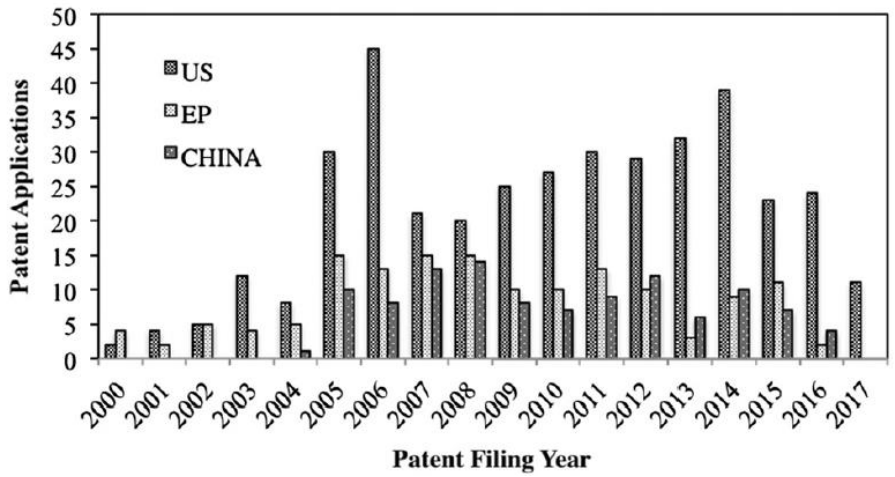

Figure 1.4: Number of patent applications, filed for RNAi technology for plants in the United States (US), Europe (EP) and China. Figure adapted from ref.[85]

1.2. Cationic polymers for dsRNA complexation

This second part focuses on the synthesis of cationic polymers which can be used for dsRNA complexation. Controlled radical polymerisation is a powerful technique to prepare a wide range of polymers with specific composition, molecular weight and architecture, such as star-like structures. 2-dimethylaminoethyl acrylate (DMAEA)-based cationic polymers, which are the focus of this work, are interesting candidates for efficient complexation of nucleic acids through electrostatic interaction. They hydrolyse over time inducing a charge shift and leading to the release of the negatively charged material as described below.[75, 77, 86-88]

1.2.1. Controlled radical polymerisation

Radical polymerisation is a versatile technique that is comptatbile with a wide range of monomers and enables the synthesis of various functional polymer materials. It is the most widely used polymerisation process in industry to synthesise low cost materials.[89] With the development of reversible-deactivation radical polymerisation (RDRP)[90] in the 1990s, also known as controlled radical polymerisation , it is now possible to synthesise well-defined polymers with controlled architectures such as star, brush, or branched polymers,[91, 92] structures which used to only be accessible by ionic polymerisation.The radical process in RDRP allows the reaction to work in less stringent conditions and with a wider range of monomers. The polymeric architecture strongly affects the material properties, thus the ability to control this parameter makes RDRP highly attractive for a broad range of applications such as nanocarriers for encapsulation of active components, lubricants, emulsifiers, rheology and surface modifiers or adhesives.[93] The control afforded by RDRP is achieved through the reversible deactivation of the radical active species to a dormant species through a control agent.[89, 90, 94, 95] The equilibrium is strongly in favour of the dormant form, meaning only a small proportion of the chains are active and growing at any given time. The instantaneous concentration in radical is therefore very low so termination and transfer events are limited. As the radical is exchanged very fast between dormant and active chains, polymer chains are able to grow simultaneously as the monomer is consumed.[96] The main RDRP techniques are Nitroxide-mediated polymerisation (NMP),[97] Atom Transfer Radical polymerisation (ATRP)[91] and reversible addition-

fragmentation transfer (RAFT).[90, 98] They all have their advantages and disadvantages as described in the next paragraphs.

1.2.1.1. NMP

NMP is based on the reversible termination mechanism by combination with a stable nitroxide radical (**Scheme 1.2**).[95, 99] At high temperature the alkoxyamine bond is cleaved, to release the active species capable of reacting with monomers, and a stable nitroxide radical. The species recombine to reform a dormant compound. The equilibrium is strongly in favour of the dormant state, thus keeping the radical concentration low to have a good control of the polymerisation and obtain well defined materials.

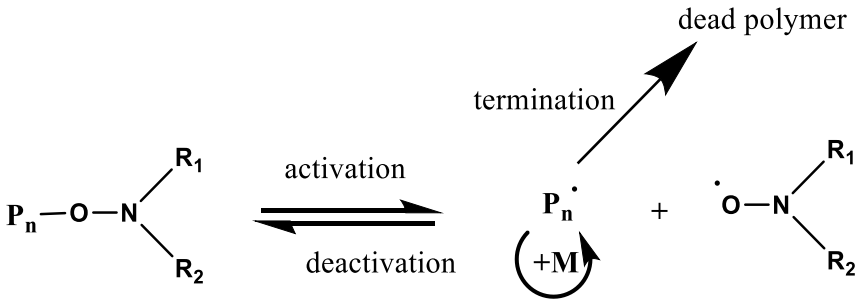

Scheme 1.2: The NMP mechanism.

Although NMP has significant advantages, such as the simplicity of procedures and polymer purity (due to the absence of metal catalyst or thiols), its application is limited due to slow polymerisation kinetics requiring high temperatures and long reaction times, limited monomer compatibility and susceptibility to side reactions.[100]

1.2.2. Metal-mediated RDRP: ATRP and Cu(0)-mediated RDRP

The ATRP activation-deactivation equilibrium is based on the reversible reaction between a dormant alkyl halide and a transition metal complex to form an oxidised transition metal complex and an active propagating radical (**Scheme 1.3**).[101, 102] This method has been developed by Matyjaszewski using copper since 1995,[103] and Sawamotto using Ruthenium, but it has also been developed using many other transition metals including iron, osmium, nickel, palladium, silver, molybdenum and

zinc.[101] Copper is still the most widely used transition metal due of its low cost, availability and efficiency.[102, 104]

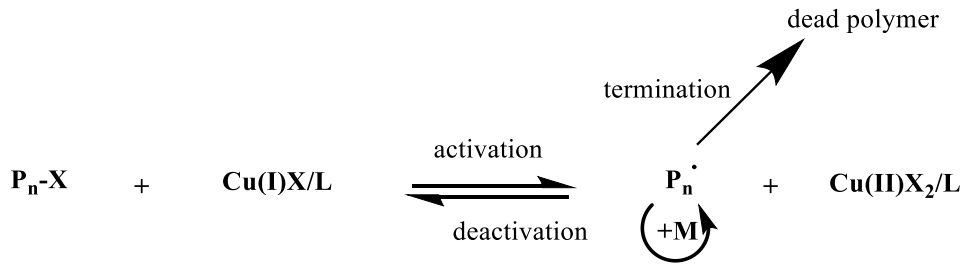

Scheme 1.3: ATRP mechanism with copper as the transition metal. X is a halogen atom and L is a ligand.

ATRP has been successfully used in academic laboratories for the past 20 years as shown by the number of research articles and patents published.[95] But commercial use has been delayed by many reasons including the high concentration of Cu catalyst required for the reaction to maintain a high polymerisation rate. New techniques have been developed to considerably reduce this concentration in the final material with a number of different activator regeneration processes (ICAR (initiators for continuous activator regeneration) using initiators, ARGET (activators regenerated by electron transfer) using a reducing agent, electrochemical and photo-mediated ATRP using free ligand).[105, 106]

Cu(0)-RDRP has shown great potential to reduce the amount of copper required. The introduction of a zerovalent metal has been reported to be an interesting solution. Two models are presented in the literature: supplemental activator and reducing agent (SARA ATRP) and single electron transfer living radical polymerisation (SET-LRP). Both represent the same components resulting in the same reaction, but the mechanism is still under debate since the two are based on two different assumptions (**Scheme 1.4**).[107] The SARA ATRP mechanism is based on the Cu(I) being the major activator of alkyl halides and Cu(0) acting as supplemental activator reducing the excess of Cu(II) to Cu(I) via comproportionation,[108] while in the SET-LRP mechanism Cu(0) is the major activator and Cu(I) instantaneously disproportionate into Cu(0) and Cu(II) in water in the presence of aliphatic amine ligands.[109, 110] However, despite this, commercial application remain limited.

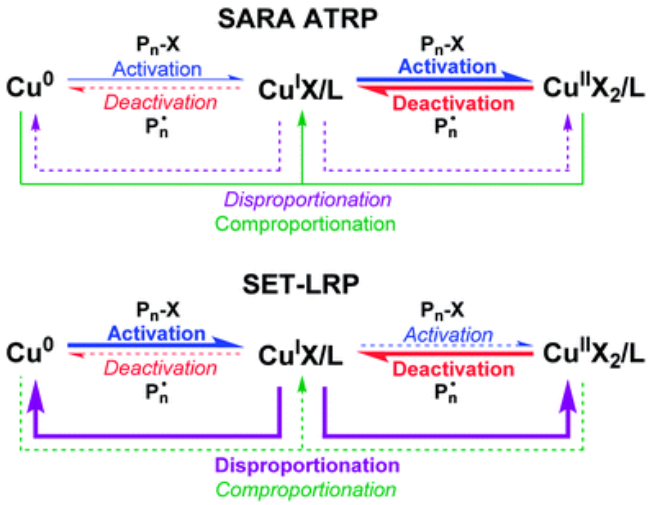

Scheme 1.4: Mechanisms of SARA ATRP and SET-LRP. Bold arrows indicate major reactions, whereas soil arrows indicate supplemental or contributing reactions and dashed arrows indicate minor reactions that can be neglected from the mechanism. ref. [107]

1.2.2.1. RAFT polymerisation

The RAFT process is similar to classic radical polymerisation, but the propagating radical is constantly transferred from one polymeric chain to another via a degenerative mechanism of addition and fragmentation in the presence of a chain transfer agent (CTA or RAFT agent) (Scheme 1.5).[94, 98, 111, 112] Unlike other RDRP techniques, RAFT requires the presence of an external radical initiator; its concentration will determine the instantaneous concentration of radicals and thus the propagation/termination rate. The design of the RAFT agent is fundamental, matching its activity to that of the monomer(s) to achieve good control over the molecular weight distribution in a given system.[113]

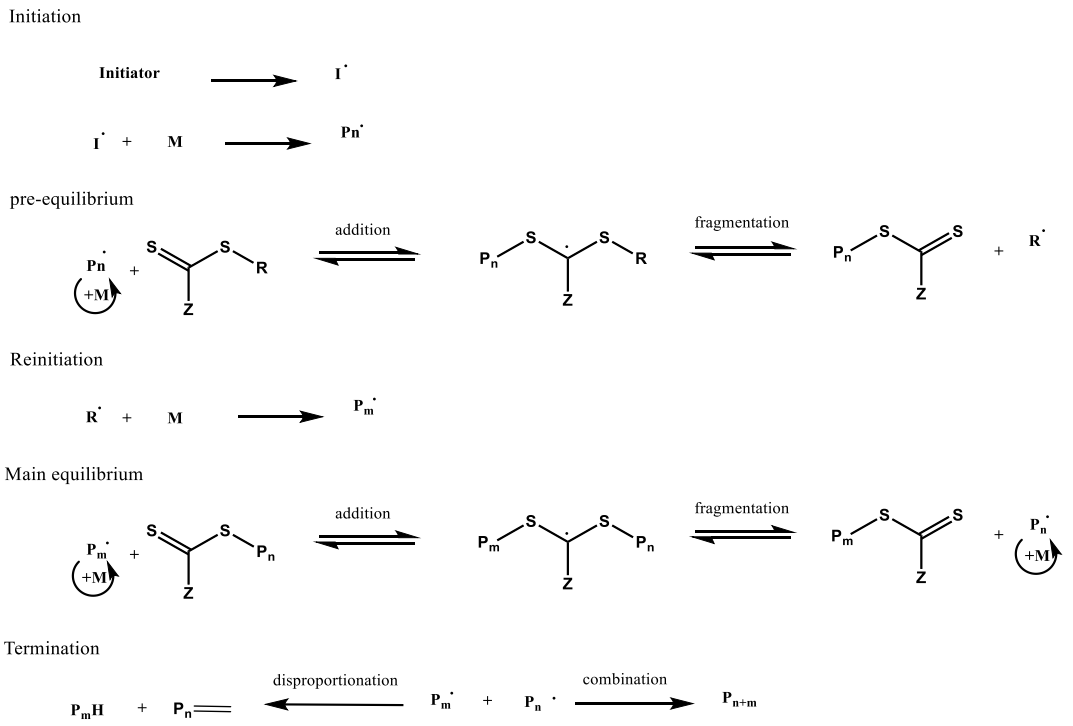

Scheme 1.5: RAFT polymerisation mechanism

RAFT is a highly versatile, simple and robust method to polymerise a wide range of monomers.[98] It allows control over the growth of the polymeric chains obtained by conventional radical polymerisation. By modifying the ratio of monomer to CTA ([M]/[CTA]), narrow dispersity polymers with tuneable molar mass (M_n) can be obtained.[98] As it is a pseudo-living polymerisation, most of the chains will retain the thiocarbonylthio moiety at the chain-end (called living chains) allowing further chain extension to produce block copolymers.[113-115] Furthermore, this property can be exploited to prepare complex architectures such as stars or brushes.[77, 92]

1.2.3. Star polymers

Star-shaped polymers are macromolecules with three or more polymeric arms connected through a central core.[116] These polymers have been extensively studied in recent years because of their interesting physical and chemical properties: compact structure, flexibility, low viscosity and high surface functionality. Their synthesis can be divided into three categories using divergent or convergent approaches.[117-119]

In the core first approach, a multifunctional initiator is used as the core from which arms are grown to form the star (Figure 1.5A).[74, 120-122] The number of arms can easily be tuned as it corresponds to the functionality of the initiator, however, it can be challenging to ensure arms grow at the same rate due to sterics around the tightly packed core affecting initiation efficiency with same DP. This approach is also limited by the possibility of the obtention of multifunctional RAFT agents with high purity for instance, to get a well-defined star polymer with a certain number of arms.

Another method is the arm-first approach, in which the linear polymeric arms are first synthesised using a controlled polymerisation technique such as RDRP, and then a bifunctional crosslinker is introduced to covalently interconnect the end of the arms to form the star-shaped structure (Figure 1.5C).[116, 123, 124] Compared to the core-first approach, the structure, composition and functionality of the arms are better controlled as the arms can be characterized separately prior to chain extension with the crosslinker.[125] It also allows for the synthesis of star polymers with higher number of arms, however, the molecular weight distribution is often broader and it can leave residual unattached arms.[118] Parameters such as the crosslinker to CTA (or initiator) ratio, radical concentration and the nature of the crosslinker are crucial to optimise the synthesis and obtain high arm incorporation and narrow molecular weight distribution.[126, 127]

Finally, the grafting-to strategy uses preformed linear arms with end functional groups that are able to react with a multifunctional core through an efficient coupling reaction (Figure 1.5B).[116, 128, 129] One of the most used chemistries for the coupling are the so-called “click” reactions, which have numerous advantages such as high yield and fast reaction times.[130, 131]

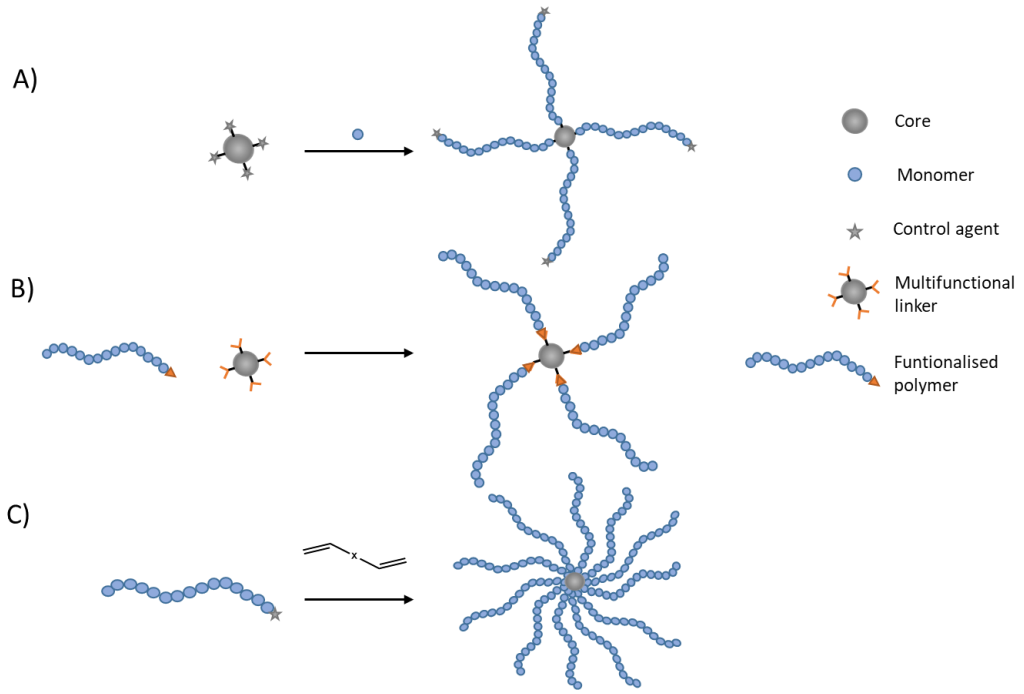

Figure 1.5: methods to synthesise stars. A) Core-first approach, B) grafting to, C) Arm-first approach.

In this thesis, the core-first approach was first used (**Chapter 2**) using RAFT polymerisation, in order to assess the potential of 4-arm star structures already investigated using Cu(0)-mediated RDRP for dsRNA protection and to compare it to core-crosslinked star structures (**Chapter 3 and 4**). The arm-first approach has been chosen for ease of preparation and the higher achievable arm density. Ideally, the polymeric arms are synthesised in a first step with full monomer conversion, so that the synthesis can be done in one-pot by direct introduction of the crosslinker without any purification step.[126]

1.2.3.1. Star polymer characterisation

Characterising complex architectures requires more advanced techniques than traditional ones employed for the analysis of linear polymers, such as gel permeation chromatography (GPC) (also known as size exclusion chromatography (SEC)) with conventional calibration or nuclear magnetic resonance (NMR). These techniques only provide limited information with regards to the polymeric architecture.[118]

Conventional GPC uses a concentration sensitive detector - typically a refractive index (RI) detector, or alternatively a UV detector. After injection of the sample into

the GPC column,the polymer molecules are separated based on their molecular size/hydrodynamic volume in the solvent. The detector situated after the column determines the amount of material at a given retention time. By using a calibration curve, the retention time can be corresponded to a molecular weight and then used to give a molecular weight distribution for the sample of interest. This curve can be generated by using polymer standards with known molecular weight and narrow dispersities. Although conventional GPC is widely used as an analytical tool to determine average molecular weigth of polymers and their dispersity, it has some limitations. The standards used for the calibration are typically linear PMMA, PS or PEO, but if the sample is composed of a different polymer, the results are only comparative and inconsistencies and deviations are observed. Moreover, star or branched polymers in general are more compact structures, therefore they have a smaller hydrodynamic volume than their linear equivalent with corresponding molecular weight. This means the molecular weight is underestimated with the use of conventional linear calibration standards.

Triple detection GPC combines light scattering and viscosimeter detectors with the refractive index (RI) detector. The RI detector gives a concentration profile and the light scattering (LS) allows for calculation of the absolute molecular weight, while the viscometer measures the viscosity of the sample giving access to more structural data. The combination of the complementary data can give access to more information on the behaviour of the polymer in solution such as absolute molecular weight, structural data without the need for a calibrant. The so called universal calibration is based on the fact that intrinsic viscosity and molecular weight are related to the hydrodynamic volume of the macromolecules, as described by the following equation.

$$V_h = k[\eta]MW \text{ or } [\eta] = k' \frac{V_h}{MW}$$

Where [η] is the intrinsic viscosity, k and k' are constants and V_h is the hydrodynamic volume of the polymer. Therefore, any calibrant can be used to generate calibration (Figure 1.6) regardless of chemistry or architecture.

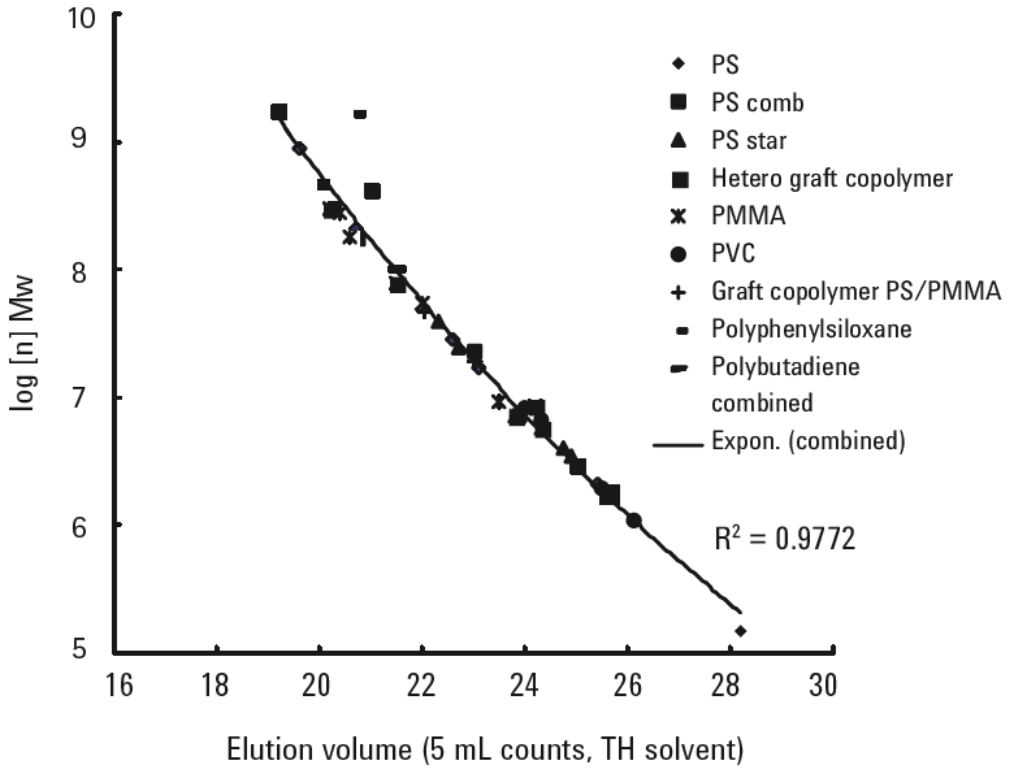

Figure 1.6: Plot of Log[η]MW=f(elution volume) for different polymers with different molecular weight, chemistry and architectures. Figure adapted from ref.[132, 133]

The viscometer detector also allows the production of a Mark-Houwink plot (Figure 1.7), showing the relationship between molecular weight and intrinsic viscosity: $[\eta] = KMW^{\alpha}$ plotted as $\log[\eta] = \log K + \alpha \log MW$. The two parameters K and α are constants and provide structural information specific to the polymer-solvent system. K is the intercept value, and is related to backbone structure. α is the slope, describing the density of the macromolecules in solution, it ranges from 0 (solid sphere) to 2 (rigid rod). Values of between 0.5 and 0.8 are typical for a polymer in a theta solvent or a random coil in a good solvent, while lower values are observed for more compact dense structures such as stars and branched polymers.

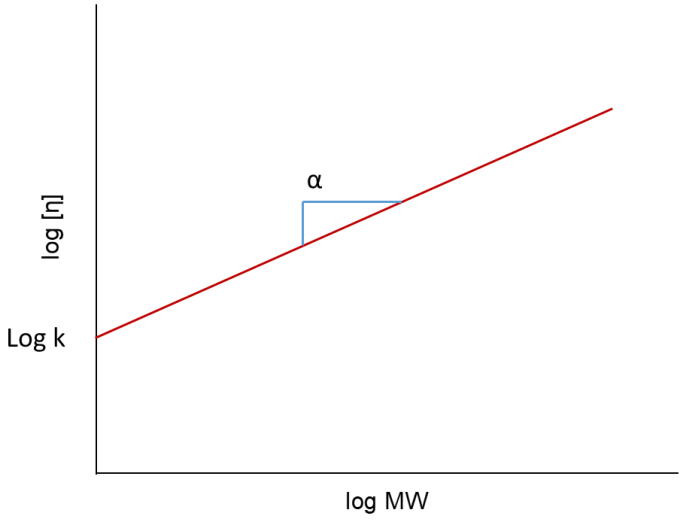

Figure 1.7: Mark-Houwink plot.

Light scattering detectors can be used to determine the absolute average molecular weight, independent of calibration standards. The amount of scattered light measured by the detectors at different angles is proportional to the size of the macromolecules, with larger molecules displaying stronger scattering intensity. Light scattering analysis does not only generate information on the molecular weight, but also on size (radius of gyration, R_g).

1.2.3.2. Other techniques to determine the size and shape

Given their small size (size < 20 nm), star polymer particles are difficult to characterise with common techniques such as dynamic light scattering (DLS) or direct imaging techniques (transmission or scanning electron microscopy (TEM/SEM) and atomic force microscopy (AFM)). Structural details are difficult to observe as they are often below the resolution limits or the material is in a collapsed globular structure.[118] AFM enables the measurement of height, length, width and volume of a molecule deposited onto a substrate, by building up a height profile map of the sample's surface and data are then treated to form an image.[134] Successful imaging of star copolymers using AFM has been achieved, as demonstrated in work by Yoshizaki *et al.*, who were able to measure the size of single molecular particles of poly(p-methoxystyrene) stars (N_{arm} = 67) on mica discs. A radius of approximately 20 nm and heights of about 2.5 nm were determined.[135] Other high quality imaging has been obtained for star-like structures with brush-like arm polymers with good resolution of the arms.[136, 137] Small

angle X-ray scattering (SAXS) can also be used to characterise the structure (size, shape, internal structure etc) of polymeric materials, and has been applied to star polymers. [138, 139] Felberg *et al*. were able to observe the structural transitions with the change of pH for their polyelectrolyte star cross-linded star polymers.[139] Additionally, Moinard *et al*. have shown the influence of the counter ion and 4-arm star concentration on the maximum intensity.[140]

1.2.4. Poly(2-dimethylaminoethyl acrylate) (pDMAEA) as hydrolysable polymer

McCool and Senogles were the first to highlight the self-catalysed hydrolysis of pDMAEA forming poly(acrylic acid) (PAA) and *N*,*N*'-dimethylaminoethanol (DMAE) (Scheme 1.6).[141] Ros *et al*. suggest that the hydrolysis involves a 5-membered ring interaction under basic conditions and 7-membered ring coordination under acidic conditons as shown in Figure 1.8.[142]

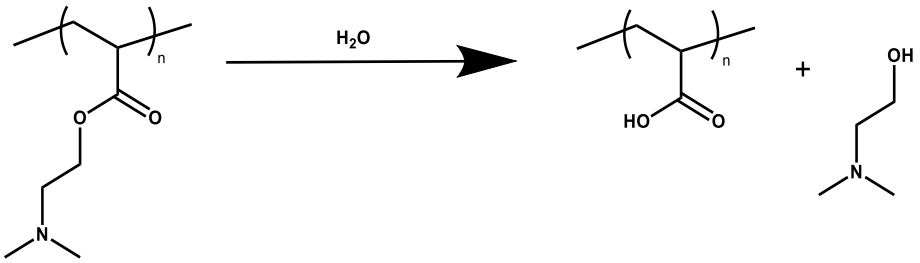

Scheme 1.6: Hydrolysis of pDMAEA

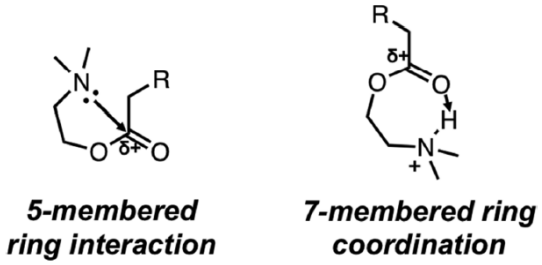

Figure 1.8: proposed interactions of dimetylamino substituent with the ester of pDMAEA under basic and acidic conditions by Ros *et al*.[142]

It is usually reported that in water at room temperature, there is a fast initial rate of hydrolysis and a slower rate reaching the plateau within a few days (around 5-10 days).[141, 143] Even though some studies[74, 143] have reported a pH-independent pDMAEA hydrolysis rate over a range of pH from 1 to 10, it has been demonstrated

recently by Ros *et al.* that it is in fact highly a pH-dependent mechanism, as shown in Figure 1.9.[142, 144] We can see that the initial rate of hydrolysis decreases dramatically between pH 13.3 and pH 3.9, with hydrolysis half-lives of about 14 min and 2.7 years, respectively (Figure 1.9b). This is consistent with a hydroxide-catalysed hydrolysis process. The initial hydrolysis rate reaches a minimum between pH 3 and 4, but increases again for strongly acidic conditions with a half-life of about 9 days at pH 0.31. After this fast initial period, the hydrolysis dramatically slows down and reach a plateau. The plateau of hydrolysis % at each pH corresponds approximately to a polymer chain with zero net charge. The reduction in hydrolysis rate can be explained by the change in electrostatic environment as reaction proceeds. The local environment is changing throughout hydrolysis with formation of the carboxylates, creating a polyampholyte. This can cause more electrostatic repulsion of the hydroxide anion, change in conformation and more hydrophobic environment. This is not a problem in the case of the acid-catalysed hydrolysis at pH 0.3 as no repulsion is expected.[142] At acidic pH at 70°C, the hydrolysis did not plateau and reached 88% after 8 days. However the experiment was not conducted further to prove it could reach full hydrolysis. In this study, they used solutions with strong buffer capacity and the pH was measured and adjusted after dissolution of the polymer. The earlier reports that showed no influence of pH were probably not adequately controlling the pH during dissolution and hydrolysis. With weak buffer capacity the solutions have similar pH, around 9 and results are in agreements with rates at pH 9 as shown in Figure 1.9a.

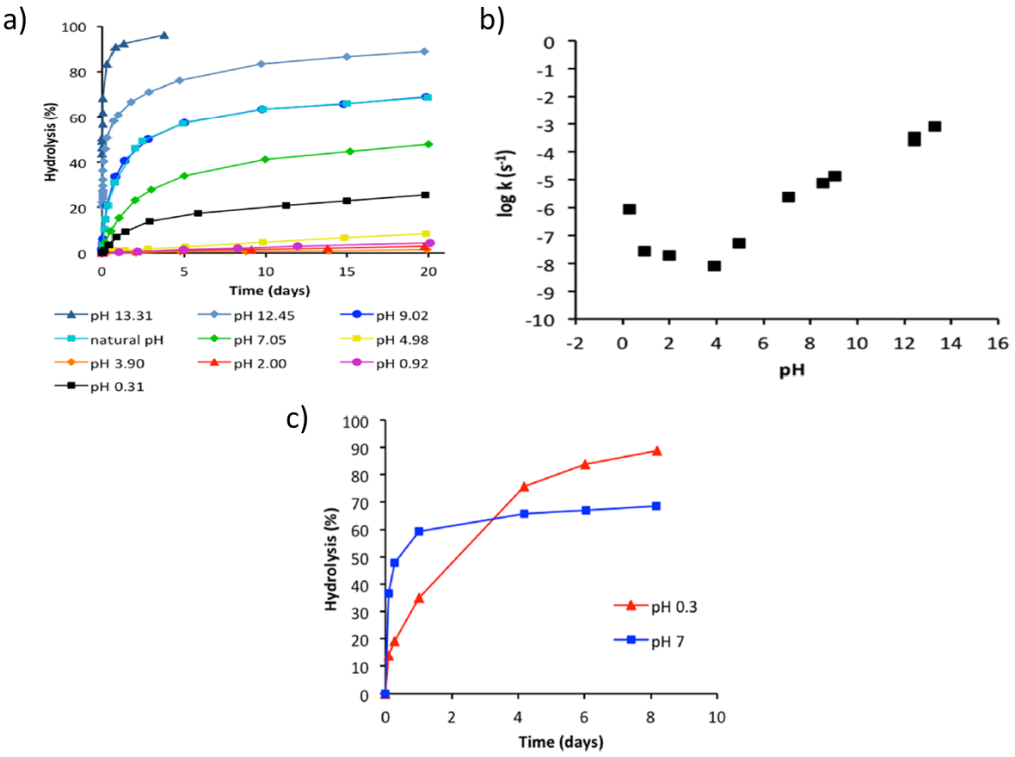

Figure 1.9: a) Hydrolysis of pDMAEA at pH from 0.31 to 13.31 at room temperature (22°C). Natural pH refers to a 0.5 wt % solution of pDMAEA (free-base form) in unbuffered D_2O b) Log k against pH plot for initial pseudo-first order rates ($k_{initial}$) of pDMAEA hydrolysis at room temperature (22°C) c) Hydrolysis of pDMAEA at pH 0.3 (acid-catalysed) and pH 7 (base-catalysed) at 70°C. Figure adapted from ref.[142]

1.3. Scope of this thesis

The aim of this work was to develop novel cationic polymers for the complexation of dsRNA, able to improve its stability in soil environment, and to control its release in order to induce RNAi in corn rootworms. Intact nucleic acid needs to be available for the pest to ingest, therefore its protection is essential to increase its viability. Hydrolysable DMAEA-based polymers have shown to be interesting materials for this application as they are able to complex dsRNA and release it over time thanks to their hydrolysis, making free dsRNA available for corn rootworms.[75, 77] However, the hydrolysis and release of the dsRNA with linear homopolymers of DMAEA are very fast, thus leading to poor soil stability of the nucleic acids. The aim was to protect the dsRNA long enough so farmers do not have to spray their fields too often. In chapter 3, pDMAEA 4-arm stars of various molecular weights made by RAFT were studied as controls, to compare their performance to new materials synthesised (**Chapter 3**) and used for complexation of dsRNA and pDNA (**Chapter 4**). First, the influence of the composition on the hydrolysis and control release of dsRNA was investigated by incorporating a non-hydrolysable comonomers, 2-dimethylaminoethyl methacrylate (DMAEMA) at different ratios. The influence of the architecture was also investigated with dense and compact star copolymers of DMAEA and DMAEMA made by the arm-first approach. The materials were synthesised using RAFT polymerisation and characterised for dsRNA complexation using agarose gel electrophoresis and ethidium bromide displacement assays as described in the next chapters. The stability of the polyplexes in soil was assessed by incubating them in soil for up to 28 days. Heparin displacement assays can be performed to simulate the impact of the presence of competing species on the binding and nucleases assays to test the ability of the cationic polymers to protect the dsRNA against degrading species.

1.4. References

1. Flood, J., The importance of plant health to food security. *Food sec.* **2010,** *2* (3), 215-231.

2. Douglas, A., Strategies for enhanced crop resistance to insect pests. *Annu. Rev. Plant Biol.* **2018,** *69*, 637-660.

3. Liu, S.; Jaouannet, M.; Dempsey, D. M. A.; Imani, J.; Coustau, C.; Kogel, K.-H. J. B. a., RNA-based technologies for insect control in plant production. *Biotechnol. Adv.* **2019**, 107463.

4. Elzen, G. W.; Hardee, D. D. J. P. M. S. f. P. S., United States Department of Agriculture-Agricultural Research Service research on managing insect resistance to insecticides. *Pest Manage. Sci.* **2003,** *59* (6-7), 770-776.

5. Vogel, E.; Santos, D.; Mingels, L.; Verdonckt, T.-W.; Broeck, J. V., RNA Interference in Insects: Protecting Beneficials and Controlling Pests. *Front. Physiol.* **2019,** *9*, 1912.

6. Fire, A.; Xu, S.; Montgomery, M. K.; Kostas, S. A.; Driver, S. E.; Mello, C. C., Potent and specific genetic interference by double-stranded RNA in Caenorhabditis elegans. *Nature* **1998,** *391* (6669), 806-811.

7. Spit, J.; Philips, A.; Wynant, N.; Santos, D.; Plaetinck, G.; Broeck, J. V. J. I. b.; biology, m., Knockdown of nuclease activity in the gut enhances RNAi efficiency in the Colorado potato beetle, Leptinotarsa decemlineata, but not in the desert locust, Schistocerca gregaria. *Insect Biochem. Mol. Biol.* **2017,** *81*, 103-116.

8. Shukla, J. N.; Kalsi, M.; Sethi, A.; Narva, K. E.; Fishilevich, E.; Singh, S.; Mogilicherla, K.; Palli, S. R., Reduced stability and intracellular transport of dsRNA contribute to poor RNAi response in lepidopteran insects. *RNA Biology* **2016,** *13* (7), 656-669.

9. Baum, J. A.; Bogaert, T.; Clinton, W.; Heck, G. R.; Feldmann, P.; Ilagan, O.; Johnson, S.; Plaetinck, G.; Munyikwa, T.; Pleau, M.; Vaughn, T.; Roberts, J., Control of coleopteran insect pests through RNA interference. *Nat. Biotechnol.* **2007,** *25* (11), 1322-1326.

10. Gordon, K. H. J.; Waterhouse, P. M., RNAi for insect-proof plants. *Nat. Biotechnol.* **2007,** *25* (11), 1231-1232.

11. Kaczmarek, J. C.; Kowalski, P. S.; Anderson, D. G., Advances in the delivery of RNA therapeutics: from concept to clinical reality. *Genome Med.* **2017,** *9* (1), 60.

12. Kunte, N.; McGraw, E.; Bell, S.; Held, D.; Avila, L.-A., Prospects, challenges and current status of RNAi through insect feeding. *Pest. Manag. Sci* **2020,** *76* (1), 26-41.

13. Dias, N. P.; Cagliari, D.; dos Santos, E. A.; Smagghe, G.; Jurat-Fuentes, J. L.; Mishra, S.; Nava, D. E.; Zotti, M. J., Insecticidal Gene Silencing by RNAi in the Neotropical Region. *Neotrop. Entomol.* **2020,** *49* (1), 1-11.

14. Gillet, F.-X.; Garcia, R. A.; Macedo, L. L. P.; Albuquerque, E. V. S.; Silva, M. C. M.; Grossi-de-Sa, M. F., Investigating Engineered Ribonucleoprotein Particles to Improve Oral RNAi Delivery in Crop Insect Pests. *Front. Physiol.* **2017,** *8*, 256.

15. Yan, S.; Qian, J.; Cai, C.; Ma, Z.; Li, J.; Yin, M.; Ren, B.; Shen, J., Spray method application of transdermal dsRNA delivery system for efficient gene silencing and pest control on soybean aphid Aphis glycines. *J. Pest Sci.* **2020,** *93* (1), 449-459.

16. Zheng, Y.; Hu, Y.; Yan, S.; Zhou, H.; Song, D.; Yin, M.; Shen, J., A polymer/detergent formulation improves dsRNA penetration through the body wall and RNAi-induced mortality in the soybean aphid Aphis glycines. *Pest Manage. Sci.* **2019,** *75* (7), 1993-1999.

17. Christiaens, O.; Swevers, L.; Smagghe, G., DsRNA degradation in the pea aphid (Acyrthosiphon pisum) associated with lack of response in RNAi feeding and injection assay. *Peptides* **2014,** *53*, 307-314.

18. Guan, R.-B.; Li, H.-C.; Fan, Y.-J.; Hu, S.-R.; Christiaens, O.; Smagghe, G.; Miao, X.-X., A nuclease specific to lepidopteran insects suppresses RNAi. *J. Biol. Chem.* **2018,** *293* (16), 6011-6021.

19. Das, S.; Debnath, N.; Cui, Y.; Unrine, J.; Palli, S. R., Chitosan, Carbon Quantum Dot, and Silica Nanoparticle Mediated dsRNA Delivery for Gene Silencing in Aedes aegypti: A Comparative Analysis. *ACS Appl. Mater. Interfaces* **2015,** *7* (35), 19530-19535.

20. Yan, S.; Ren, B.; Zeng, B.; Shen, J., Improving RNAi efficiency for pest control in crop species. *BioTechniques* **2020**.

21. Kanasty, R.; Dorkin, J. R.; Vegas, A.; Anderson, D., Delivery materials for siRNA therapeutics. *Nat. Mater* **2013,** *12* (11), 967.

22. Cooper, A. M. W.; Silver, K.; Zhang, J.; Park, Y.; Zhu, K. Y., Molecular mechanisms influencing efficiency of RNA interference in insects. *Pest Manage. Sci.* **2019,** *75* (1), 18-28.

23. Zotti, M. J.; Smagghe, G., RNAi Technology for Insect Management and Protection of Beneficial Insects from Diseases: Lessons, Challenges and Risk Assessments. *Neotrop. Entomol.* **2015,** *44* (3), 197-213.

24. Sugahara, R.; Tanaka, S.; Shiotsuki, T., RNAi-mediated knockdown of SPOOK reduces ecdysteroid titers and causes precocious metamorphosis in the desert locust Schistocerca gregaria. *Dev. Biol.* **2017,** *429* (1), 71-80.

25. Majidiani, S.; PourAbad, R. F.; Laudani, F.; Campolo, O.; Zappalà, L.; Rahmani, S.; Mohammadi, S. A.; Palmeri, V., RNAi in Tuta absoluta management: effects of injection and root delivery of dsRNAs. *J. Pest Sci.* **2019,** *92* (4), 1409-1419.

26. Cagliari, D.; Dias, N. P.; Galdeano, D. M.; dos Santos, E. Á.; Smagghe, G.; Zotti, M. J., Management of Pest Insects and Plant Diseases by Non-Transformative RNAi. *Front Plant Sci* **2019,** *10*, 1319.

27. Zhao, Y.; Sui, X.; Xu, L.; Liu, G.; Lu, L.; You, M.; Xie, C.; Li, B.; Ni, Z.; Liang, R., Plant-mediated RNAi of grain aphid CHS1 gene confers common wheat resistance against aphids. *Pest Manage. Sci.* **2018,** *74* (12), 2754-2760.

28. Guo, W.; Bai, C.; Wang, Z.; Wang, P.; Fan, Q.; Mi, X.; Wang, L.; He, J.; Pang, J.; Luo, X.; Fu, W.; Tian, Y.; Si, H.; Zhang, G.; Wu, J., Double-Stranded RNAs High-Efficiently Protect Transgenic Potato from Leptinotarsa decemlineata by Disrupting Juvenile Hormone Biosynthesis. *J. Agric. Food. Chem.* **2018,** *66* (45), 11990-11999.

29. Head, G. P.; Carroll, M. W.; Evans, S. P.; Rule, D. M.; Willse, A. R.; Clark, T. L.; Storer, N. P.; Flannagan, R. D.; Samuel, L. W.; Meinke, L. J., Evaluation of SmartStax and SmartStax PRO maize against western corn rootworm and northern corn rootworm: efficacy and resistance management. *Pest Manage. Sci.* **2017,** *73* (9), 1883-1899.

30. Bolognesi, R.; Ramaseshadri, P.; Anderson, J.; Bachman, P.; Clinton, W.; Flannagan, R.; Ilagan, O.; Lawrence, C.; Levine, S.; Moar, W.; Mueller, G.; Tan, J.; Uffman, J.; Wiggins, E.; Heck, G.; Segers, G., Characterizing the mechanism of action of double-stranded RNA activity against western corn rootworm (Diabrotica virgifera virgifera LeConte). *PLoS One* **2012,** *7* (10), e47534-e47534.

31. Zhang, J.; Khan, S. A.; Heckel, D. G.; Bock, R., Next-Generation Insect-Resistant Plants: RNAi-Mediated Crop Protection. *Trends Biotechnol.* **2017,** *35* (9), 871-882.

32. Zha, W.; Peng, X.; Chen, R.; Du, B.; Zhu, L.; He, G., Knockdown of midgut genes by dsRNA-transgenic plant-mediated RNA interference in the hemipteran insect Nilaparvata lugens. *PLoS One* **2011,** *6* (5), e20504-e20504.

33. San Miguel, K.; Scott, J. G., The next generation of insecticides: dsRNA is stable as a foliar-applied insecticide. *Pest Manage. Sci.* **2016,** *72* (4), 801-809.

34. Mitter, N.; Worrall, E. A.; Robinson, K. E.; Li, P.; Jain, R. G.; Taochy, C.; Fletcher, S. J.; Carroll, B. J.; Lu, G. Q.; Xu, Z. P., Clay nanosheets for topical delivery of RNAi for sustained protection against plant viruses. *Nature Plants* **2017,** *3* (2), 16207.

35. Zhu, F.; Xu, J.; Palli, R.; Ferguson, J.; Palli, S. R., Ingested RNA interference for managing the populations of the Colorado potato beetle, Leptinotarsa decemlineata. *Pest Manage. Sci.* **2011,** *67* (2), 175-182.

36. Christiaens, O.; Tardajos, M. G.; Martinez Reyna, Z. L.; Dash, M.; Dubruel, P.; Smagghe, G., Increased RNAi Efficacy in Spodoptera exigua via the Formulation of dsRNA With Guanylated Polymers. *Front. Physiol.* **2018,** *9*, 316.

37. Castellanos, N. L.; Smagghe, G.; Sharma, R.; Oliveira, E. E.; Christiaens, O., Liposome encapsulation and EDTA formulation of dsRNA targeting essential genes increase oral RNAi-caused mortality in the Neotropical stink bug Euschistus heros. *Pest Manage. Sci.* **2019,** *75* (2), 537-548.

38. Lin, Y.-H.; Huang, J.-H.; Liu, Y.; Belles, X.; Lee, H.-J., Oral delivery of dsRNA lipoplexes to German cockroach protects dsRNA from degradation and induces RNAi response. *Pest Manage. Sci.* **2017,** *73* (5), 960-966.

39. He, B.; Chu, Y.; Yin, M.; Müllen, K.; An, C.; Shen, J., Fluorescent Nanoparticle Delivered dsRNA Toward Genetic Control of Insect Pests. *Adv. Mater.* **2013,** *25* (33), 4580-4584.

40. Thairu, M. W.; Skidmore, I. H.; Bansal, R.; Nováková, E.; Hansen, T. E.; Li-Byarlay, H.; Wickline, S. A.; Hansen, A. K., Efficacy of RNA interference knockdown using aerosolized short interfering RNAs bound to nanoparticles in three diverse aphid species. *Insect Mol. Biol.* **2017,** *26* (3), 356-368.

41. Joga, M. R.; Zotti, M. J.; Smagghe, G.; Christiaens, O., RNAi Efficiency, Systemic Properties, and Novel Delivery Methods for Pest Insect Control: What We Know So Far. *Front. Physiol.* **2016,** *7*, 553.

42. Dubelman, S.; Fischer, J.; Zapata, F.; Huizinga, K.; Jiang, C.; Uffman, J.; Levine, S.; Carson, D., Environmental fate of double-stranded RNA in agricultural soils. *PLoS One* **2014,** *9* (3), e93155-e93155.

43. Fischer, J. R.; Zapata, F.; Dubelman, S.; Mueller, G. M.; Jensen, P. D.; Levine, S. L., Characterizing a novel and sensitive method to measure dsRNA in soil. *Chemosphere* **2016,** *161*, 319-324.

44. Bachman, P.; Fischer, J.; Song, Z.; Urbanczyk-Wochniak, E.; Watson, G., Environmental Fate and Dissipation of Applied dsRNA in Soil, Aquatic Systems, and Plants. *Front Plant Sci* **2020,** *11*, 21-21.

45. Song, H.; Fan, Y.; Zhang, J.; Cooper, A. M. W.; Silver, K.; Li, D.; Li, T.; Ma, E.; Zhu, K. Y.; Zhang, J., Contributions of dsRNases to differential RNAi efficiencies between the injection and oral delivery of dsRNA in Locusta migratoria. *Pest Manage. Sci.* **2019,** *75* (6), 1707-1717.

46. Song, H.; Zhang, J.; Li, D.; Cooper, A. M. W.; Silver, K.; Li, T.; Liu, X.; Ma, E.; Zhu, K. Y.; Zhang, J., A double-stranded RNA degrading enzyme reduces the efficiency of oral RNA interference in migratory locust. *Insect Biochem. Mol. Biol.* **2017,** *86*, 68-80.

47. Peng, Y.; Wang, K.; Fu, W.; Sheng, C.; Han, Z., Biochemical Comparison of dsRNA Degrading Nucleases in Four Different Insects. *Front. Physiol.* **2018,** *9*, 624.

48. Rivera-Vega, L. J.; Acevedo, F. E.; Felton, G. W., Genomics of Lepidoptera saliva reveals function in herbivory. *Curr. Opin. Insect. Sci.* **2017,** *19*, 61-69.

49. Garbutt, J. S.; Bellés, X.; Richards, E. H.; Reynolds, S. E., Persistence of double-stranded RNA in insect hemolymph as a potential determiner of RNA interference success: Evidence from Manduca sexta and Blattella germanica. *J. Insect Physiol.* **2013,** *59* (2), 171-178.

50. Barra, G. B.; Santa Rita, T. H.; Vasques, J. d. A.; Chianca, C. F.; Nery, L. F. A.; Costa, S. S. S., EDTA-mediated inhibition of DNases protects circulating cell-free DNA from ex vivo degradation in blood samples. *Clin. Biochem.* **2015,** *48* (15), 976-981.

51. Parsons, K. H.; Mondal, M. H.; McCormick, C. L.; Flynt, A. S., Guanidinium-Functionalized Interpolyelectrolyte Complexes Enabling RNAi in Resistant Insect Pests. *Biomacromolecules* **2018,** *19* (4), 1111-1117.

52. Hegedus, D.; Erlandson, M.; Gillott, C.; Toprak, U., New Insights into Peritrophic Matrix Synthesis, Architecture, and Function. *Annu. Rev. Entomol.* **2008,** *54* (1), 285-302.

53. Baia-da-Silva, D. C.; Alvarez, L. C. S.; Lizcano, O. V.; Costa, F. T. M.; Lopes, S. C. P.; Orfanó, A. S.; Pascoal, D. O.; Nacif-Pimenta, R.; Rodriguez, I. C.; Guerra, M. d. G. V. B.; Lacerda, M. V. G.; Secundino, N. F. C.; Monteiro, W. M.; Pimenta, P. F. P., The role of the peritrophic matrix and red blood cell concentration in Plasmodium vivax infection of Anopheles aquasalis. *Parasites & Vectors* **2018,** *11* (1), 148.

54. Huvenne, H.; Smagghe, G., Mechanisms of dsRNA uptake in insects and potential of RNAi for pest control: a review. *J. Insect Physiol.* **2010,** *56* (3), 227-235.

55. Lim, Z. X.; Robinson, K. E.; Jain, R. G.; Sharath Chandra, G.; Asokan, R.; Asgari, S.; Mitter, N., Diet-delivered RNAi in Helicoverpa armigera – Progresses and challenges. *J. Insect Physiol.* **2016,** *85*, 86-93.

56. Cappelle, K.; de Oliveira, C. F. R.; Van Eynde, B.; Christiaens, O.; Smagghe, G., The involvement of clathrin-mediated endocytosis and two Sid-1-like transmembrane proteins in double-stranded RNA uptake in the Colorado potato beetle midgut. *Insect Mol. Biol.* **2016,** *25* (3), 315-323.

57. Pinheiro, D. H.; Vélez, A. M.; Fishilevich, E.; Wang, H.; Carneiro, N. P.; Valencia-Jiménez, A.; Valicente, F. H.; Narva, K. E.; Siegfried, B. D., Clathrin-dependent endocytosis is associated with RNAi response in the western corn rootworm, Diabrotica virgifera virgifera LeConte. *PLoS One* **2018,** *13* (8), e0201849.

58. Saleh, M.-C.; van Rij, R. P.; Hekele, A.; Gillis, A.; Foley, E.; O'Farrell, P. H.; Andino, R., The endocytic pathway mediates cell entry of dsRNA to induce RNAi silencing. *Nat. Cell Biol.* **2006,** *8* (8), 793-802.

59. Yoon, J.-S.; Gurusamy, D.; Palli, S. R., Accumulation of dsRNA in endosomes contributes to inefficient RNA interference in the fall armyworm, Spodoptera frugiperda. *Insect Biochem. Mol. Biol.* **2017,** *90*, 53-60.

60. Selby, L. I.; Cortez-Jugo, C. M.; Such, G. K.; Johnston, A. P. R., Nanoescapology: progress toward understanding the endosomal escape of polymeric nanoparticles. *WIREs Nanomed Nanobiotechnol.* **2017,** *9* (5), e1452.

61. Benjaminsen, R. V.; Mattebjerg, M. A.; Henriksen, J. R.; Moghimi, S. M.; Andresen, T. L., The Possible "Proton Sponge " Effect of Polyethylenimine (PEI) Does Not Include Change in Lysosomal pH. *Mol. Ther.* **2013,** *21* (1), 149-157.

62. Akinc, A.; Thomas, M.; Klibanov, A. M.; Langer, R., Exploring polyethylenimine-mediated DNA transfection and the proton sponge hypothesis. *J. Gene Med.* **2005,** *7* (5), 657-663.

63. Taning, C. N. T.; Christiaens, O.; Berkvens, N.; Casteels, H.; Maes, M.; Smagghe, G., Oral RNAi to control Drosophila suzukii: laboratory testing against larval and adult stages. *J. Pest Sci.* **2016,** *89* (3), 803-814.

64. Tariq, K.; Ali, A.; Davies, T. G. E.; Naz, E.; Naz, L.; Sohail, S.; Hou, M.; Ullah, F., RNA interference-mediated knockdown of voltage-gated sodium channel (MpNav) gene causes mortality in peach-potato aphid, Myzus persicae. *Scientific Reports* **2019,** *9* (1), 5291.

65. Sugahara, R.; Tanaka, S.; Jouraku, A.; Shiotsuki, T., Geographic variation in RNAi sensitivity in the migratory locust. *Gene* **2017,** *605*, 5-11.

66. Zhang, X.; Zhang, J.; Zhu, K. Y., Chitosan/double-stranded RNA nanoparticle-mediated RNA interference to silence chitin synthase genes through larval feeding in the African malaria mosquito (Anopheles gambiae). *Insect Mol. Biol.* **2010,** *19* (5), 683-693.

67. Au - Zhang, X.; Au - Mysore, K.; Au - Flannery, E.; Au - Michel, K.; Au - Severson, D. W.; Au - Zhu, K. Y.; Au - Duman-Scheel, M., Chitosan/Interfering RNA Nanoparticle Mediated Gene Silencing in Disease Vector Mosquito Larvae. *JoVE* **2015,** (97), e52523.

68. Mysore, K.; Flannery, E. M.; Tomchaney, M.; Severson, D. W.; Duman-Scheel, M., Disruption of Aedes aegypti olfactory system development through chitosan/siRNA nanoparticle targeting of semaphorin-1a. *PLoS Negl Trop Dis* **2013,** *7* (5), e2215-e2215.

69. Li, J.; Qian, J.; Xu, Y.; Yan, S.; Shen, J.; Yin, M., A Facile-Synthesized Star Polycation Constructed as a Highly Efficient Gene Vector in Pest Management. *ACS Sustain. Chem. Eng.* **2019,** *7* (6), 6316-6322.

70. Avila, L. A.; Chandrasekar, R.; Wilkinson, K. E.; Balthazor, J.; Heerman, M.; Bechard, J.; Brown, S.; Park, Y.; Dhar, S.; Reeck, G. R.; Tomich, J. M., Delivery of lethal dsRNAs in insect diets by branched amphiphilic peptide capsules. *J. Controlled Release* **2018,** *273*, 139-146.

71. Whyard, S.; Singh, A. D.; Wong, S., Ingested double-stranded RNAs can act as species-specific insecticides. *Insect Biochem. Mol. Biol.* **2009,** *39* (11), 824-832.

72. Moghimi, S. M.; Symonds, P.; Murray, J. C.; Hunter, A. C.; Debska, G.; Szewczyk, A., A two-stage poly (ethylenimine)-mediated cytotoxicity: implications for gene transfer/therapy. *Mol. Ther.* **2005,** *11* (6), 990-995.

73. Bauer, M.; Tauhardt, L.; Lambermont-Thijs, H. M. L.; Kempe, K.; Hoogenboom, R.; Schubert, U. S.; Fischer, D., Rethinking the impact of the protonable amine density on cationic polymers for gene delivery: A comparative study of partially hydrolyzed poly(2-ethyl-2-oxazoline)s and linear poly(ethylene imine)s. *Eur. J. Pharm. Biopharm.* **2018,** *133*, 112-121.

74. Whitfield, R.; Anastasaki, A.; Truong, N. P.; Wilson, P.; Kempe, K.; Burns, J. A.; Davis, T. P.; Haddleton, D. M., Well-defined PDMAEA stars via Cu (0)-mediated reversible deactivation radical polymerization. *Macromolecules* **2016,** *49* (23), 8914-8924.

75. Whitfield, R.; Anastasaki, A.; Truong, N. P.; Cook, A. B.; Omedes-Pujol, M.; Loczenski Rose, V.; Nguyen, T. A.; Burns, J. A.; Perrier, S. b.; Davis, T. P., Efficient Binding, Protection, and Self-Release of dsRNA in Soil by Linear and Star Cationic Polymers. *ACS Macro Lett.* **2018,** *7*, 909-915.

76. Cook, A. Highly branched and hyperbranched polymers : synthesis, characterisation, and application in nucleic acid delivery. University of Warwick, 2018.

77. Cook, A.; Peltier, R.; Hartlieb, M.; Whitfield, R.; Moriceau, G.; Burns, J.; Haddleton, D.; Perrier, S., Cationic and hydrolysable branched polymers by RAFT for complexation and controlled release of dsRNA. *Polym. Chem.* **2018**.

78. Funhoff, A. M.; van Nostrum, C. F.; Lok, M. C.; Fretz, M. M.; Crommelin, D. J. A.; Hennink, W. E., Poly(3-guanidinopropyl methacrylate): A Novel Cationic Polymer for Gene Delivery. *Bioconjugate Chem.* **2004,** *15* (6), 1212-1220.

79. Al-Dosari, M. S.; Gao, X., Nonviral Gene Delivery: Principle, Limitations, and Recent Progress. *The AAPS Journal* **2009,** *11* (4), 671.

80. Zhi, D.; Bai, Y.; Yang, J.; Cui, S.; Zhao, Y.; Chen, H.; Zhang, S., A review on cationic lipids with different linkers for gene delivery. *Adv. Colloid Interface Sci.* **2018,** *253*, 117-140.

81. Junquera, E.; Aicart, E., Recent progress in gene therapy to deliver nucleic acids with multivalent cationic vectors. *Adv. Colloid Interface Sci.* **2016,** *233*, 161-175.

82. Donna T. Ward, J. R. Method and composition for treating insects. 2019.

83. Kun Yan Zhu, X. Z., Jianzhen Zhang Double-stranded RNA-based nanoparticles for gene silencing. 2014.

84. Pedro Coelho, C. W. Improved insect control strategies utilizing pheromones and RNAi. 2017.

85. Mat Jalaluddin, N. S.; Othman, R. Y.; Harikrishna, J. A., Global trends in research and commercialization of exogenous and endogenous RNAi technologies for crops. *Crit. Rev. Biotechnol.* **2019,** *39* (1), 67-78.

86. Truong, N. P.; Gu, W.; Prasadam, I.; Jia, Z.; Crawford, R.; Xiao, Y.; Monteiro, M. J., An influenza virus-inspired polymer system for the timed release of siRNA. *Nat. Commun.* **2013,** *4*, 1902.

87. Truong, N. P.; Jia, Z.; Burgess, M.; Payne, L.; McMillan, N. A.; Monteiro, M. J., Self-catalyzed degradable cationic polymer for release of DNA. *Biomacromolecules* **2011,** *12* (10), 3540-3548.

88. Liao, X.; Walden, G.; Falcon, N. D.; Donell, S.; Raxworthy, M. J.; Wormstone, M.; Riley, G. P.; Saeed, A., A direct comparison of linear and star-shaped poly (dimethylaminoethyl acrylate) polymers for polyplexation with DNA and cytotoxicity in cultured cell lines. *Eur. Polym. J.* **2017,** *87*, 458-467.

89. Moad, G.; Solomon, D. H., *The chemistry of radical polymerization*. Elsevier: 2006.

90. Aubrey, D. J.; Richard, G. J.; Graeme, M., Terminology for reversible-deactivation radical polymerization previously called "controlled" radical or "living" radical polymerization (IUPAC Recommendations 2010). *Pure Appl. Chem.* **2009,** *82* (2), 483-491.

91. Matyjaszewski, K.; Tsarevsky, N. V., Macromolecular Engineering by Atom Transfer Radical Polymerization. *J. Am. Chem. Soc.* **2014,** *136* (18), 6513-6533.

92. Gregory, A.; Stenzel, M. H., Complex polymer architectures via RAFT polymerization: From fundamental process to extending the scope using click chemistry and nature's building blocks. *Prog. Polym. Sci.* **2012,** *37* (1), 38-105.

93. Destarac, M., Industrial development of reversible-deactivation radical polymerization: is the induction period over? *Polym. Chem.* **2018,** *9* (40), 4947-4967.

94. Barner-Kowollik, C., *Handbook of RAFT polymerization*. John Wiley & Sons: 2008.

95. Corrigan, N.; Jung, K.; Moad, G.; Hawker, C. J.; Matyjaszewski, K.; Boyer, C., Reversible-deactivation radical polymerization (Controlled/living radical polymerization): From discovery to materials design and applications. *Prog. Polym. Sci.* **2020,** *111*, 101311.

96. Stenzel, M. H.; Barner-Kowollik, C., The living dead – common misconceptions about reversible deactivation radical polymerization. *Materials Horizons* **2016,** *3* (6), 471-477.

97. Hawker, C. J.; Bosman, A. W.; Harth, E., New Polymer Synthesis by Nitroxide Mediated Living Radical Polymerizations. *Chem. Rev.* **2001,** *101* (12), 3661-3688.

98. Perrier, S. b., 50th Anniversary Perspective: RAFT Polymerization・A User Guide. *Macromolecules* **2017,** *50* (19), 7433-7447.

99. Nicolas, J.; Guillaneuf, Y.; Lefay, C.; Bertin, D.; Gigmes, D.; Charleux, B., Nitroxide-mediated polymerization. *Prog. Polym. Sci.* **2013,** *38* (1), 63-235.

100. Grubbs, R. B., Nitroxide-Mediated Radical Polymerization: Limitations and Versatility. *Polym. Rev.* **2011,** *51* (2), 104-137.

101. Matyjaszewski, K.; Xia, J., Atom Transfer Radical Polymerization. *Chem. Rev.* **2001,** *101* (9), 2921-2990.

102. Pintauer, T.; Matyjaszewski, K., Structural aspects of copper catalyzed atom transfer radical polymerization. *Coord. Chem. Rev.* **2005,** *249* (11), 1155-1184.

103. Wang, J.-S.; Matyjaszewski, K., Controlled/"living" radical polymerization. atom transfer radical polymerization in the presence of transition-metal complexes. *J. Am. Chem. Soc.* **1995,** *117* (20), 5614-5615.

104. Pintauer, T.; Matyjaszewski, K., Atom transfer radical addition and polymerization reactions catalyzed by ppm amounts of copper complexes. *Chem. Soc. Rev.* **2008,** *37* (6), 1087-1097.

105. Matyjaszewski, K.; Jakubowski, W.; Min, K.; Tang, W.; Huang, J.; Braunecker, W. A.; Tsarevsky, N. V., Diminishing catalyst concentration in atom transfer radical polymerization with reducing agents. *Proceedings of the National Academy of Sciences* **2006,** *103* (42), 15309.

106. Jakubowski, W.; Matyjaszewski, K., Activators Regenerated by Electron Transfer for Atom-Transfer Radical Polymerization of (Meth)acrylates and Related Block Copolymers. *Angew. Chem. Int. Ed.* **2006,** *45* (27), 4482-4486.

107. Konkolewicz, D.; Wang, Y.; Krys, P.; Zhong, M.; Isse, A. A.; Gennaro, A.; Matyjaszewski, K., SARA ATRP or SET-LRP. End of controversy? *Polym. Chem.* **2014,** *5* (15), 4396-4417.

108. Zhang, Y.; Wang, Y.; Peng, C.-h.; Zhong, M.; Zhu, W.; Konkolewicz, D.; Matyjaszewski, K., Copper-Mediated CRP of Methyl Acrylate in the Presence of Metallic Copper: Effect of Ligand Structure on Reaction Kinetics. *Macromolecules* **2012,** *45* (1), 78-86.

109. Rosen, B. M.; Jiang, X.; Wilson, C. J.; Nguyen, N. H.; Monteiro, M. J.; Percec, V., The disproportionation of Cu(I)X mediated by ligand and solvent into Cu(0) and Cu(II)X2 and its implications for SET-LRP. *J. Polym. Sci., Part A: Polym. Chem.* **2009,** *47* (21), 5606-5628.

110. Levere, M. E.; Nguyen, N. H.; Leng, X.; Percec, V., Visualization of the crucial step in SET-LRP. *Polym. Chem.* **2013,** *4* (5), 1635-1647.

111. Moad, G.; Rizzardo, E., A 20th anniversary perspective on the life of RAFT (RAFT coming of age). *Polym. Int.* **2020,** *69* (8), 658-661.

112. Chiefari, J.; Chong, Y. K.; Ercole, F.; Krstina, J.; Jeffery, J.; Le, T. P. T.; Mayadunne, R. T. A.; Meijs, G. F.; Moad, C. L.; Moad, G.; Rizzardo, E.; Thang, S. H., Living Free-Radical Polymerization by Reversible Addition−Fragmentation Chain Transfer: The RAFT Process. *Macromolecules* **1998,** *31* (16), 5559-5562.

113. Keddie, D. J.; Moad, G.; Rizzardo, E.; Thang, S. H., RAFT Agent Design and Synthesis. *Macromolecules* **2012,** *45* (13), 5321-5342.

114. Gody, G.; Maschmeyer, T.; Zetterlund, P. B.; Perrier, S., Pushing the Limit of the RAFT Process: Multiblock Copolymers by One-Pot Rapid Multiple Chain Extensions at Full Monomer Conversion. *Macromolecules* **2014,** *47* (10), 3451-3460.

115. Gody, G.; Maschmeyer, T.; Zetterlund, P. B.; Perrier, S., Rapid and quantitative one-pot synthesis of sequence-controlled polymers by radical polymerization. *Nat. Commun.* **2013,** *4* (1), 2505.

116. Yang, D. P.; Oo, M. N. N. L.; Deen, G. R.; Li, Z.; Loh, X. J., Nano-Star-Shaped Polymers for Drug Delivery Applications. *Macromol. Rapid Commun.* **2017,** *38* (21), 1700410.

117. Georgiou, T. K., Star polymers for gene delivery. *Polym. Int.* **2014,** *63* (7), 1130-1133.

118. Ren, J. M.; McKenzie, T. G.; Fu, Q.; Wong, E. H. H.; Xu, J.; An, Z.; Shanmugam, S.; Davis, T. P.; Boyer, C.; Qiao, G. G., Star Polymers. *Chem. Rev.* **2016,** *116* (12), 6743-6836.

119. Rohini Anandrao, P.; Aloorkar, N. H.; Kulkarni, A. S.; Ingale, D. J., Star Polymers: An Overview. *Int. J. Pharm. Sci. Nanotech* **2012,** *5* (2).

120. Barner-Kowollik, C.; Davis, T. P.; Stenzel, M. H., Synthesis of Star Polymers using RAFT Polymerization: What is Possible? *Aust. J. Chem.* **2006,** *59* (10), 719-727.

121. Allison-Logan, S.; Karimi, F.; Sun, Y.; McKenzie, T. G.; Nothling, M. D.; Bryant, G.; Qiao, G. G., Highly Living Stars via Core-First Photo-RAFT Polymerization: Exploitation for Ultra-High Molecular Weight Star Synthesis. *ACS Macro Lett.* **2019,** *8* (10), 1291-1295.

122. Bekhradnia, S.; Diget, J. S.; Zinn, T.; Zhu, K.; Sande, S. A.; Nyström, B.; Lund, R., Charged Star Diblock Copolymers in Dilute Solutions: Synthesis, Structure, and Chain Conformations. *Macromolecules* **2015,** *48* (8), 2637-2646.

123. Chen, Q.; Cao, X.; Xu, Y.; An, Z., Emerging Synthetic Strategies for Core Cross-Linked Star (CCS) Polymers and Applications as Interfacial Stabilizers: Bridging Linear Polymers and Nanoparticles. *Macromol. Rapid Commun.* **2013,** *34* (19), 1507-1517.

124. Gao, H.; Matyjaszewski, K., Structural Control in ATRP Synthesis of Star Polymers Using the Arm-First Method. *Macromolecules* **2006,** *39* (9), 3154-3160.

125. Blencowe, A.; Tan, J. F.; Goh, T. K.; Qiao, G. G., Core cross-linked star polymers via controlled radical polymerisation. *Polymer* **2009,** *50* (1), 5-32.

126. Bray, C.; Peltier, R.; Kim, H.; Mastrangelo, A.; Perrier, S., Anionic multiblock core cross-linked star copolymers via RAFT polymerization. *Polym. Chem.* **2017,** *8* (36), 5513-5524.

127. Ferreira, J.; Syrett, J.; Whittaker, M.; Haddleton, D.; Davis, T. P.; Boyer, C., Optimizing the generation of narrow polydispersity ‘arm-first’ star polymers made using RAFT polymerization. *Polym. Chem.* **2011,** *2* (8), 1671-1677.

128. Xiaoqi, Y.; Jianbo, L.; Tianbin, R., Synthesis of miktoarm star-shaped and inverse star-block copolymers by a combination of ring-opening polymerization and click chemistry. *e-Polymers* **2018,** *18* (6), 559-568.

129. Barner-Kowollik, C.; Du Prez, F. E.; Espeel, P.; Hawker, C. J.; Junkers, T.; Schlaad, H.; Van Camp, W., "Clicking" Polymers or Just Efficient Linking: What Is the Difference? *Angew. Chem. Int. Ed.* **2011,** *50* (1), 60-62.

130. Binder, W. H.; Sachsenhofer, R., 'Click' Chemistry in Polymer and Materials Science. *Macromol. Rapid Commun.* **2007,** *28* (1), 15-54.

131. Kolb, H. C.; Finn, M. G.; Sharpless, K. B., Click Chemistry: Diverse Chemical Function from a Few Good Reactions. *Angew. Chem. Int. Ed.* **2001,** *40* (11), 2004-2021.

132. Saunders, G.; MacCreath, B., Application compendium. *Agilent Technologie* **2010**.

133. Grubisic, Z.; Rempp, P.; Benoit, H., A universal calibration for gel permeation chromatography. *J. Polym. Sci., Part B: Polym. Phys.* **1996,** *34* (10), 1707-1713.

134. Eaton, P.; West, P., *Atomic force microscopy*. Oxford university press: 2010.

135. Yoshizaki, T.; Kanazawa, A.; Kanaoka, S.; Aoshima, S., Quantitative and Ultrafast Synthesis of Well-Defined Star-Shaped Poly(p-methoxystyrene) via One-Pot Living Cationic Polymerization. *Macromolecules* **2016,** *49* (1), 71-79.

136. Amamoto, Y.; Higaki, Y.; Matsuda, Y.; Otsuka, H.; Takahara, A., Programmed Thermodynamic Formation and Structure Analysis of Star-like Nanogels with Core Cross-linked by Thermally Exchangeable Dynamic Covalent Bonds. *J. Am. Chem. Soc.* **2007,** *129* (43), 13298-13304.

137. Burdyńska, J.; Li, Y.; Aggarwal, A. V.; Höger, S.; Sheiko, S. S.; Matyjaszewski, K., Synthesis and Arm Dissociation in Molecular Stars with a Spoked Wheel Core and Bottlebrush Arms. *J. Am. Chem. Soc.* **2014,** *136* (36), 12762-12770.

138. Schnablegger, H.; Singh, Y. J. A. A. P. G., The SAXS guide: getting acquainted with the principles. **2011**, 1-124.

139. Felberg, L. E.; Doshi, A.; Hura, G. L.; Sly, J.; Piunova, V. A.; Swope, W. C.; Rice, J. E.; Miller, R.; Head-Gordon, T., Structural transition of nanogel star polymers with pH by controlling PEGMA interactions with acid or base copolymers. *Mol. Phys.* **2016,** *114* (21), 3221-3231.

140. Moinard, D.; Taton, D.; Gnanou, Y.; Rochas, C.; Borsali, R., SAXS from Four-Arm Polyelectrolyte Stars in Semi-Dilute Solutions. *Macromol. Chem. Phys.* **2003,** *204* (1), 89-97.

141. McCool, M.; Senogles, E., The self-catalysed hydrolysis of poly (N, N-dimethylaminoethyl acrylate). *Eur. Polym. J.* **1989,** *25* (7-8), 857-860.

142. Ros, S.; Wang, J.; Burke, N. A. D.; Stöver, H. D. H., A Mechanistic Study of the Hydrolysis of Poly[N,N-(dimethylamino)ethyl acrylates] as Charge-Shifting Polycations. *Macromolecules* **2020,** *53* (9), 3514-3523.

143. Truong, N. P.; Jia, Z.; Burges, M.; McMillan, N. A.; Monteiro, M. J., Self-catalyzed degradation of linear cationic poly (2-dimethylaminoethyl acrylate) in water. *Biomacromolecules* **2011,** *12* (5), 1876-1882.

144. Ros, S.; Kleinberger, R. M.; Burke, N. A.; Rossi, N. A.; Stöver, H. D., Charge-Shifting Polycations with Tunable Rates of Hydrolysis: Effect of Backbone Substituents on Poly [2-(dimethylamino) ethyl acrylates]. *Macromolecules* **2018**.

Chapter 2: Method

2.1. Materials

Sodium Hydroxide (Sigma-Aldrich), agarose (Sigma-Aldrich), Tris-Borate-EDTA buffer (TBE), Gel loading dye purple (6X) (BioLabs), GelRed (Biotium), ethidium bromide (Sigma-Aldrich, 500 mg/mL), heparin (Sigma-Aldrich), TRI Reagent (Sigma-Aldrich), Polyvinylsulfonate solution (PVS, Sigma-Aldrich, 30 wt. % in water, technical grade), EGTA (Sigma-Aldrich, 97%), chloroform-d (Sigma-Aldrich, 99.8% D atom), sterile water molecular biology reagent (Sigma-Aldrich). DsRNA and soil were provided by Syngenta.

2.2. Analytical techniques

Gel permeation chromatography (GPC) was performed in DMF as eluent, an Agilent infinity II MDS instrument equipped with differential refractive index (DRI), viscometry (VS), dual angles light scattering (LS) and variable wavelength UV detectors was utilised. The system was equipped with 2 x PLgel Mixed D columns (300 x 7.5 mm) and PLgel 5 µm guard column. The eluent used was DMF with 5 mmol NH_4BF_4 additive. Samples were run at 1 mL/min at 50°C. Poly(methyl methacrylate) standards (Agilent EasyVials) were used for calibration between 955,000 – 550 $g.mol^{-1}$. Analyte samples were filtered through a nylon membrane with 0.22 μm pore size before injection. Respectively, experimental molar mass ($M_{n,SEC}$) and dispersity ($Đ$) values of synthesised polymers were determined by conventional calibration using Agilent GPC/SEC software (version A.02.01).

Proton nuclear magnetic resonance spectra (^{1}H NMR) were recorded on a Bruker Advance 300 or 400 (300 or 400 MHz) at 27°C using $CDCl_3$ or D_2O as solvents. Chemical shift values (δ) reported in ppm, and the residual proton signal of the solvent used as internal standard.

2.3. Agarose gel electrophoresis

Polyplexes were prepared at various N/P ratios by mixing the correct amount of polymer stock solution with 25 µL of a stock solution of dsRNA at 0.1 mg/mL for a total solution of 50 µL. Polyplexes were vortexed and incubated for 30 min. Prior to loading, 25 µL of loading dye was added to each sample. Agarose gel was prepared by heating agarose (2 g) dissolved in 200 mL of 10% TBE buffer in the microwave until complete dissolution. The solution was cooled down for 20 minutes and 22 µL of GelRed was added. The mixture was poured into the gel caster and combed was inserted. The gel was left to set for 25 minutes at room temperature. The agarose gel electrophoresis were run in 10% TBE buffer. 15 µL of polyplexes were loaded into the agarose gel wells. Gel electrophoresis was performed at 100 V for 30 minutes with dsRNA. The final gels were visualised under UV illumination.

2.4. Ethidium bromide displacement assay

DsRNA or pDNA (15 µg/mL) and ethidium bromide (1 µg/mL) were incubated for 10 minutes at room temperature. And 50 µL of this solution was transferred to a 96 wellplate containing polymers at different concentrations corresponding to the different N/P ratios. After 20 minutes incubation before measuring fluorescence intensity (λ_{Ex} = 525 nm, λ_{Em} = 605 nm) using Biotek instruments Citation 3 cell imaging multi-mode reader. The maximum fluorescence was defined with controls containing only dsRNA or pDNA with ethidium bromide.

2.5. Soil stability assay

Method 1:

200 µL of polyplexes (N/P 5) was added to 0.5 g of soil in a tube and the samples were incubated for 0, 1, 2, 3, 7, 10, 14, 21 and 28 days. 50 µL of a 10 mg/mL heparin solution was added to the sample and incubated for 2 minutes at room temperature. 1 mL of TRI Reagent was then added and the samples was vortexed well followed by a 5 min incubation. The sample was then stored at -20 ˚C. At the end of the 28 days, all samples were let to warm up to room temperature and 200 µL of chloroform was added. The samples were vortexed and incubated for 3 minutes at room temperature.

Samples were centrifuged for 15 minutes at 12 000 g. The supernatant (400 µL) was transferred into a new tube and isopropanol was added to precipitate the dsRNA. After 10 minutes incubation, the tubes were centrifuged for 10 minutes at 12 000 g. After removal of the supernatant, the pellet was washed twice with 500 µL of 70% ethanol and centrifuged 5 minutes at 12 000 g. After removal of the supernatant, the samples were centrifuged 1 minute at 12 000 g. The pellet was left to dry for 5 minutes and resuspended in 200 µL water. Agarose gel electrophoresis was used to visualise the results of the assay. 5 µL of the dsRNA solution was mixed with 5 µL water and 5 µL of loading dye.

Method 2:

200 µL of polyplexes (N/P 5) was added to 0.5 g of soil in a tube and the samples were incubated for 0, 1, 2, 3, 7, 10, 14, 21 and 28 days. The degradation reaction was stopped by freezing the samples (-20 °C). At the end of the 28 days, all samples were let to warm up to room temperature. 5 µL of 25% Polyvinylsulfonate (PVS) solution, 80 µL of 0.5 M EGTA solution and 315 µL of water are added in the tubes. After that the soil had been resuspended by mixing vigourously the tubes, the samples were centrifuged at 12 000 rpm for 15 min at room temperature. The supernatant was transferred into a new tube and 5 µL into a black 96-well plate with 100 µL of water and 20 µL of 200X GelRed. The plate was gently mixed on a thermos-mixer at 350 rpm for a few second and incubated in the dark for 10 min. The plate was read on a fluorescence plate reader (λ_{Ex} = 300 nm, λ_{Em} = 590 nm).

Chapter 3: PDMAEA 4-arm Stars by RAFT

3.1. Abstract

PDMAEA 4-arm stars made by Cu(0)-RDRP are reported in the literature to be able to delay the degradation in soil by up to two weeks compared to one week for the linear equivalent and to release the dsRNA and make it available for ingestion by the pest.[1] The potential of these structures was further studied here; four 4-arm stars with different molecular weights (7 500 – 15 700 g/mol) were synthesised using RAFT polymerisation. Stable polymers were obtained with high conversions (80 – 90 %) and no star-star coupling. All stars were able to efficiently complex the dsRNA as shown by the agarose gel electrophoresis results and ethidium bromide displacement assays. Little effect of the molecular weight was observed on complexation, with slightly more polymer needed to fully complex the dsRNA with the smaller star (N/P 2) compared to the higer molecular weight star (N/P 1). However, no prolonged protection of dsRNA was observed in the presence of dsRNases or in soil with any of the stars, due to the fast hydrolysis of the DMAEA side chains resulting in the fast release of the dsRNA. Therefore, the change in architecture was not enough to obtain a good protection of the nucleic acids.

3.2. Introduction

As seen in **chapter 1**, RNAi is an efficient tool to replace the classic broad-spectrum chemical pesticides by targeting specifically one or a range of pest species.[2] However, dsRNA is quickly degraded in the environment, especially in live soil.[3, 4] Nucleases, ions and the microbial community present in live soil are mainly responsible for the degradation of dsRNA. Therefore, the use of a vector to transport and protect the nucleic acids from the enzymes present in soil is essential.[5] Cationic polymers have shown to be efficient vectors to transport RNA and DNA by binding electrostatically to form a polyplex.[6] They are interesting for their ease of synthesis and production as well as good reproducibility, their low immunogenicity and their tuneable physical and chemical properties. Among cationic polymers, poly(2-dimethylaminoethyl acrylate) (pDMAEA) is a good candidate for the complexation of dsRNA, and its ability to hydrolyse to poly(acrylic acid) enables the release of the nucleic acids without any external trigger.[7, 8] However, the protection of dsRNA in soil environment is particularly challenging as many competing species (mainly ions) are present, thus inducing low stability of the complex. Whitfield *et al*. reported improved protection in soil with the use of pDMAEA polymers with a 4-arm star architecture (M_n= 6 200 g/mol, $Đ$=1.14) compared to a linear equivalent (M_n= 5 600 g/mol, $Đ$=1.18).[1] The stability of dsRNA in soil was improved and delayed to up to 2 weeks as shown in Figure 3.1 wherease the linear chain was only able to delay it to up to 7 days. In this work, the materials were synthesised using Cu(0)-mediated RDRP for its fast rate of reaction with low amount of catalyst required to obtain polymers with good control over molecular weight and dispersity. The polymerisation of DMAEA was stopped at low conversion in order to avoid side reactions leading to termination due to the high reactivity of the tertiary amine functionality and to keep the dispersity low, at around 1.1. When the reaction was left longer, a high molecular weight shoulder was observed, with dispersity increasing significantly. The polymerisation of DMAEA has always been reported to be problematic compared to other acrylate or similar monomers due to side reactions and chain transfer regardless of the technique used. The range of molecular weight is usually limited to a maximum of around 10 000 g/mol due to side reactions, with dispersities around 1.2 to 1.3 until very recently when Ros *et al*. reported the polymerisation of DMAEA using RAFT in

a mixture of dioxane and water at pH 3-4 resulting in a higher molecular weight polymer (M_n=31 200 g/mol, $Đ$=1.25). [8-12] However, reports on the synthesis of DMAEA-based polymers is still limited.

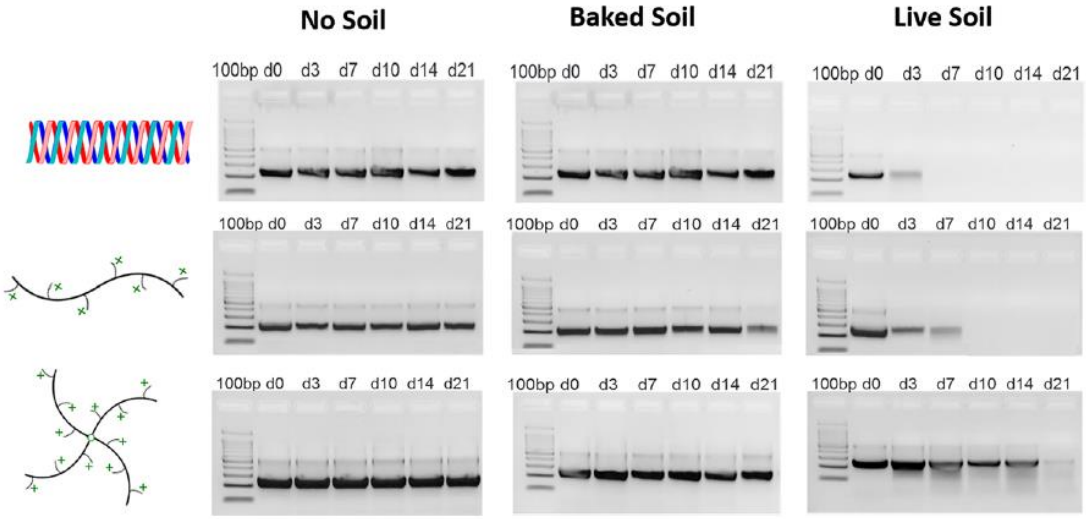

Figure 3.1: Evaluation of naked dsRNA, linear pDMAEA/dsRNA complex and star pDMAEA/dsRNA complex in no soil, baked soil and live soil. Samples were formed and incubated at room temperature for different time periods (d = day 0, 3, 7, 10, 14, 21). DsRNA was extracted from soil and samples loaded onto 2% w/v agarose gel (100 V, 30 min) for subsequent analysis. Figure adapted from ref.[1]

The promising results reported by Whitfield *et al*. were encouraging, thus, in this present chapter, we are looking at the potential of pDMAEA 4-arm star structures of different molecular weights (7 400 – 15 700 g/mol). The aim was to then investigate the design of new potential materials to improve complexation, control of the release of the dsRNA and stability of the polyplexes in live soil. In this work, the pDMAEA materials were reproduced using RAFT polymerisation to compare them with the materials reported in the next chapters. RAFT polymerisation was chosen for its high versatility toward a wide range of monomers[13] and the ability to reach higher monomer conversion and higher molecular weight for the synthesis of pDMAEA.[10, 14]

3.3. Results and discussion

3.3.1. Synthesis of 4 arms pDMAEA stars

In order to compare the new materials to the 4-arm stars synthesised previously by Cu(0) RDRP,[1] RAFT was used to synthesise similar stars with DMAEA. Four stars of molecular weight going from 7 400 to 15 700 g/mol by targeting DPs up to 80 were synthesised using the core-first approach.

A tetra functional (propanoic acid)yl butyl trithiocarbonate (PABTC) RAFT agent was synthesised since it controls of the polymerisation of acrylate monomers, including DMAEA. The tetra functional PABTC was synthesised by the esterification of pentaerythritol with 2-bromopropionyl bromide. The product was then reacted with the product of the reaction of butanethiol and carbone disulphide in acetone (Scheme 3.1). The resulting 4-arm CTA was purified by flash column chromatography to give a clean product as evidence by ^{1}H NMR (Figure A3.1) with 23% yield.

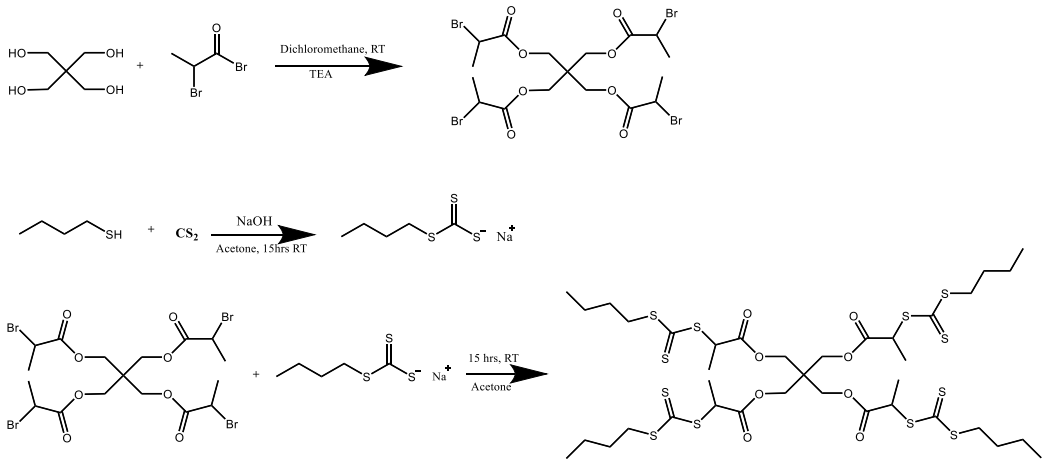

Scheme 3.1: Multifunctional RAFT agent synthesis

The 4-arms CTA was used to polymerise DMAEA in dioxane at various arm DPs from 13 to 80, by varying the ratio of monomer to CTA ([M]/[CTA]). The monomer concentration was kept low enough to avoid star-star coupling ([M]= 2 M). No initiator was used as the reaction was performed under blue light at room temperature. The blue light is able to fragment the CTA without the need of an external source of radical. The reaction was performed under blue light, which triggers the fragmentation of the CTA, and therefore avoid the use of a free radical initiator.[15-17] Moreover, this allows to work at lower temperatures, thus preventing termination and

chain transfer reaction. Polymers with higher conversion (89%) and slightly narrower dispersities (1.28) were obtained with blue light compared to thermal initiation (81%, $Đ$=1.35) for a targeted DP of 13. Conversions were determined by ^{1}H NMR spectroscopy by following the decrease of the peak corresponding to the vinyl protons of DMAEA at 5.5 ppm. Molecular weights were determinded by gel permeation chromatography (GPC) in DMF with PMMA calibration, using an RI detector.

The 4-arms star pDMAEA were obtained with conversions varying from 80% to 90% (Table 3.1). Increasing the DP seemed to increase the dispersity (up to 1.7) with more tailing at low molecular weight (Figure 3.2). Additionally, lower conversion was obtained for higher molecular weight. Compared to Cu(0)-mediated RDRP, polymers were obtained with higher dispersities.[18] However, RAFT allows the reaction to proceed to high conversion with no observation of major star-star coupling as evidenced by GPC results, no shoulder at high molecular weight could be observed. Yet, the limitation in molecular weight and higher dispersities can be observed at the higher targeted DPs due to side reaction and transfer to dimethylaminoethanol small molecules.

Table 3.1: 4-arm star pDMAEA. Conversion was determined by ^{1}H NMR and molar mass were determined by DMF-GPC with pMMA standards.

Polymer	**DP targetted**	**Conversion (%)**	$M_{n,th}$ **(g.mol^{-1})**	$M_{n,GPC}$ **(g.mol^{-1})**	$M_{w,GPC}$ **(g.mol^{-1})**	$Đ$
4-pDMAEA_11	13	89	7 500	7 400	9 500	1.28
4-pDMAEA_38	40	90	22 700	16 700	25 000	1.49
4-pDMAEA_47	50	90	28 100	15 500	24 100	1.59
4-pDMAEA_67	80	80	44 500	15 700	26 800	1.71

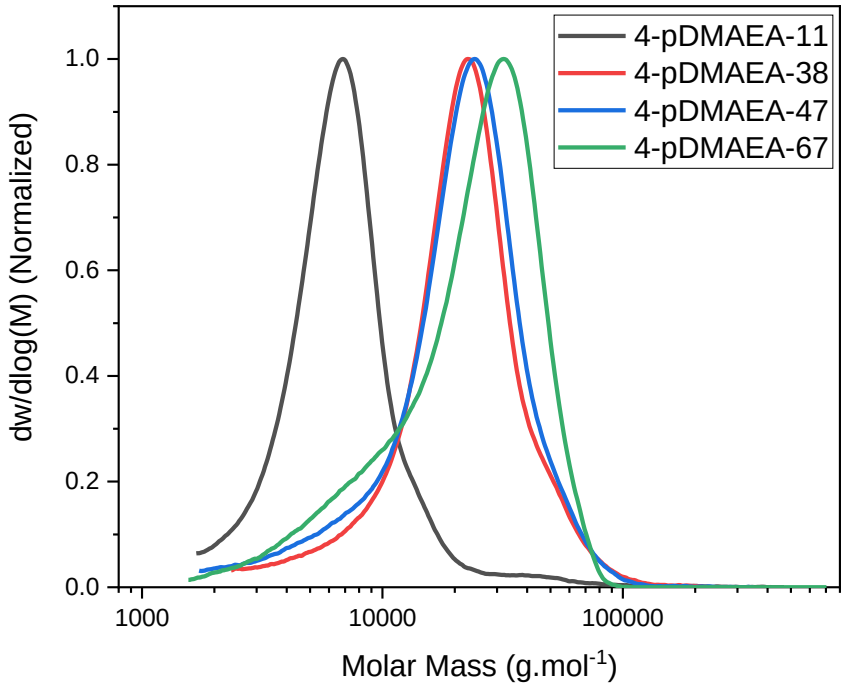

Figure 3.2: DMF-GPC traces of the 4-arms pDMAEA stars at final DP of 11, 38, 47 and 67.

3.3.2. Complexation and characterisation of polyplexes

The 4 star pDMAEA polymers were used for the complexation of dsRNA. This was assessed by agarose gel electrophoresis and ethidium bromide assay.

Gel electrophoresis is based on negatively charged species such as the nucleic acids moving down with the current while a positively charged complex will stay in the well at the top of the gel. By varying the ratio of nitrogen from the polymer to phosphorus from the nucleic acid (N/P ratio), the amount of polymer necessary to fully complex the dsRNA can be determined. Complexation was assessed with dsRNA at N/P ratios from 0 to 10. Full complexation was observed at N/P 1 for the three higher molecular weight star polymers (Figure 3.3b-c), while an N/P ratio of 2 was necessary to fully complex the dsRNA with the star pDMAEA with an arm DP of 11 (Figure 3.3a).

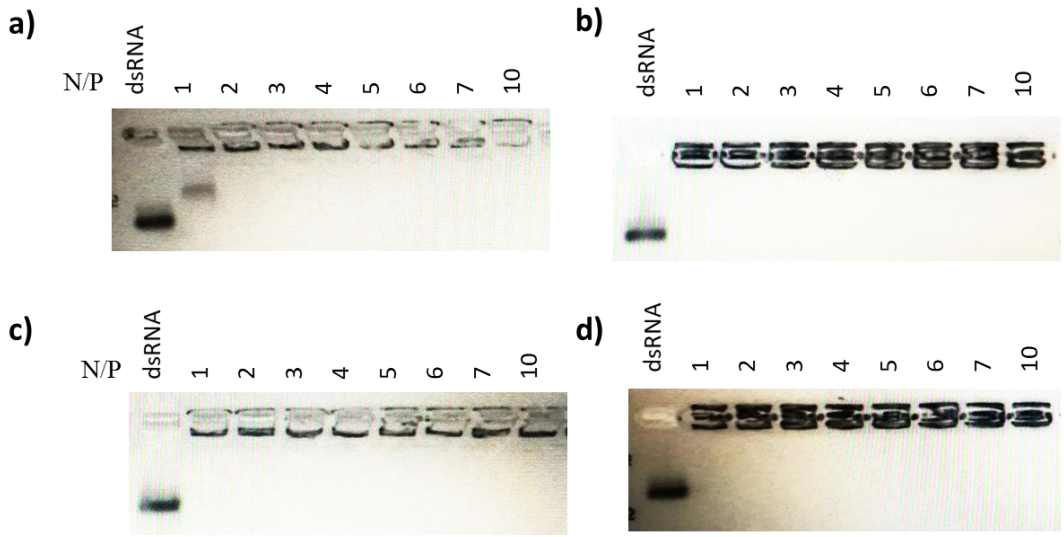

Figure 3.3: Agarose gel electrophoresis pictures of complexation of dsRNA with a) 4-pDMAEA_11 b) 4-pDMAEA_38 c) 4-pDMAEA_47 d) 4-pDMAEA_68.

Fluorescence spectroscopy can also be used to measure the interactions between the polymer and dsRNA. When the fluorescent cationic dyes ethidium bromide (EtBr) or GelRed, intercalate with the base pairs of the nucleic acids, an increase in fluorescence is observed.[19, 20] Therefore, the formation of the polyplex can be observed by a decrease of EtBr fluorescence as the dsRNA interacts with the cationic polymer instead. The relative percentage of displaced nucleic acids which is then binding to the cationic polymer chains can be calculated. By using PEI as a reference, we observed good complexation at N/P 2 and the displacement stayed the same at higher N/P ratios. The three stars with higher arm DP were able to bind a maximum of 89 to 92% of dsRNA at N/P 1, while 4-pDMAEA_11 could bind a maximum of 87% of dsRNA at N/P 2 (Figure 3.4). This is in agreement with what was observed for the complexation with the agarose gel electrophoresis. The binding of dsRNA was slightly stronger for higher molecular weight 4-arms pDMAEA polymers. A decrease in relative bound dsRNA could be observed with the pDMAEA polymers as 91% of the dsRNA was displaced at N/P 1 for 4-pDMAEA_38 and 75% at N/P 10. This was likely to be due to the increasing concentration of polymer required to target higher N/P ratios which lead to increasing pH (from around 7.1 for N/P 1 to 8.3 for N/P 10) thus leading to less charged polymers.

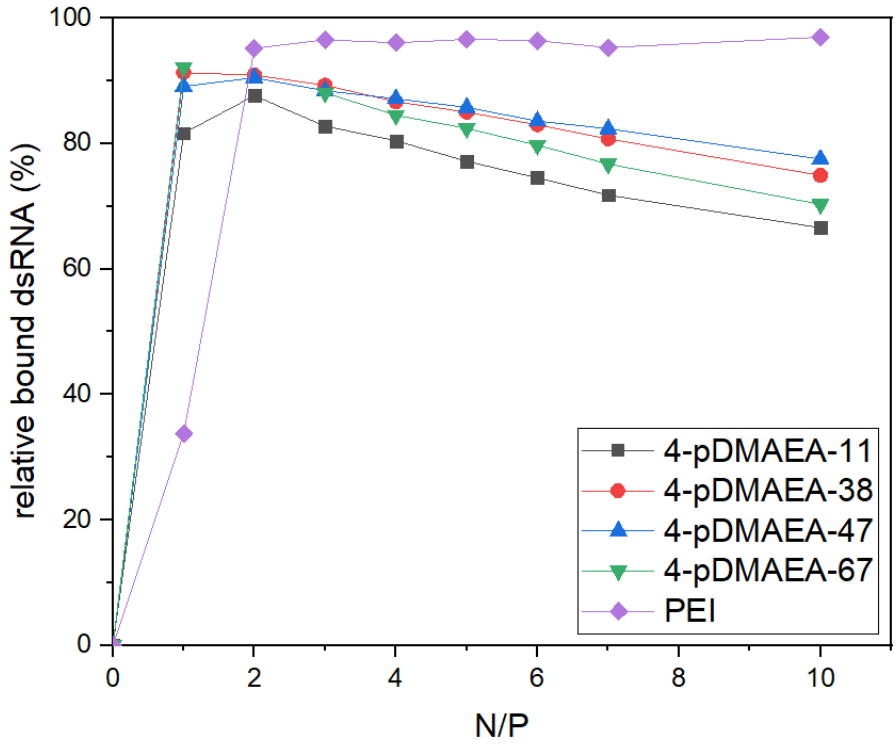

Figure 3.4: Ethidium bromide displacement assay for 4-arm star pDMAEA with arm DP of 11, 38, 47 and 67 and branched PEI.

3.3.3. Heparin displacement assays

The stability of the polyplex in the presence of competing species can be estimated using heparin dissociation assays.[21] Heparin is a competing polyanion with high negative charge density disrupting the electrostatic interaction and leading to dissociation when the concentration is high enough.[22, 23] Heparin was added at increasing concentration in the polyplex solution and agarose gel electrophoresis was used to observe any decomplexation of the dsRNA after 20 minutes incubation (Figure 3.5). Results showed stability of the polyplexes up to medium concentrations for all stars. When concentration was close to 0.3 mg/mL, free dsRNA could be observed, except in the case of the complex obtained with the star with the highest molecular weight. This observation supports the idea that the high molecular weight might help to give a better binding and protection of the nucleic acids.

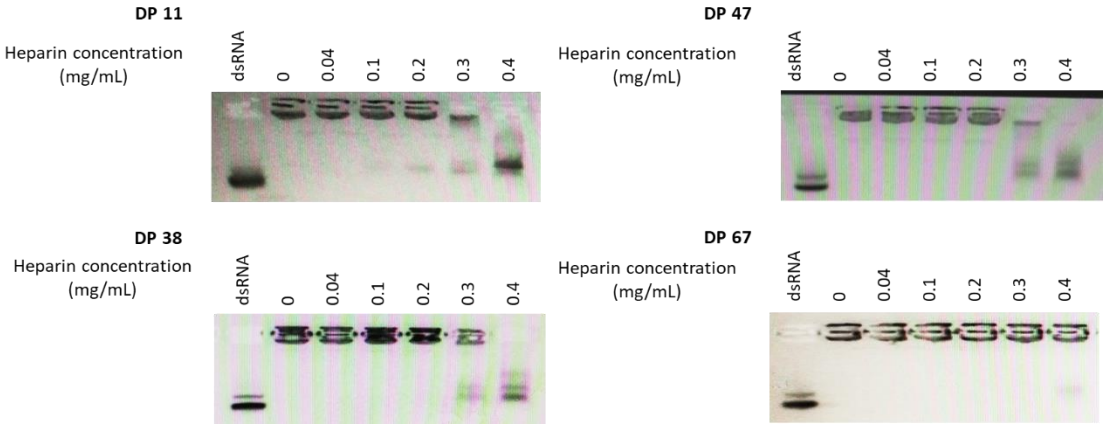

Figure 3.5: Heparin displacement assay. 5 µL heparin solution of increasing concentration were added to the polyplex solution at N/P 5 and incubated for 20 minutes upon gel electrophoresis run (100V, 30 min).

3.3.4. Soil stability

The soil stability assay allows us to test the polymers' ability to protect the dsRNA in environmental conditions. Stability in the live soil is particularly challenging since it is composed of many chemicals, nucleases and a microbial community, that can lead to decomplexation and degradation of the nucleic acids.[3, 24] The ability of these materials to protect the dsRNA in soil conditions was assessed in order to compare to the results obtained by Whitfield *et al.*[1] The dsRNA was complexed with the polymers in sterile water at a N/P ratio of 5, and added to a sample of live soil, enough to humidify it. Samples were incubated for up to 10 days at room temperature and were frozen at chosen time points to stop any further degradation. It is expected some dsRNA is released in the soil, and quickly degraded, while some dsRNA remain complexed and thus protected from degradation by the polymer. Naked dsRNA is used as a negative control and PEI as a positive control, since it is known to provide good protection, and no release of the dsRNA. PVS was then added to induce the dsRNA decomplexion. GelRed dye was used as a dye in order to measure fluorescence and quantify the amount of dsRNA left.

Results presented in Figure 3.6 show that the fluorescence of the samples with formulated dsRNA were higher than the one of the naked nucleic acids at day 1, indicating the polymers were able to limit the degradation. However, it quickly decreased at day 2 and beyond, thus indicating that most dsRNA has been degraded. The positive control with PEI showed high fluorescence, which suggests the dsRNA

was well protected during the time of the experiment. Therefore, we can conclude that very little protection was provided. This result was surprising as it is in contradiction with previous results from Whitfield *et al*. where pDMAEA stars provided good protection for up to 14 days (Figure 3.1).[1] The experiment was repeated for 4-pDMAEA_11 and 4-pDMAEA_38 as a controls, the same results were obtained, the dsRNA was completely degraded after 3 days. However, it was also shown by Whitfield *et al*. that the dsRNA was fully released in about 3 days in sterile water at a N/P of 5,[1] these results are supported by Cook *et al*.. [25] Therefore, it is unlikely that the release would be slower in soil than in pure water, especialy considering all the competing species present in soil. This results could be explained by a difference in activity between the soil used by Whitfield *et al*. and the soil used in this study, it could also be due to experimental. Thus, it seems the protection is still not strong enough with this type of architecture using simply DMAEA units as the nucleic acids is released too quickly in the soil.

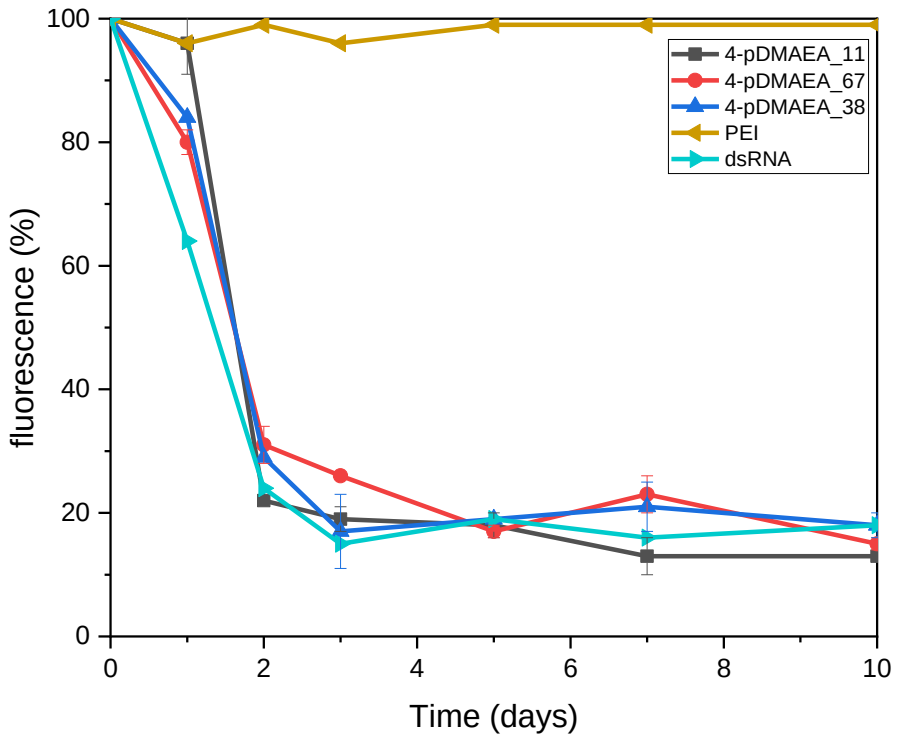

Figure 3.6: Soil stability assay. Fluorescence of GelRed after incubation (for 1, 2, 3, 5,7 and 10 days) in soil with naked dsRNA (negative control) and dsRNA formulated with pDMAEA 4-arm stars at arm DP 11, 38 and 67 and PEI (positive control) at N/P 5 with a final concentration of dsRNA of 1 mg/mL.

3.4. Conclusion

4-arm pDMAEA stars were successfully synthesised using RAFT polymerisation in order to compare their ability to protect dsRNA in soil to the one previously reported by Whitfield *et al*. using Cu(0)-mediated RDRP.[1] Four different molecular weight polymers were produced to investigate if the size / arm length would affect complexation and protection of dsRNA in a soil environment. Compared to the polymer previously reported, the dispersities of the RAFT star polymers were higher, with more tailing at low molecular weight, but the reactions were performed to higher conversions without significant star-star coupling. Star polymers made by RAFT were stable after purification and could be stored dry which represent a significant advantage over Cu(0)-mediated RDRP.

Successful complexation with dsRNA was evidenced with the four different stars, with the low molecular weight star (4-pDMAEA_11) being slightly less efficient at low N/P ratio as evidenced by agarose gel electrophoresis and ethidium bromide displacement assays. However, the increased stability in soil compared to linear chains reported in the litterature[1] has not been observed with this architecture, with the molecular weight having no effect. This can be explained by the release of the dsRNA is still fast (less than 3 days). The key aspect might be to first control the release of the dsRNA in a solution such as water before testing it in soil. Previous work in our group suggests that a combination of branched type architecture and the introduction of a non-hydrolysable monomer would give a delayed release, with good stability of polyplex.[14, 25] The copolymerisation of DMAEA with 20% of (2-dimethylaminoethyl methacrylate) DMAEMA showed that the dsRNA was fully released after 7 days instead of 1 day for the fully hydrolysable homopolymer.[14] These materials showed promising results, despite exhibiting high dispersities.

The next two chapters will investigate the effect of incorporating DMAEMA in a polymeric architecture, by first focusing on the hydrolysis of linear copolymers (**Chapter 3**) and the release of dsRNA and protection in soil (**Chapter 4**). Then, novel dense and branched architectures, based on arm-first p(DMAEA-DMAEMA) star polymers, which exhbit better control over structure and molecular weight, will be investigated.

3.5. Experimental

3.5.1. Materials

Pentaerythritol (Sigma-Aldrich, 99%), 2-bromopropionyl bromide (Sigma-Aldrich, 97%), triethylamine (TEA; Sigma-Aldrich, 99.5%), butanethiol (Sigma-Aldrich, 99%), carbone disulfide (Sigma-Aldrich, 99.9%), 2-(Dimethylamino)ethyl acrylate (DMAEA; Sigma-Aldrich, 98%), dry dichloromethane (DCM; Sigma-Aldrich), Sodium Hydroxyde (Sigma-Aldrich), agarose (Sigma-Aldrich), gelred (Biotium), Tris-Borate-EDTA buffer (TBE), Orange G/blue loading dye (6X) (Alfa Aesar), chloroform-d (Sigma-Aldrich, 99.8% D atom), sterile water (Sigma-Aldrich). DsRNA was provided by Syngenta. The soil was provided dried by Syngenta and sieved through a 2mm sieve and used within one year. The DMAEA monomer was passed through alumina prior to use.

3.5.2. Analytical techniques

Refer to method chapter.

3.5.3. Synthesis

3.5.3.1. Synthesis of the tetrafunctional PABTC

The pentaerythitol (1.18 g, 8.69 mmol, 1 eq.) was dissolved in 120 mL dry dichloromethane, and TEA (7.3 mL, 52.1 mmol, 6 eq.) was added to the solution which was then cooled down in an ice bath. The 2-bromopropionyl bromide (7.3 mL, 69.5 mmol, 8 eq.) was added slowly into the cold solution. The solution quickly turned to clear orange upon addition. The reaction was left overnight. The solution was filtered and washed with acid (HCl) 3 times, base (NaOH) 3 times and water and brine. The organic phase was dried over anhydrous magnesium sulfate, filtered and the solvent was removed under reduced pressure to give the intermediated product as an orange-brown solid. The IR showed no residual alcohol at 3 300 cm^{-1} and a ester bond at 1736 cm^{-1}.

The second step was adapted from the synthesis of PABTC reported in the literature.[26]

Butanethiol (3 mL, 28.5 mmol, 1 eq.) was dissolved in 20 mL acetone and a sodium hydroxide solution (1.25 g in 6 mL water, 31.3 mmol). The resulting solution was stirred for 30 minutes at room temperature. The solution is then treated with carbon disulfide (1.8 mL, 29.2 mmol, 1.025 eq.) to give a yellow solution that is stirred for 30 min. The solution is then cooled down with an ice bath. The product from step 1 was dissolved in 20 mL acetone and added drop-wise to the reaction mixture. The reaction was left to stir overnight. The product was extracted with DCM and washed with brine. The solution was dried over anhydrous magnesium sulfate, filtered and the solvent was removed under reduced pressure to give an orange oil. The product was purified by silica gel column chromatography (eluent: Hexane/ethyl acetate) to yield a viscous orange liquid with 26% yield. ^{1}H NMR (400 MHz, $CDCl_3$): δ=4.82 (1H, t, J=7.4 Hz, -C**H**-CH_3), 4.06 (2H, m, -C**H**$_2$-O-CO-), 3.35 (2H, m, -S-C**H**$_2$-CH_2-CH_2-CH_3), 1.68 (2H, m, -S-CH_2-C**H**$_2$-CH_2-CH_3), 1.58 (3H, d, J=7.3 Hz -CH-C**H**$_3$), 1.43 (2H, m, -S-CH_2-CH_2-C**H**$_2$-CH_3), 0.93 (2H, t, J=7.4 Hz, -S-CH_2-CH_2-CH_2-C**H**$_3$). ^{13}C NMR (400 MHz, $CDCl_3$): δ (ppm) = 221.8, 170.5, 62.8, 47.3, 42.2, 37.1, 29.8, 22.1, 16.4, 13.6 (Figure A3.2).

3.5.3.2. Synthesis of star polymers

For a typical polymerisation in which [DMAEA]:[CTA] = 52:1, tetrafunctional PABTC (39.14 mg, 0.04 mmol), DMAEA (286.4 mg, 2.0 mmol), and dioxane (1.70 mL) were added to a vial equipped with a magnetic stirrer and deoxygenated by bubbling with nitrogen for 20 minutes. The vial was place in a blue light reactor (460 nm) at ambient temperature for 15 hours. Monomer conversions are determined by ^{1}H NMR. The polymer is precipitated 3 times in Hexane and dried under vacuum. The final material was analysed by DMF-GPC (Figure 3.2) and ^{1}H NMR (Figure A3.3).

3.5.4. Agarose gel electrophoresis

Refer to method chapter.

3.5.5. Ethidium bromide displacement assay

Refer to method chapter.

3.5.6. Heparin displacement assay.

Refer to method chapter.

3.5.7. Soil stability assay

Refer to method 2 in method chapter.

3.6. References

1. Whitfield, R.; Anastasaki, A.; Truong, N. P.; Cook, A. B.; Omedes-Pujol, M.; Loczenski Rose, V.; Nguyen, T. A.; Burns, J. A.; Perrier, S. b.; Davis, T. P., Efficient Binding, Protection, and Self-Release of dsRNA in Soil by Linear and Star Cationic Polymers. *ACS Macro Lett.* **2018,** *7*, 909-915.

2. Liu, S.; Jaouannet, M.; Dempsey, D. M. A.; Imani, J.; Coustau, C.; Kogel, K.-H. J. B. a., RNA-based technologies for insect control in plant production. *Biotechnol. Adv.* **2019**, 107463.

3. Dubelman, S.; Fischer, J.; Zapata, F.; Huizinga, K.; Jiang, C.; Uffman, J.; Levine, S.; Carson, D., Environmental fate of double-stranded RNA in agricultural soils. *PLoS One* **2014,** *9* (3), e93155-e93155.

4. Joga, M. R.; Zotti, M. J.; Smagghe, G.; Christiaens, O., RNAi Efficiency, Systemic Properties, and Novel Delivery Methods for Pest Insect Control: What We Know So Far. *Front. Physiol.* **2016,** *7*, 553.

5. Vogel, E.; Santos, D.; Mingels, L.; Verdonckt, T.-W.; Broeck, J. V., RNA Interference in Insects: Protecting Beneficials and Controlling Pests. *Front. Physiol.* **2019,** *9*, 1912.

6. Yin, H.; Kanasty, R. L.; Eltoukhy, A. A.; Vegas, A. J.; Dorkin, J. R.; Anderson, D. G., Non-viral vectors for gene-based therapy. *Nat. Rev. Genet* **2014,** *15* (8), 541-555.

7. Truong, N. P.; Gu, W.; Prasadam, I.; Jia, Z.; Crawford, R.; Xiao, Y.; Monteiro, M. J., An influenza virus-inspired polymer system for the timed release of siRNA. *Nat. Commun.* **2013,** *4*, 1902.

8. Truong, N. P.; Jia, Z.; Burges, M.; McMillan, N. A.; Monteiro, M. J., Self-catalyzed degradation of linear cationic poly (2-dimethylaminoethyl acrylate) in water. *Biomacromolecules* **2011,** *12* (5), 1876-1882.

9. Gurnani, P.; Blakney, A. K.; Terracciano, R.; Petch, J. E.; Blok, A. J.; Bouton, C. R.; McKay, P. F.; Shattock, R. J.; Alexander, C., The In Vitro, Ex Vivo, and In Vivo Effect of Polymer Hydrophobicity on Charge-Reversible Vectors for Self-Amplifying RNA. *Biomacromolecules* **2020,** *21* (8), 3242-3253.

10. Ros, S.; Wang, J.; Burke, N. A. D.; Stöver, H. D. H., A Mechanistic Study of the Hydrolysis of Poly[N,N-(dimethylamino)ethyl acrylates] as Charge-Shifting Polycations. *Macromolecules* **2020,** *53* (9), 3514-3523.

11. Truong, N. P.; Jia, Z.; Burgess, M.; Payne, L.; McMillan, N. A.; Monteiro, M. J., Self-catalyzed degradable cationic polymer for release of DNA. *Biomacromolecules* **2011,** *12* (10), 3540-3548.

12. Liao, X.; Walden, G.; Falcon, N. D.; Donell, S.; Raxworthy, M. J.; Wormstone, M.; Riley, G. P.; Saeed, A., A direct comparison of linear and star-shaped poly (dimethylaminoethyl acrylate) polymers for polyplexation with DNA and cytotoxicity in cultured cell lines. *Eur. Polym. J.* **2017,** *87*, 458-467.

13. Perrier, S. b., 50th Anniversary Perspective: RAFT Polymerization· A User Guide. *Macromolecules* **2017,** *50* (19), 7433-7447.

14. Cook, A.; Peltier, R.; Hartlieb, M.; Whitfield, R.; Moriceau, G.; Burns, J.; Haddleton, D.; Perrier, S., Cationic and hydrolysable branched polymers by RAFT for complexation and controlled release of dsRNA. *Polym. Chem.* **2018**.

15. Yeow, J.; Sugita, O. R.; Boyer, C., Visible Light-Mediated Polymerization-Induced Self-Assembly in the Absence of External Catalyst or Initiator. *ACS Macro Lett.* **2016,** *5* (5), 558-564.

16. McKenzie, T. G.; Fu, Q.; Wong, E. H. H.; Dunstan, D. E.; Qiao, G. G., Visible Light Mediated Controlled Radical Polymerization in the Absence of Exogenous Radical Sources or Catalysts. *Macromolecules* **2015,** *48* (12), 3864-3872.

17. McKenzie, T. G.; Wong, E. H. H.; Fu, Q.; Sulistio, A.; Dunstan, D. E.; Qiao, G. G., Controlled Formation of Star Polymer Nanoparticles via Visible Light Photopolymerization. *ACS Macro Lett.* **2015,** *4* (9), 1012-1016.

18. Whitfield, R.; Anastasaki, A.; Truong, N. P.; Wilson, P.; Kempe, K.; Burns, J. A.; Davis, T. P.; Haddleton, D. M., Well-defined PDMAEA stars via Cu (0)-mediated reversible deactivation radical polymerization. *Macromolecules* **2016,** *49* (23), 8914-8924.

19. Lepecq, J. B.; Paoletti, C., A fluorescent complex between ethidium bromide and nucleic acids: Physical—Chemical characterization. *J. Mol. Biol.* **1967,** *27* (1), 87-106.

20. Geall, A. J.; Blagbrough, I. S., Rapid and sensitive ethidium bromide fluorescence quenching assay of polyamine conjugate–DNA interactions for the

analysis of lipoplex formation in gene therapy. *J. Pharm. Biomed. Anal.* **2000,** *22* (5), 849-859.

21. Kwok, A.; Hart, S. L., Comparative structural and functional studies of nanoparticle formulations for DNA and siRNA delivery. *Nanomed. Nanotechnol. Biol. Med.* **2011,** *7* (2), 210-219.

22. Richter, F.; Martin, L.; Leer, K.; Moek, E.; Hausig, F.; Brendel, J. C.; Traeger, A., Tuning of endosomal escape and gene expression by functional groups, molecular weight and transfection medium: a structure–activity relationship study. *J. Mater. Chem. B* **2020,** *8* (23), 5026-5041.

23. Wagner, M.; Rinkenauer, A. C.; Schallon, A.; Schubert, U. S., Opposites attract: influence of the molar mass of branched poly(ethylene imine) on biophysical characteristics of siRNA-based polyplexese. *RSC Advances* **2013,** *3* (31), 12774-12785.

24. Fischer, J. R.; Zapata, F.; Dubelman, S.; Mueller, G. M.; Jensen, P. D.; Levine, S. L., Characterizing a novel and sensitive method to measure dsRNA in soil. *Chemosphere* **2016,** *161*, 319-324.

25. Cook, A. Highly branched and hyperbranched polymers : synthesis, characterisation, and application in nucleic acid delivery. University of Warwick, 2018.

26. Larnaudie, S. C.; Brendel, J. C.; Jolliffe, K. A.; Perrier, S., Cyclic peptide–polymer conjugates: Grafting-to vs grafting-from. *J. Polym. Sci., Part A: Polym. Chem.* **2016,** *54* (7), 1003-1011.

3.7. Appendix

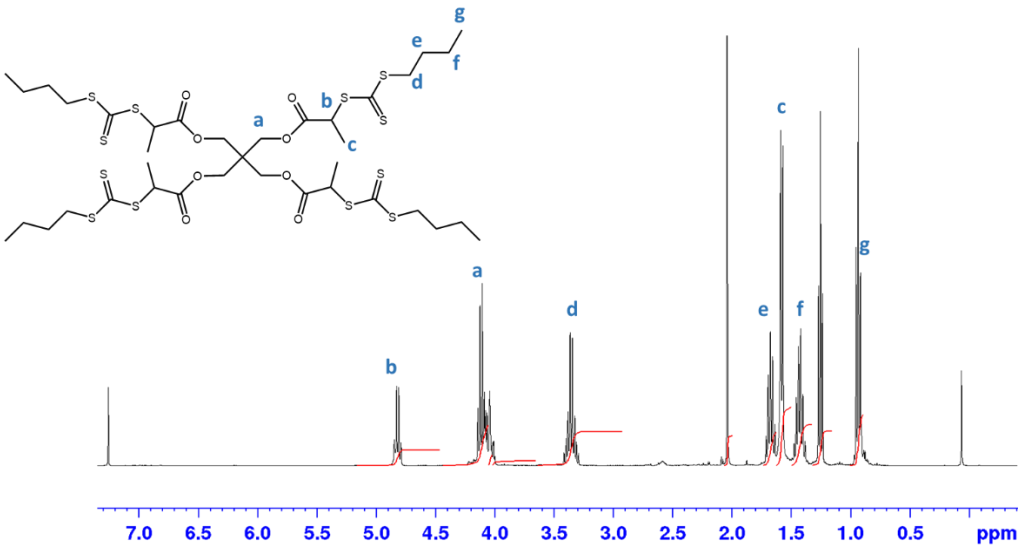

Figure A3.1: ^{1}H NMR spectrum (400 MHz, $CDCl_3$, 128 scans) of the multifunctional RAFT agent after purification by column chromatography.

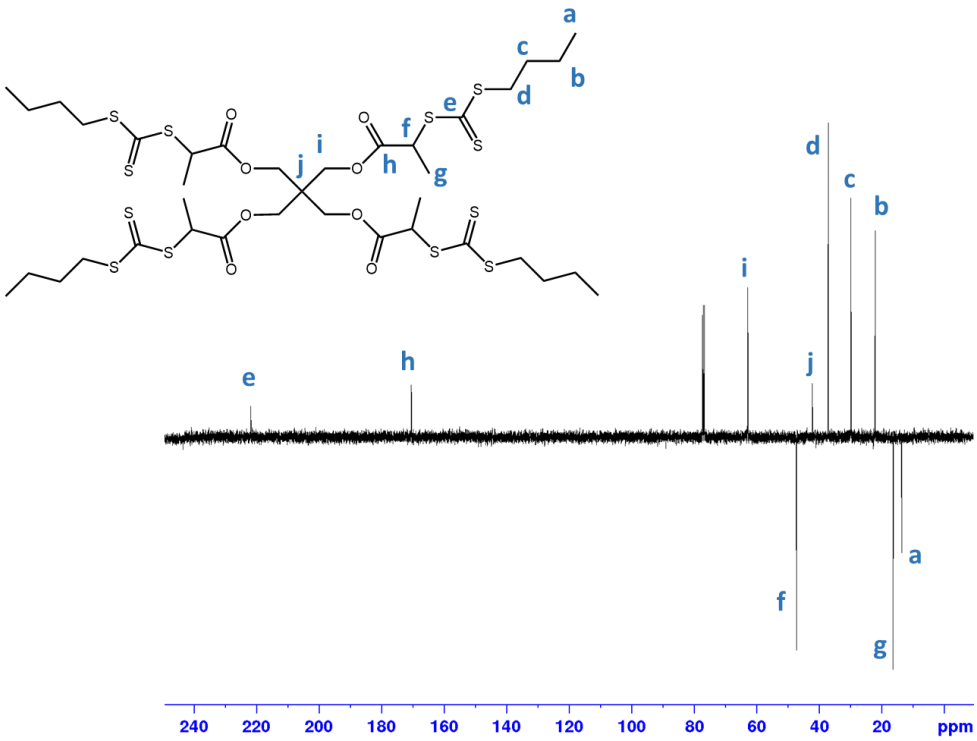

Figure A3.2: ^{13}C NMR spectrum (400 MHz, $CDCl_3$, 512 scans) of the multifunctional RAFT agent after purification by column chromatography.

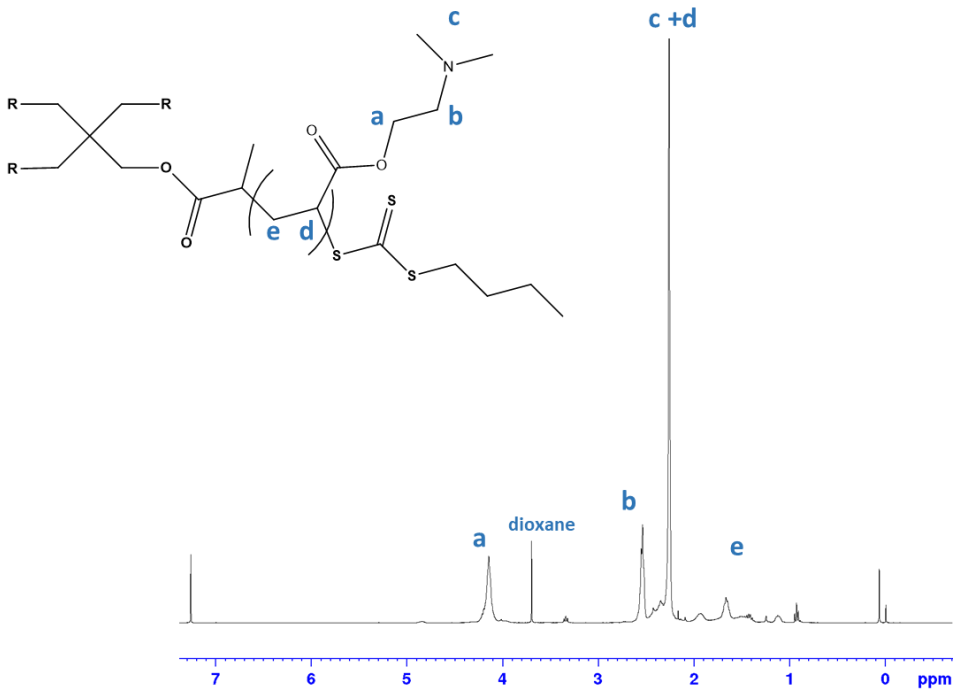

Figure A3.3: ^{1}H NMR (400 MHz, $CDCl_3$, 128 scans) spectrum of 4-pDMAEA_11 after precipitation in hexane.

Chapter 4: Synthesis and Hydrolysis of Linear and Star pDMAEA-DMAEMA Copolymers.

4.1. Abstract

In this work, a series of copolymers of DMAEA and 2-(dimethylamino)ethyl methacrylate (DMAEMA), as a cationic non-hydrolysable comonomer, were synthesised by RAFT polymerisation with different ratios of hydrolysable monomers from 100% to 50% DMAEA. Increasing amount of DMAEMA resulted in slower and lower hydrolysis. In order to study the influence of the architecture on the hydrolysis of the copolymers of DMAEA and DMAEMA (DMAEA:DMAEMA = 80:20), dense and compact star copolymers were prepared using RAFT, by the arm-first approach. Successful chain extensions of p($DMAEA_{80}$-*stat*-$DMAEMA_{20}$) were achieved with acrylamide monomers, therefore, a bisacrylamide crosslinker was used for the formation of the stars. *N*-Acrylmorpholine (NAM) was incorporated before crosslinking as a non-cationic monomer, either as a block or statistically integrated, to obtain soluble stars after purification and drying. Stars with a high number of well-defined arms (N_{arm} ~ 55 – 100) and dispersities between 1.7 and 2.3 were obtained. The architecture had a small impact on hydrolysis with slightly lower hydrolysis percentages observed for the stars compared to their corresponding arms. This is likely to be because of their compact structures, as access to chains closer to the center of the core may be more limited. These results have shown the hydrolysis could be tuned by incorporating DMAEMA and that the dense star architecture had only a small impact on the hydrolysis of the DMAEA side chains, reducing slightly the proportion of hydrolysed fraction.

4.2. Introduction: Effect of composition and architecture on pDMAEA hydrolysis

Given the fast hydrolysis of pDMAEA in water[1-7] discussed in chapter 1, attempts to tune the hydrolysis and the effect of comonomers on the hydrolysis have been reported in a few studies. Ros *et al.* studied different systems with a cationic comonomer 3-aminopropylmethacrylamide (APM), a neutral/hydrophilic comonomer hydroxyethylacrylate (HEA), and an anionic comonomer acrylic acid (AA) (Figure 4.2b). The copolymers containing the cationic APM units displayed the fastest hydrolysis, with higher APM content leading to increased DMAEA hydrolysis (Figure 4.2a). APM is non hydrolysable, but its positive charge plays a role in the net charge of the polymer chain. For the copolymer with only 24% DMAEA, the hydrolysis went to completion at 37°C. This polymer still possessed a significant net cationic charge (calculated from the fraction of cationic (APM+DMAEA) and anionic (AA) units), whereas copolymers with 88% DMAEA reached a zero net charge at just 55% hydrolysis (Figure 4.2c). Hydrolysis slowed as the chains were getting closer to zero net charge but none of them crossed zero to become negatively charged.[5] With the introduction of anionic AA comonomer, the hydrolysis of DMAEA was slower than the other polymers, as only 14% was reached in 20 days. This was explained by the net charge being close to neutral when the polymer may be more hydrophobic and in a collapsed conformation. This corresponds to the composition at which the hydrolysis of pDMAEA reaches a plateau. The AA units might also interact with the DMAEA and disrupt the intramolecular activation pathways of the hydrolysis. On the other hand, the copolymerisation with the neutral and hydrophilic HEA comonomers had very little impact.

The effect of the hydrophilicity/hydrophobicity was also studied by copolymerising DMAEA with a second hydrolysable comonomer, 2-hydroxymethyl acrylate (DHMA). The homopolymer of DHMA hydrolysed faster than pDMAEA, with about 80% of the side chains hydrolysed in 2 days at pH 7, at room temperature, whereas less than 20% were hydrolysed for pDMAEA in the same conditions. The hydroxymethyl substituent might interact with the ester carbonyl oxygen and increase the electrophilicity as well as increasing the hydrophilicity of the polymer. When DHMA and DMAEA were copolymerised, the speed of the hydrolysis of the resulting

copolymer increased when the ratio of DHMA to DMAEA increases.[6] Gurnani *et al*. further studied the influence of the hydrophilicity by copolymerising DMAEA with either a hydrophilic (HEA) or hydrophobic, butyl acrylate (BA), comonomer . Higher hydrolysis is reached for the more hydrophilic copolymers. By spacing the DMAEA units with BA, the pH dependency of pDMAEA was increased whereas by spacing them with HEA the pH dependency was reduced.[8] The copolymerisation of DMAEA with its methacrylate version DMAEMA which is nonhydrolysable[6] was also seen to slow down the hydrolysis. Two different compositions were reported, 80% DMAEA and 20% DMAEA relative to DMAEMA. When the copolymer with 80% DMAEA reached a plateau at about 60% hydrolysis of DMAEA, the one with 20% DMAEA reached only 25% in 20 days.[9] From these studies we can conclude the addition of comonomers or substituents (DHMA or DMAEMA) and change of environments (hydrophilicity/hydrophobicity, pH and net charge) can have a strong effect on the hydrolysis rates of the DMAEA side chains.

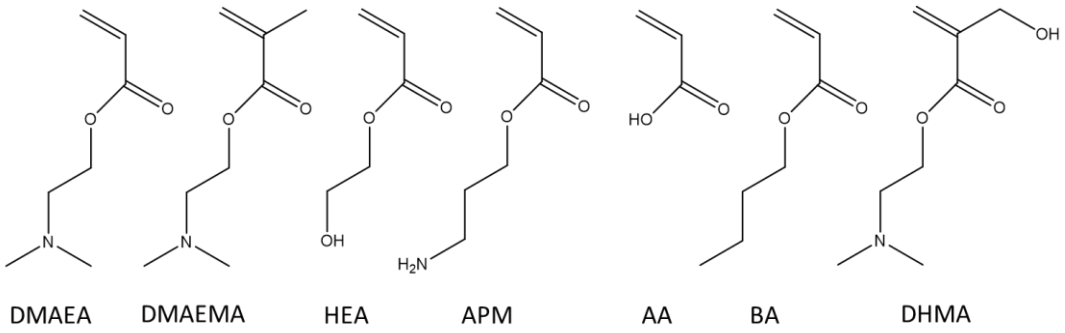

Figure 4.1: DMAEA and its different comonomers studied in literature: DMAEMA, HEA, APM, AA, BA, DHMA.

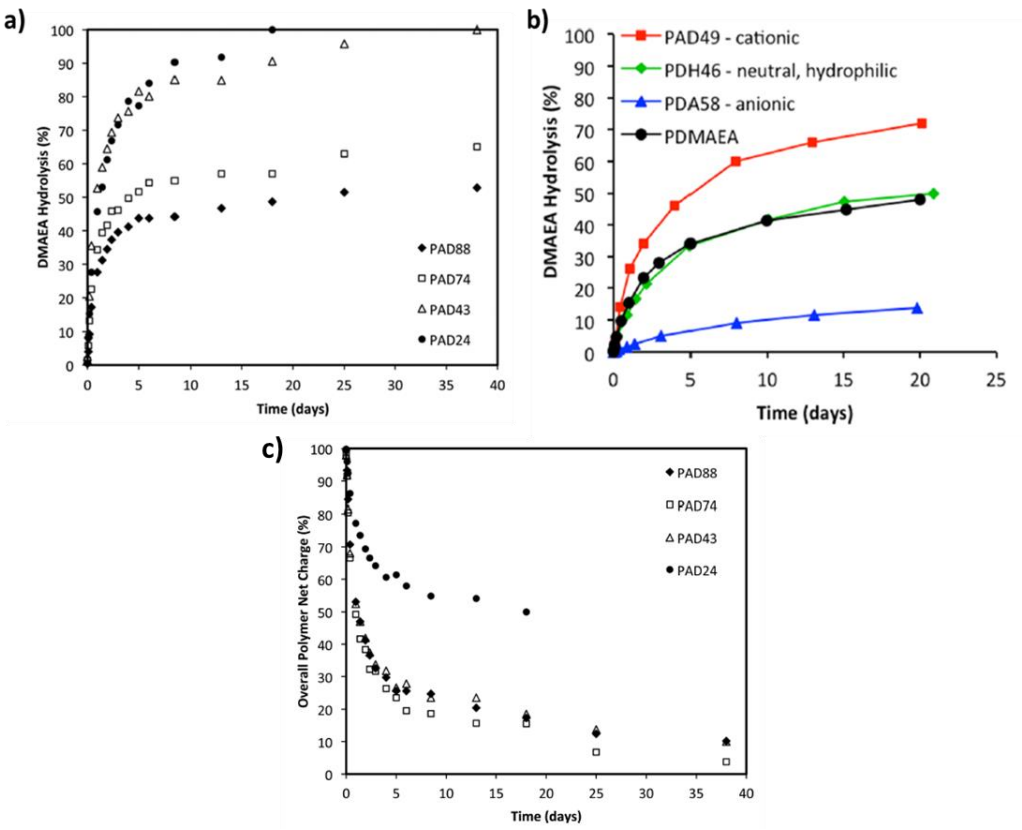

Figure 4.2: Hydrolysis of DMAEA units for a) p(DMAEA-co-APM) at pH 7 and 37°C shown as percent of DMAEA hydrolysed for different ratios of DMAEA:APM from 88% to 24% DMAEA adapted from ref 46.[5] b) for p(DMAEA-co-APM) (PAD49), p(DMAEA-co-HEA) (PDH46), p(DMAEA-co-AA) (pDA58) and pDMAEA at pH 7 and room temperature (22°C) adapted from ref. 43.[7] c) Overall net charge (or excess of cationic groups) calculated from fractions of cationic (APM + DMAEA) and anionic (AA) adapted from ref.[5]

Studies on the effect of the polymeric architecture have shown minimal effect on the hydrolysis. Whitfield *et al.* reported four and eight arms pDMAEA star homopolymers made by the core-first approach compared to linear equivalent.[4] Cook *et al.* looked at branched architectures copolymers of DMAEA and DMAEMA.[9] Both these studies concluded there was no effect of these architectures on the hydrolysis of the DMAEA side chains. The impact on hydrolysis of DMAEA units localised in the core of star polymers has been studied by Rolph *et al.*. The polymer was synthesised by the arm-first approach (polyacrylates arms), chains were extended with DMAEA and a diacrylate cross-linker. Monomers were fed to produce stars with approximately 20, 15 and 10% crosslinking density. It was expected that by increasing crosslinking density to give a less mobile core, thus less mobile pendant functionality and more localized build-up of negative charge, the kinetics would be slower and maximum

hydrolysis lower. However, little difference was observed between star and linear polymers, in 300 minutes at room temperature, 26% hydrolysis was reached whereas 34% for the linear polymer, though, at 50°C, the difference is more apparent.[10]

Since the hydrolysis of homopolymers of DMAEA and the release of nucleic acids are too fast to observe a prolonged protection of dsRNA in soil conditions, even with a 4-am star architecture as evidenced in chapter 2, the incorporation of DMAEMA as non-hydrolysable comonomers to slow down the hydrolysis was further investigated in this chapter. Linear copolymers with different ratios of DMAEA:DMAEMA were prepared to study the influence on the hydrolysis profile. In a second part, new architectures of copolymers of DMAEA and DMAEMA were investigated. Dense star copolymers were synthesised by the arm-first approach in order to obtain a structure with a high number of arms and with improved control compared to the branched polymers previously studied.[9] The branched structures of DMAEA and DMAEMA showed promising results but the poor control over the molecular weight and structure makes it difficult to determine how it is more efficient at protecting the dsRNA. The arm-first approach enables good control over the arm size and composition. The hydrolysis of such architecture was compared to the one of their arms to investigate the impact of architecture as demonstrated in the literature.[4, 9]

4.3. Results and discussions

4.3.1. Synthesis of p(DMAEA-*co*-DMAEMA) linear copolymer

4.3.1.1. Polymer synthesis and characterisation

RAFT polymerisation was used for its fine control over the molecular weight, dispersity, chain-end fidelity, and also for its compatibility toward amine functionalised monomers.[11, 12] A series of poly(DMAEMA-*co*-DMAEA) were synthesised (Scheme 4.1) with ratios of monomers DMAEA:DMAEMA of 100:0, 90:10, 80:20, 70:30 and 50:50 in order to finely tune the rate of hydrolysis and final fraction of hydrolysis. A homopolymer of DMAEMA was synthesised as control. As acrylates and methacrylates were copolymerised, (4-cyano pentanoic acid)yl ethyl trithiocarbonate (CPAETC), a CTA that has been shown to efficiently control the polymerisation of both acrylate and methacrylates[9, 13] was used, with 4,4′-Azobis(4-cyanovaleric acid) (ACVA) as initiator at 70°C over 24 hours (Scheme 4.1). To obtain molecular weights of 7,500 g.mol^{-1}, a degree of polymerisation (DP) of 50 was targeted. The amount of initiator was kept low at a ratio of control transfer agent to initiator ([CTA]:[I]) of 20, in order to reduce the fraction of dead chains.

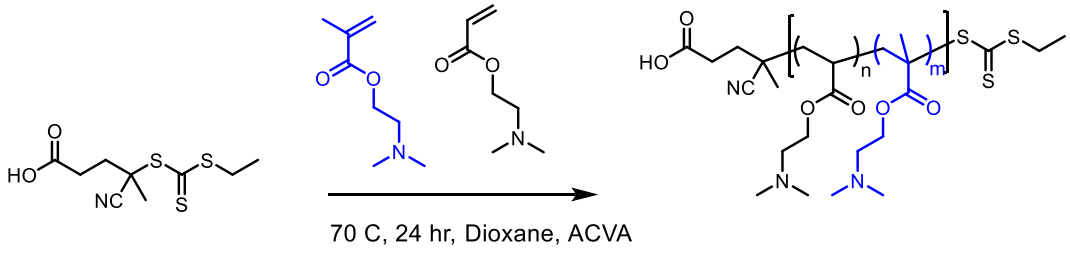

Scheme 4.1: RAFT copolymerisation of DMAEA and DMAEMA ([M]=4M, [CTA]/[I]=20, DP=50).

Conversions were determined by ^{1}H NMR spectroscopy by following the decrease of signal for vinyl protons of DMAEA and DMAEMA at 5.5 ppm and 5.8 ppm respectively (Figure A 4.1). Copolymers were obtained with conversion between 80 and 86% and almost full conversion (>99%) was obtained for the pDMAEMA homopolymer. Molecular weights were determined by GPC, in DMF eluent with

PMMA standards, using RI and UV detectors. Results are presented in Table 4.1 and showed dispersities around 1.2 and a good overlap between RI and UV traces at λ=309 nm is observed (Figure A4.2) indicating the presence of the trithiocarbonate functionality at the chain end.

Table 4.1: Characterisation data of the different copolymers p(DMAEA-co-DMAEMA)$_{50}$. Conversion is determined by ^{1}H NMR and molar mass are determined by DMF-GPC with PMMA standards.

Polymer	DMAEA content (%)	Conversion (%)	$M_{n,th}$ (g.mol^{-1})	$M_{n,\,GPC}$ (g.mol^{-1})	$M_{w,\,GPC}$ (g.mol^{-1})	$Đ$
L$_{100}$	100	80	7 400	7 100	8 600	1.23
L$_{90}$	90	83	7 500	6 600	8 100	1.22
L$_{80}$	80	86	7 600	6300	7 600	1.20
L$_{70}$	70	85	7 600	6 500	7 800	1.20
L$_{50}$	50	81	7 800	6 200	7 500	1.21
L$_{0}$	0	>99	8 100	8 000	9 300	1.16

4.3.1.2. Optimisation of the polymer synthesis

Star synthesis following the arm-first approach in one-pot requires the system to reach full conversion. Parameters such as the choice of initiator, temperature, concentration of the monomer and CTA to initiator ratio ([CTA]/[I]) were varied in order to modify reactivity and kinetics to improve the final conversion of the polymerisation (Table 4.2). Neither the nature of the initiator nor temperature improved the final conversion (entries 01-03), slightly higher final conversions were obtained by decreasing the amount of initiator (entries 03-06), or by increasing the monomer concentration from 3 M to 4 M (entries 02 and 07), up to a maximum of 95%. It was then decided to keep the [CTA]/[I] ratio at 20 to keep initiator concentration low and decrease the number of dead chains (entry 07). The monomer concentration was increased to 4 M instead of 3 M as reaction was a slightly faster and the control was still good ($Đ$ <1.25). These parameters were chosen to keep a good balance between conversion, reaction time and livingness which is required to proceed with the next steps. As full conversion was not reached even after optimisation, intermediated purification steps were conducted for the star synthesis.

Table 4.2: Conditions of polymerisation of 80% DMAEA and 20% DMAEMA copolymers and final conversion results after 24 hours determined by ^{1}H NMR spectroscopy.

Entry	T (°C)	[M] (molar)	[CTA]/[I]	I	Conversion (%)
01	90	3	20	V40	85
02	90	3	20	V86	85
03	70	3	25	ACVA	90
04	70	3	30	ACVA	90
05	70	3	40	ACVA	86
06	70	3	15	ACVA	95
07	70	4	20	ACVA	92
08	70	4	15	ACVA	93
09	70	4	40	ACVA	75
10	70	4	30	ACVA	90
11	60	4	20	ACVA	70
12	80	4	20	ACVA	75
13	80	4	20	V40	85

With these new conditions, polymerisation of 80% DMAEA and 20% DMAEMA was followed by ^{1}H NMR spectroscopy and GPC (Figure 4.3). DMAEMA was incorporated faster into the polymer than the acrylate, meaning that the copolymer will possess a light gradient composition. These results are in agreement with the reactivity ratios determined in previous work in the group: $r_{DMAEMA} = 2.13$ and $r_{DMAEA} = 0.69$.[9] While DMAEMA went to full conversion, DMAEA reached a plateau at only 70%. The linear increase of molar mass with conversion and low dispersities ($Đ$ <1.25) are characteristic features of controlled radical polymerisation.

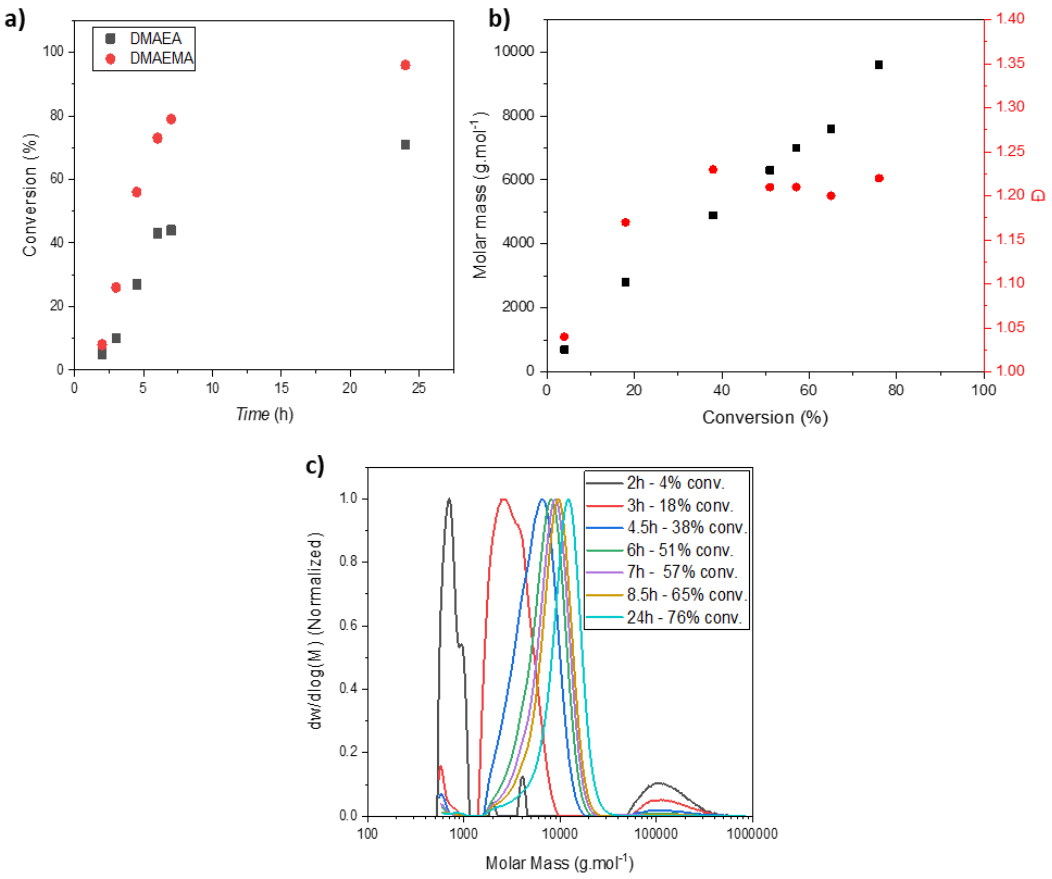

Figure 4.3: Kinetic study of the copolymersisation of DMAEA and DMAEMA with 80% DMAEA [DMAEA]:[DMAEMA]:[CTA]:[I] = 40:10:1:0.05. a) evolution of conversions of DMAEA and DMAEMA as a function of time, b) evolution of Mn and Đ with conversion, c)DMF- GPC traces of p(DMAEA-co-DMAEMA) at different conversions.

4.3.2. Hydrolysis study: influence of the composition

The hydrolysis of the polymers were performed *in situ* in NMR tubes, at a concentration of 10 mg/mL in D_2O, and the reaction was followed by ^1H NMR spectroscopy at room temperature. Figure 4.4 shows the spectra of homopolymer of DMAEA over 13 days. When hydrolysis of the DMAEA side chain occurs, intensity of the peaks at 4.2 ppm, 2.7 ppm and 2.3 ppm decrease and sharp peaks appear (3.8 ppm, 2.9 ppm and 2.6 ppm) due to small molecule by-product DMAE. The integrations of DMAE peaks in comparison to peak at 4.2ppm were used to calculate the fraction of hydrolysis.

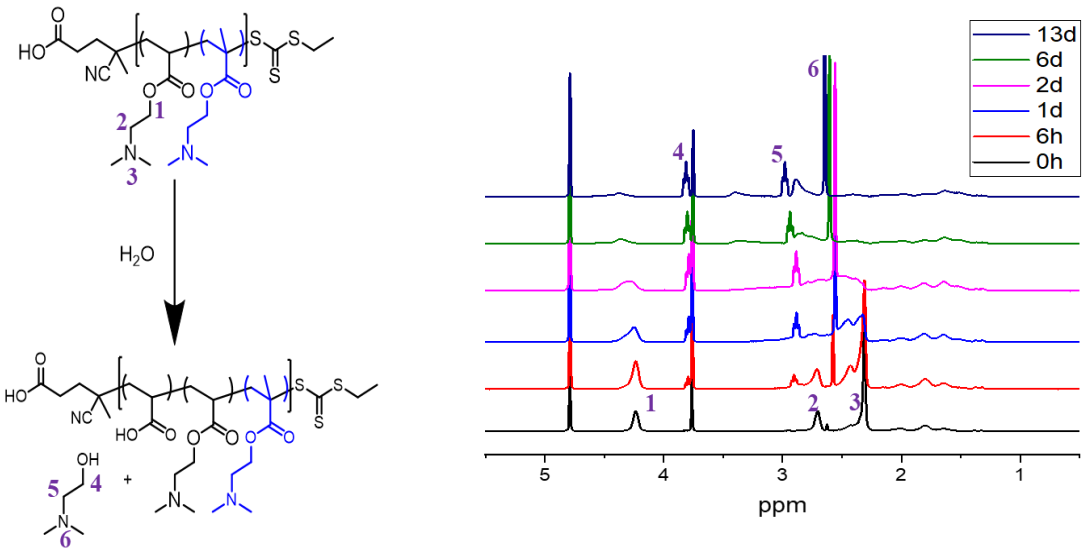

Figure 4.4: ^{1}H NMR spectra of $pDMAEA_{50}$-$DMAEMA_{0}$ in D_2O at room temperature for 0 hours, 6 hours, 1 day, 2 days, 6 days, 13 days.

Figure 4.5a shows the resulting overall side chains hydrolysis kinetic profiles for the five different copolymers. pDMAEMA homopolymer was used as a control, no hydrolysis could be observed even after 60 days. For all polymers with DMAEA, after a fast initial period, the hydrolysis dramatically slowed down and reached a plateau within a few days in all cases. This is consistent with what has been observed in the literature.[2, 4-9, 14]

The hydrolysis of the homopolymer of DMAEA reached the highest plateau (75% hydrolysis after 29 days) which is consistent with the results showed in the literature at a natural pH (around 9).[7] The ratio of DMAEA:DMAEMA clearly has an effect on hydrolysis as shown in Figure 4.5. Lower final fraction of hydrolysis are observed when the proportion of DMAEA in the polymer decreases; for 100% DMAEA, 70% hydrolysis is reached after 29 days whereas only 20% is reached for the copolymer with 50% DMAEA. Alternatively the data can be considered in terms of the % of DMAEA hydrolysed specifically, rather than all monomer units, which gives a better comparison of the ease of hydrolysis for different comonomer compositions. For all polymers with more than 70% DMAEA, about 70% of the DMAEA side chains were hydrolysed after 29 days, whereas for the copolymers with 50% DMAEA only 50% of the DMAEA is hydrolysed. Nethertheless, the rate of DMAEA hydrolysis at the beginning seems to decrease with increasing DMAEMA content. A reason could be the increased hydrophobicity of the methacrylate polymer

backbone units reducing access of water to the ester units. Compared to what have been observed with other cationic comonomers by Ros *et al*. a decrease in hydrolysed DMAEA side chains was observed with DMAEMA.[5, 7] If all the side chains were charged, there were still 75% of positive side chains, therefore the assumption that the plateau is reached when the overall charge is neutral was not verified here. Given the pH (pH around 9) at this polymer concentration (10 mg/mL), it is likely that not all DMAEA or DMAEMA side chains are positively charged. Moreover, DMAEMA is more hydrophobic and flexible.

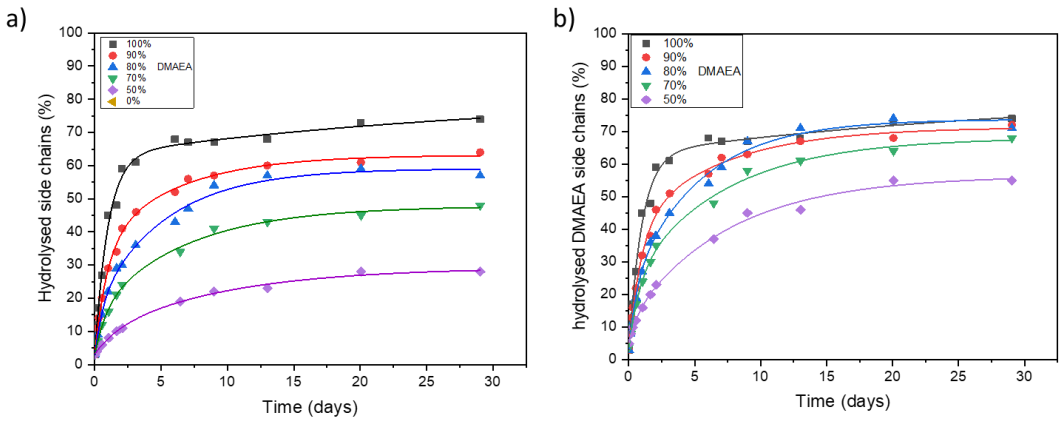

Figure 4.5: Hydrolysis kinetics of copolymers of 100%, 90%, 80%, 70% and 50% DMAEA in D_2O determined using ^1H NMR spectroscopy. percentage hydrolysis a) of all side chains b) of DMAEA side chains.

4.3.3. Star copolymers

The objective here was to synthesise well-defined star-shaped copolymers of DMAEA and DMAEMA in order to compare the kinetics of hydrolysis and release of dsRNA with their linear equivalents. The arm-first approach enables the synthesis to start from the already characterised linear pDMAEMA-DMAEA copolymers and directly chain extend them with a suitable crosslinker to interconnect the arms to form stars.[15-18] The composition of the arms was chosen at 80% DMAEA and 20% DMAEA since the hydrolysis was slowed down and lowered down significantly, enabling a slower release of the dsRNA (see chapter 4).

4.3.3.1. Investigation of chain extension of pDMAEA-based polymers

The synthesis of stars by the arm-first approach requires an efficient chain extension, to ensure arm crosslinking and to minimise the quantity of unattached linear side products. A range of difunctional crosslinking monomers are available, and the choice of monomer family can have a large impact on chain extension efficiency due to the RAFT fragmentation mechanism. An acrylate monomer was first considered as DMAEA has the same polymerisable function and diacrylate crosslinkers have been used to make branched copolymer structures[9] or stars[10] with DMAEA, however no chain extension are reported in the literature using RAFT. Whitfield *et al*. successfully chain extended pDMAEA with methyl acrylate (MA) using Cu(0)-mediated RDRP.[19] To make sure acrylates are suitable for chain extension of the p(DMAEA-*stat*-DMAEMA) copolymer, MA was used as a model monomer. However, the chain extension with MA ([M]/[mCTA]=50) from pDMAEA homopolymer showed poor reinitiation. The GPC trace revealed only small fraction of the first block shifted to higher molecular weight (Figure 4.6a). For the pDMAEMA homopolymer, the chain extension was slightly improved but still unsatisfactory (Figure 4.6b). The same trend was observed from chain extension of p(DMAEA-*stat*-DMAEMA) copolymer, a limited shift was observed with tailing at low molecular weight (Figure 4.6c). Chain extension from a statistical copolymer of MA and methyl methacrylate (MMA) was performed as a control. The GPC results showed a clear extension, even if some tailing could still be observed (Figure 4.6c). It was concluded that the poor chain extension came from the functionality of the monomers and particularly in the case of DMAEA.

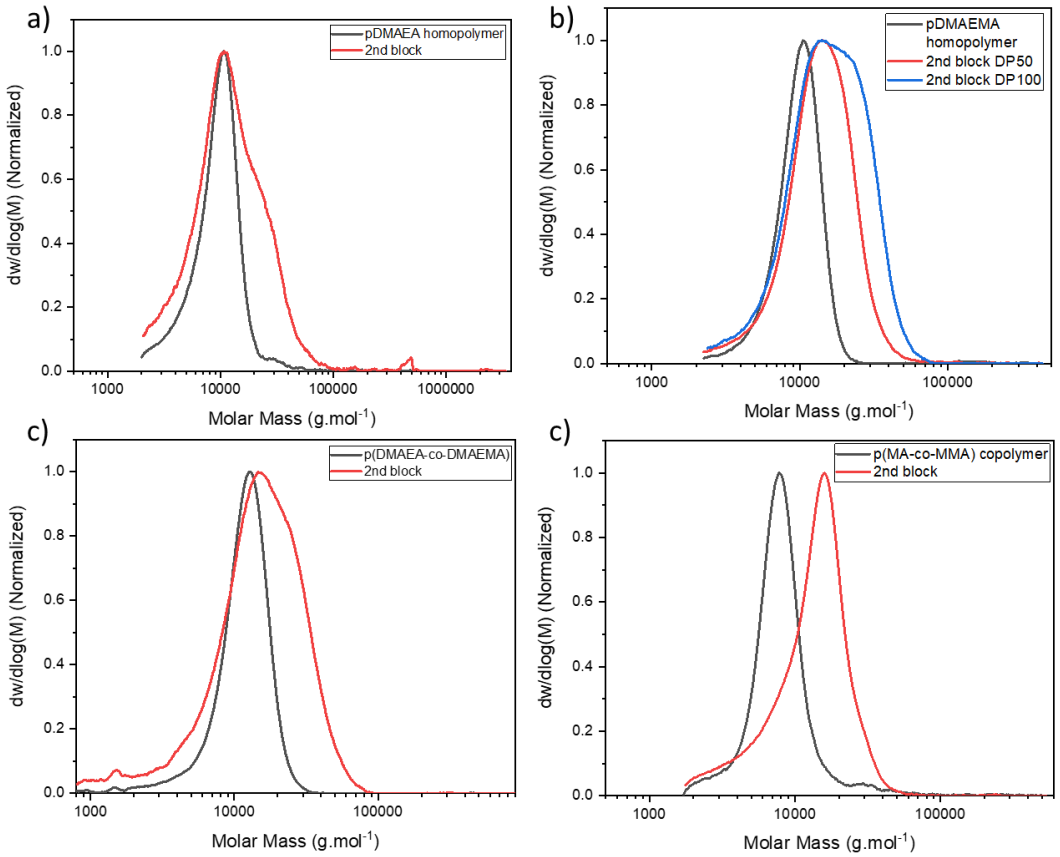

Figure 4.6: DMF-GPC traces of chain extension with methyl acrylate (MA) ([M]=0.5 M) of a) pDMAEA homopolymer b) pDMAEMA homopolymer c) p(DMAEA$_{80}$-co-DMAEMA$_{20}$) copolymer d) p(MA$_{80}$-co-MMA$_{20}$) copolymer.

As the reinitiation with an acrylate was not efficient, an extension of p(DMAEA-*co*-DMAEMA) with an acrylamide monomer, *N*-acryloylmorpholine (NAM), was performed to assess macroCTA reactivity. The reaction reached almost full conversion of NAM as shown by ^{1}H NMR with almost total disappearance of the vinyl peaks at 6.5, 6.3 and 5.7 ppm. The GPC traces (Figure 4.7) showed a much improved chain extension, with a clear shift to higher molecular weight, although a small amount of macroCTA still did not reinitiate. From these results, the usage of an acrylamide based crosslinker was identified as the most suitable choice.

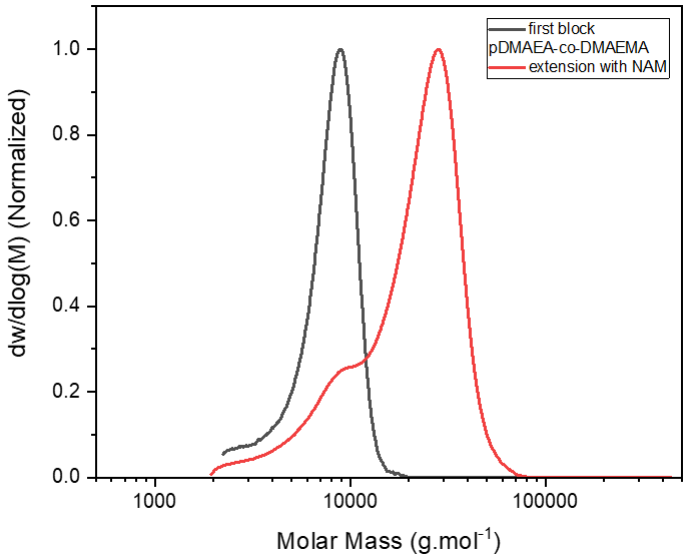

Figure 4.7: DMF-GPC traces of chain extension of p($DMAEA_{80}$-co-$DMAEMA_{20}$) with NAM ([M]=0.5M).

4.3.3.2. From linear to star copolymers the arm-first approach

Methylenbis(acrylamide) was chosen as crosslinker (CL) to synthesise the stars by the arm-first approach. Purified linear copolymer L_{80} composed of 80% DMAEA previously synthesised was used as macroCTA (mCTA) for chain extension.[20] ACVA was used as initiator (I) at 70°C over 5 hours (Scheme 4.2) and a [CL]:[mCTA] ratio of 3, a [CTA]:[I] ratio of 20 and a crosslinker concentration of 0.2 M were chosen for this reaction. The chain extension was followed by ^{1}H NMR spectroscopy and DMF GPC (Figure 4.8). This showed that 90% the double bonds of the crosslinker was consumed in four hours. GPC clearly provides evidence of the arms crosslinking into star copolymers, with the formation of a higher molecular weight species increasing in size over the course of the reaction as seen in Figure 4.10. At the end of the reaction, star copolymers were obtained with a good dispersity ($Đ$=1.30) and molecular weight of 152 000 g.mol^{-1}. Stars were then precipitated in cold diethyl ether to remove the non-incorporated arms and dried (Figure 4.9). However, this purification resulted in a material that was completely insoluble after drying. This might be due to the high charge of the polymer as this has been observed with other 100% cationic core-crosslinked stars.

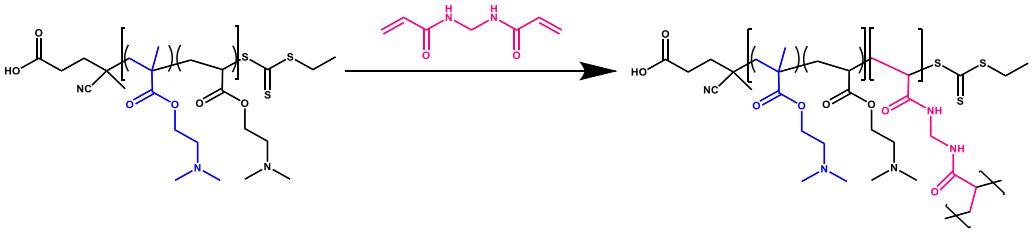

Scheme 4.2: Crosslinking of linear arm copolymers to form stars using a bisacrylamide difunctional monomer (Methylenbis(acrylamide)).

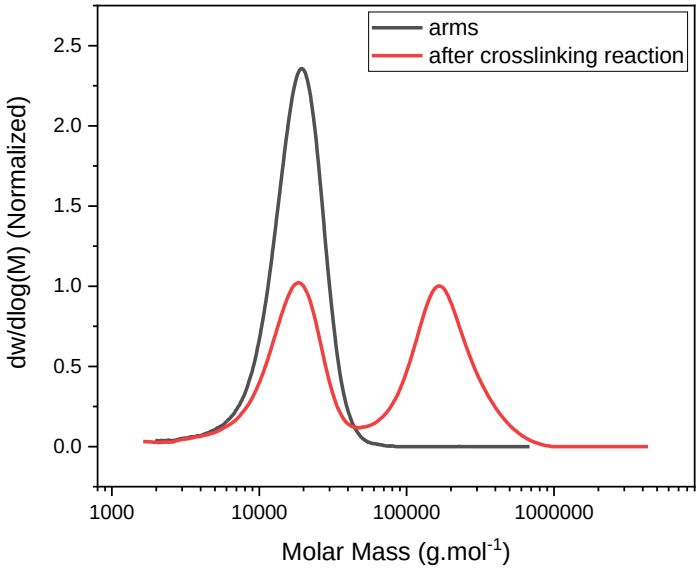

Figure 4.8: GPC traces of arms and stars after crosslinking reaction for 4 hours.

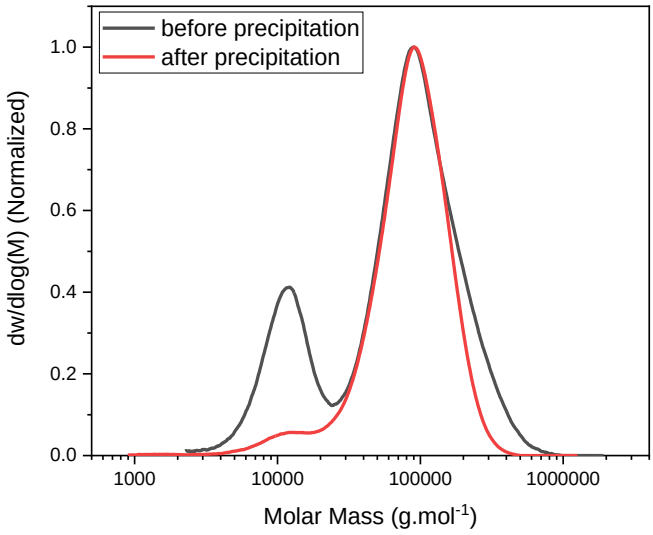

Figure 4.9: DMF-GPC traces of the final product before and after precipitation.

Introducing a block of non-cationic NAM prior to the crosslinking of the purified block copolymer in a second step enabled to solubilise the stars (Scheme 4.3). Since the introduction of the second block of NAM led to higher molecular weight materials (the DP of NAM was 30 in addition to the DP 50 of the first block), two new stars were synthesised, with a first block of DMAEA and DMAEMA of DPs 25 and 12 (80% DMAEA), respectively, instead of a total DP of 50, and chain extended after purification with NAM targeting a DP 15 and 7, respectively. The stars were purified by precipitation in a mixture of solvents, 70% cold diethyl ether and 30% dichloromethane, to selectively remove the unreacted arms.

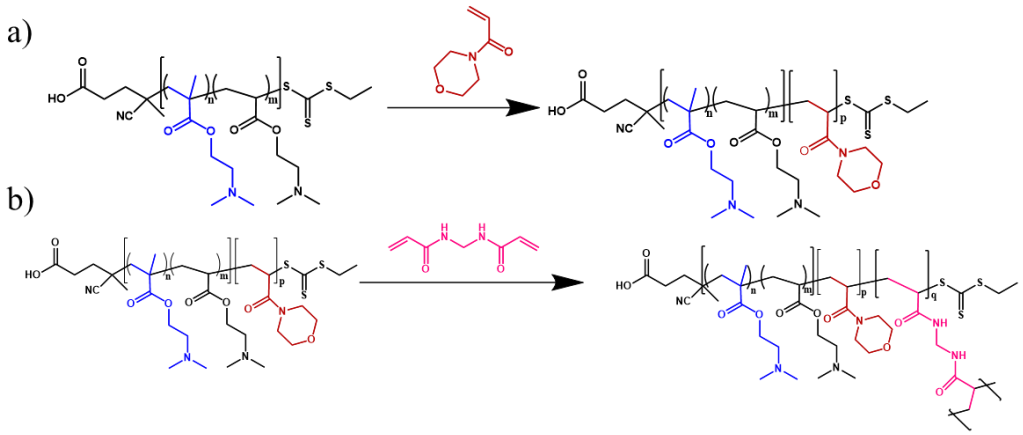

Scheme 4.3: a) Chain extension of pDMAEA-stat-DMAEMA with NAM ([M]= 2 M, [M]/[mCTA]=15 or 7, [mCTA]/[I]=20) and b) crosslinking with bisacrylamide monomer ([CL]=0.2M, [CL]/[mCTA]=3, [mCTA]/[I]=20).

Table 4.3: Kinetic data for the crosslinking of the pDMAEA-stat-DMAEMA-b-NAM arms ([CL]=0.2M, [CL]/[mCTA]=3, [mCTA]/[I]=20).

Time min	Conv. (%)	$M_{n,\ GPC\ CHCl3}$ (g/mol)	$M_{w,\ GPC\ CHCl3}$ (g/mol)	$Đ$
0	0	12 800	15 800	1.23
25	18	40 400	48 200	1.19
35	40	56 400	68 300	1.21
55	60	68 000	90 400	1.33
90	80	93 300	128 000	1.37
180	95	119 900	194 300	1.62

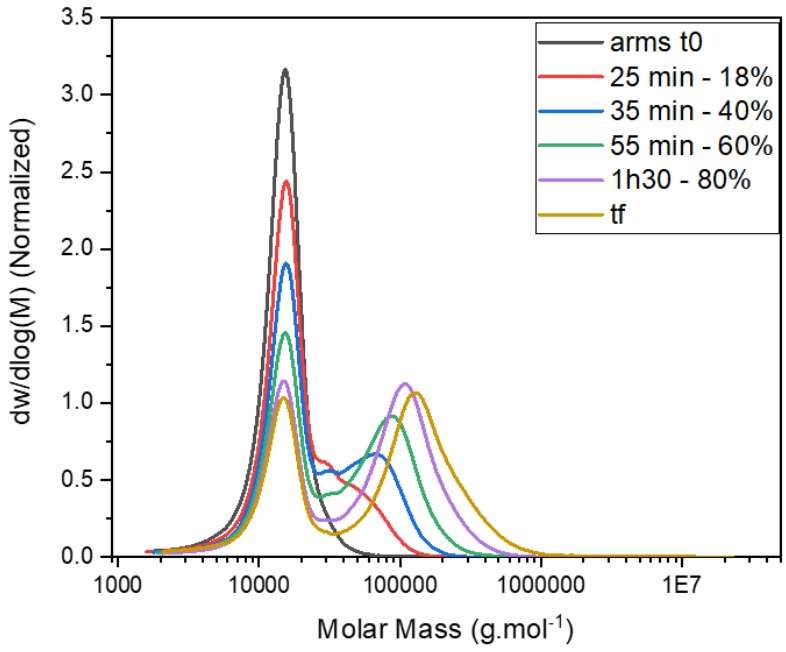

Figure 4.10: GPC traces of the kinetic of star formation ([CL]=0.2M, [CL]/[mCTA]=3, [mCTA]/[I]=20).

4.3.4. Star copolymer characterisation

The batch of star copolymers described above were characterised by DMF-GPC and ^{1}H NMR spectroscopy, and results are presented in Table 4.4 and Figure 4.12. For the block-copolymers and the stars, triple detection was used allowing the determination of different constants such as α and K values. The core crosslinked star copolymers made of the well-defined block copolymers ($Đ$ < 1.1) showed higher dispersities ($Đ$=2.2 - 2.35) as it is sometimes expected from such structures. Mark-houwink plots yielded lower alpha values (α=0.24-0.31) than their respective arms (α=0.35-0.41).

The number of arm per stars, N_{arm}, can be calculated using the absolute molecular weight of the stars, it corresponds to the ratio of the average molecular weight of the stars ($M_{w,star,\ MALS}$) to the average molecular weight of the arms ($M_{w,arm,GPC}$) :

$$N_{arm} = \frac{M_{w,star,MALS}}{M_{w,arm,GPC}}$$

The arm incorporation can be calculated from the output of the RI detector by plotting dw/dlogM out of absolute molecular weight squared determined by light scattering against retention time (**Figure 4.11**) with equation below:

$$Inc. = \frac{nb\ arms\ in\ stars}{nb\ total\ arms} = \frac{N_{arm} * A_{star}}{A_{arms} + N_{arm} * A_{star}}$$

Where A_{star} and A_{arms} are the areas under their corresponding peak (**Figure 4.11**)

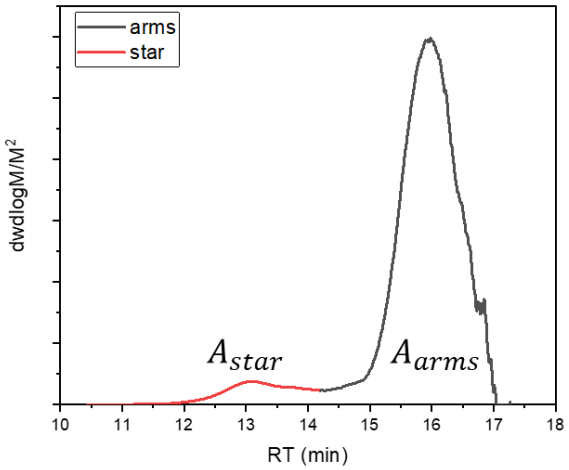

Figure 4.11: Integration of arm peak and stars peak from RI signal. Plot of dw/dlogM out of absolute molecular weight square determined by light scattering against retention time.

Stars with longer arms have an average of 100 arms per star while the one with smaller arms have an average of 65 arms per star as calculated. For the stars with longer arms, 75% of the linear chains were incorporated and 83% for the one with shorter arms. Shorter arms were easier to incorporate as there was less steric hindrance, and the number of arms per star was lower. Hydrodynamic radius (R_H) of the 2 stars are in agreement as R_H of the bigger one is double (11 nm) the one of the smaller one (5.5 nm).

Table 4.4: Characterisation of star polymers. Conversion is determined by ^{1}H NMR and molar mass are determined by DMF-GPC, absolute molecular weight from light scattering detection, α=Kuhn-Mark-Houwink-Sakurada parameter from viscometry detector, N_{arm} = number of arms per star, arm incorporation is calculated from RI detector.

	Code	$M_{n,th}$ g/mol	Conv. %	$M_{n,\ GPC\ DMF}$ g/mol	$M_{w,\ GPC\ DMF}$ g/mol	*Đ*	*α*	R_H nm	N_{arm}	arm incorp. %
$L_{(DMAEA-stat-DMAEMA)_{25}}$		3500	91	11100	11300	1.02	-	-	-	-
$L_{(DMAEA-s-DMAEMA)_{25}-b-NAM_{12}}$		5500	95	15300	16600	1.09	0.41	-	-	-
$S_{(DMAEA-s-DMAEMA)_{25}-b-NAM_{12}}$	Star 1	-	99	383900	868800	2.26	0.31	11	100	75
$L_{(DMAEA-stat-DMAEMA)_{12}}$		1800	89	9100	9900	1.09	-	-	-	-
$L_{(DMAEA-s-DMAEMA)_{12}-b-NAM_{7}}$		2800	97	6200	6500	1.06	0.35	-	-	-
$S_{(DMAEA-s-DMAEMA)_{12}-b-NAM_{7}}$	Star 2	-	99	41300	95800	2.32	0.24	5.5	65	83
$L_{(DMAEA-s-DMAEMA-s-NAM)_{40}}$		5600	91	12500	13900	1.11	0.55	-	-	-
$S_{(DMAEA-s-DMAEMA-s-NAM)_{40}}$	Star 3	-	98	228 800	380 800	1.66	0.28	10	55	50

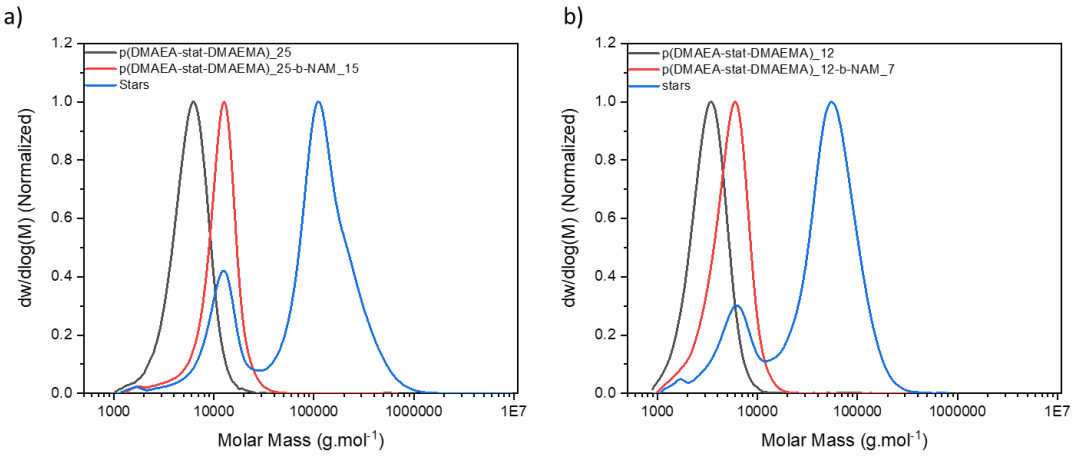

Figure 4.12: DMF-GPC traces of formation of stars from first block of pDMAEA-stat-DMAEMA to star with a first block of a) DP 25 and b) DP12 after chain extension with NAM ([CL]=2M, [M]/[mCTA]= a)15 and b)7, [mCTA]/[I]=20) and crosslinking with bisacrylamide ([CL]=0.2M, [CL]/[mCTA]=3, [mCTA]/[I]=20).

In order to make the synthesis simpler, NAM was copolymerised with DMAEA and DMAEMA in one-step to yield a statistical copolymer, rather than a block as previously described. The reaction kinetics were followed by ^{1}H NMR spectroscopy and DMF-GPC (Figure 4.13). All three monomers were incorporated, DMAEMA was still incorporated the fastest, then NAM and DMAEA making the copolymer slightly gradient. The linear increase of molar mass with conversion and low dispersities ($Đ$=1.3) are characteristic features of controlled radical polymerisation. After purification, the linear chains were crosslinked with the same conditions as used previously and then purified to remove the unreacted arms. Alpha values for the formed stars are in the range of the others: 0.28 in agreement with star formation as a compact structure (Table 4.4).

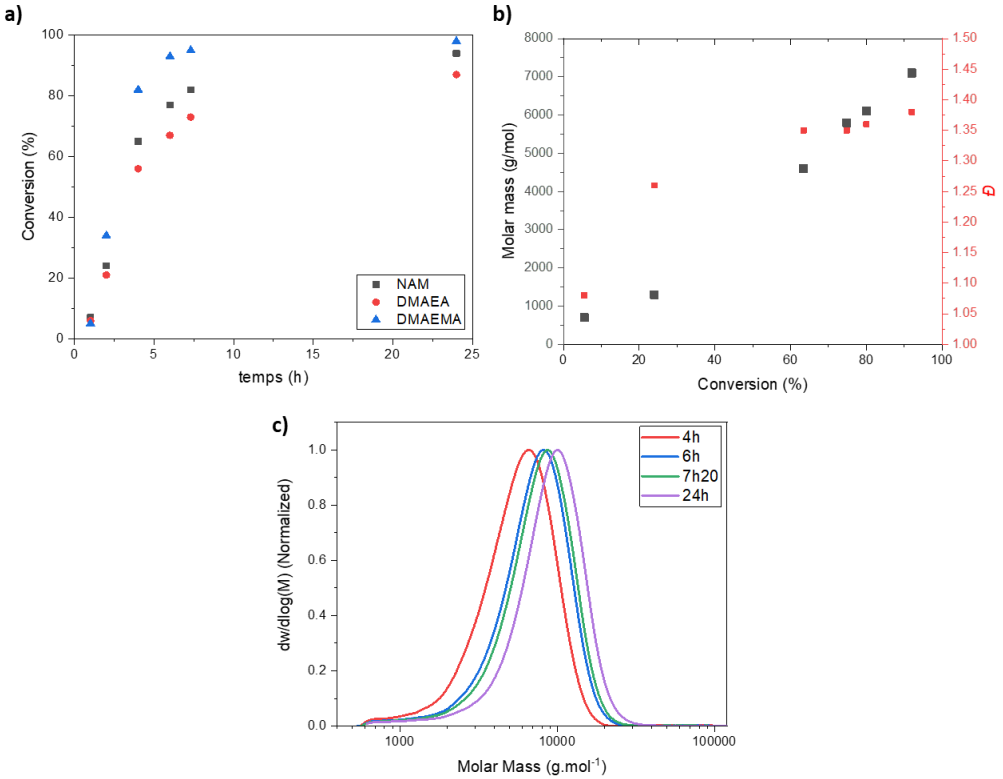

Figure 4.13: Copolymerisation of NAM with DMAEA and DMAEMA ([DMAEA]:[DMAEMA]:[NAM]:[CTA]:[I]= 20:5:15:1:0.05) a) evolution of conversion with time, conversion calculated by 1H NMR b) Mn=f(conversion) plot. c) DMF-GPC traces of copolymerisation.

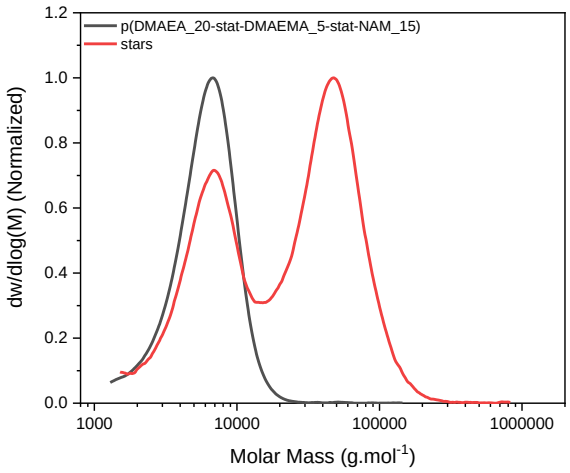

Figure 4.14: GPC traces of star formation from the statistical copolymer of DMAEA, DMAEMA and NAM.

Stars were further characterised using SAXS and AFM. SAXS data were fitted to a polydisperse star polymer model (Figure 4.16). This model describes the scattering from linear Gaussian polymer chains crosslinked to a central core. The zero-angle intensity (I_0) is proportional to the concentration and size of the individual stars. Other input parameters include the radius of gyration (R_g) of the individual polymer chains within the star, and the number of arms. Here, the number of arms was fixed according to the number of arms determined through GPC analysis. The R_g was fit to a lognormal distribution, where the number averaged R_g and the standard deviation were fitted parameters. The number average $\overline{R_g}$ was calculated for the three stars (Table 4.5), Star 1 had a $\overline{R_g}$ of 77 Å, while Star 3 with the same arm length had a $\overline{R_g}$ of 98 Å but with a higher standard deviation (0.59). Star 1 was better defined with a standard deviation of 0.22 (Figure 4.16b). This was supported by AFM images (Figure 4.17), more aggregation could be observed with Star 3 whereas better defined spheres could be observed for Star 1. Star 2 had a smaller $\overline{R_g}$ (71 Å) with a higher standard deviation of 0.50. This could also be observed with AFM, where small stars could be seen but also bigger aggregates.

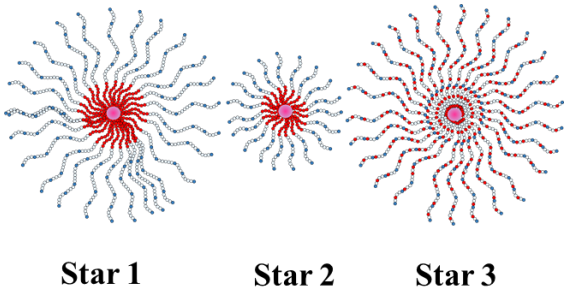

Figure 4.15: Star representation. Light blue circles represent DMAEA, darker blue circles correspond to DMAEMA monomer, red circles corresponds to NAM and the pink center represent the crosslinked core linking the arms with the bisacrylamide difunctional monomer.

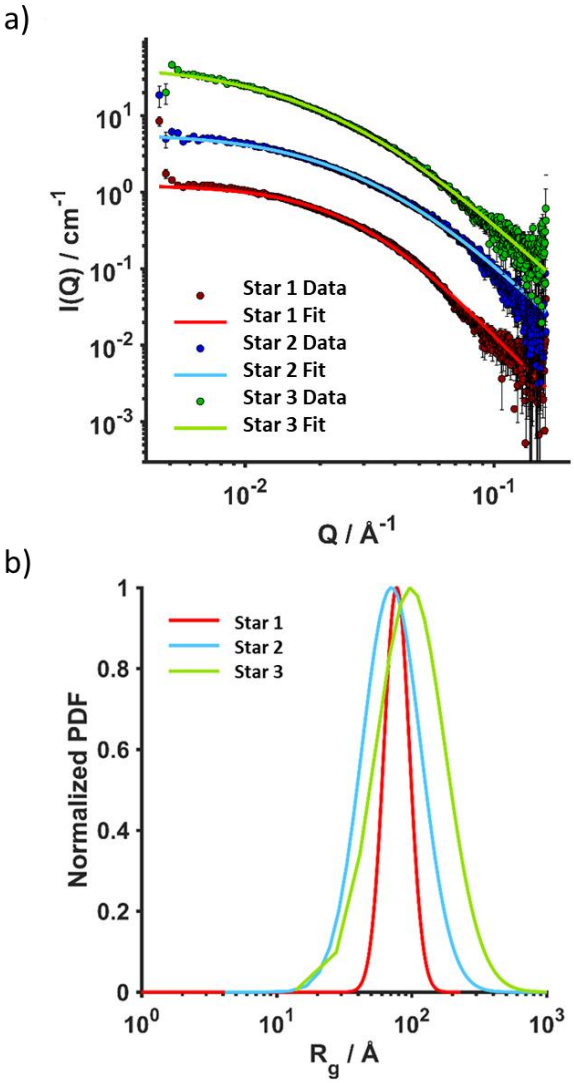

Figure 4.16: SAXS analysis in DMF (2 mg/mL, 25°C). of star 1, star 2 and star 3. a) overlay of raw data and fittings (polydisperse star polymer model), b) Radius of gyration fit to a lognormal distribution.

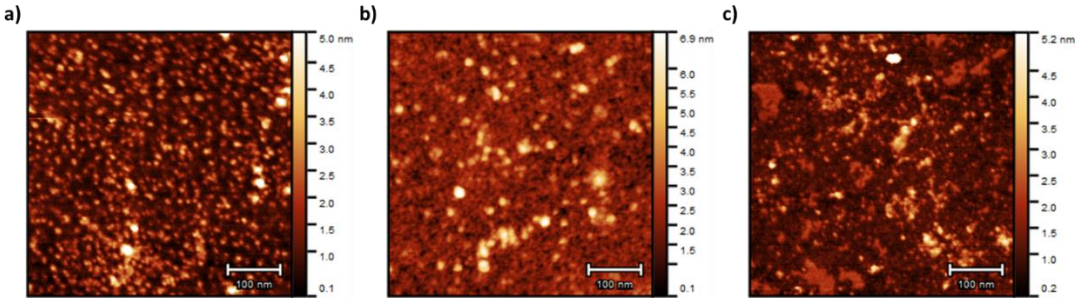

Figure 4.17: AFM pictures of a) Star 1, b) Star 2 and c) Star 3. The samples were prepared at 0.025 mg/mL onto freshly cleaved mica.

Table 4.5: Structural parameters obtained by fitting SAXS data of the star copolymers. Error values represent the standard error associated with the fitted values. N_{arms} represents the number of arms within each star and was held constant throughout the fitting procedure based on the number of arms determined via SEC analyses. $\overline{R_g}$ represents the number averaged radius of gyration of individual polymer chains within the star. σ represents the standard deviation of the lognormal distribution in R_g.

Parameter	**Polymer**		
	Star 1	**Star 2**	**Star 3**
$\boldsymbol{I_0}$ / cm^{-1}	1.23 ± 0.01	1.13 ± 0.01	1.74 ± 0.02
$\boldsymbol{N_{arms}}$	100	65	55
$\boldsymbol{\overline{R_g}}$ / Å	77.32 ± 0.16	70.77 ± 0.21	97.89 ± 0.46
$\boldsymbol{\sigma}$	0.22 ± 0.01	0.50 ± 0.01	0.59 ± 0.01

4.3.5. Study of the hydrolysis of DMAEA: influence of the architecture

After successful synthesis of the desired star copolymers, the impact of the compact star architecture on the hydrolysis of the DMAEA side chains was investigated in the same conditions as those used for the linear chains.

The change from a linear to star structure is not expected to have significant influence on the hydrolysis, as indicated by previous research on branched architectures and stars with low number of arms.[9, 10, 21] To confirm this, the hydrolysis of these structures were compared to their linear arms. Initially, all star copolymers hydrolysed quickly, exhibiting 30% hydrolysis in 2 days (Figure 4.18a). Following this initial rapid phase, the rate of hydrolysis decreased, especially for the smaller star, Star 3, which continue to slowly hydrolyse from 33% at 2 days to 52% at 62 days. The star made of statistical DMAEA, DMAEMA and NAM arms reached 68% hydrolysis in 62 days. This might be due to the presence of the hydrophilic NAM units which improve accessibility of water molecules inside the dense structure. Compared to their arms, the hydrolysis of the stars was slowed down more for the stars and the final hydrolysis was lower as hydrolysis reached 56% and 52% for the two stars whereas it reached 62% for both the arms (Figure 4.18c and d). The accessibility to the reactive units and hydrophilicity of the polymer seems to influence the rate and extent of hydrolysis after the initial period.

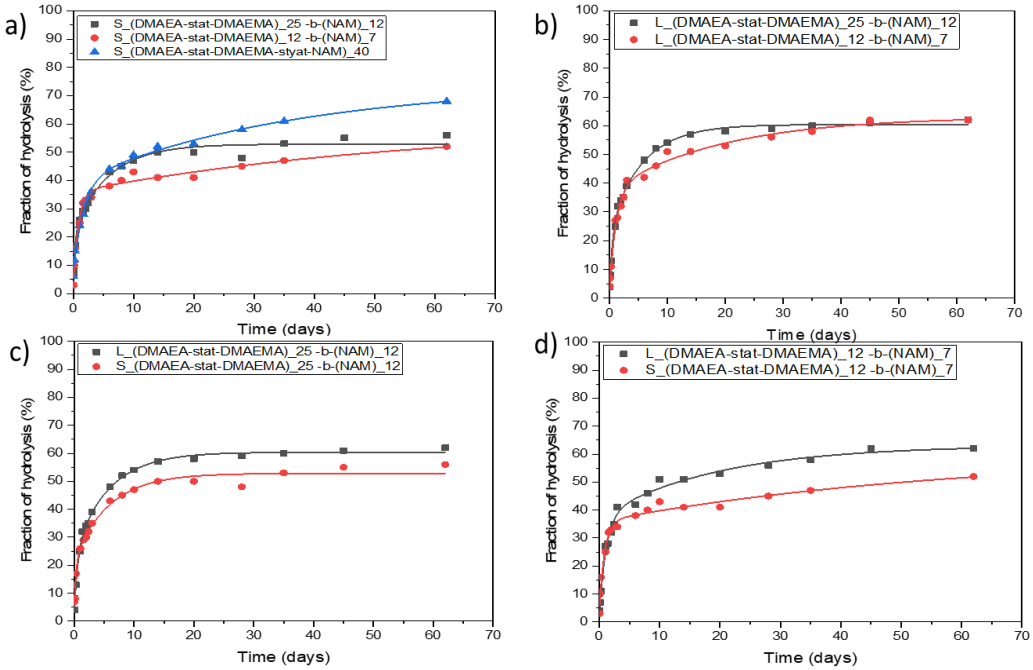

Figure 4.18: Hydrolysis study of stars compared to linear arms at room temperature in D_2O a) comparison of the 3 different stars b) comparison of the 3 different arms c) comparison of bigger stars with DP 25 of DMAEA and DMAEMA arms with corresponding arms d) comparison of smaller stars with DP 12 of DMAEA and DMAEMA arms with corresponding arms.

4.4. Conclusions

The aim of this chapter was to synthesise different copolymers of hydrolysable DMAEA and non-hydrolysable DMAEMA in order to study the influence of the composition on the hydrolysis of the DMAEA side chains and to look at the influence of the architecture with dense and compact star pDMAEA-DMAEMA structure.

A series of well-defined linear copolymer of DMAEA and DMAEMA were obtained (M_n ~ 7000 – 8 000 g/mol, $Đ$ <1.25) with conversions between 80 and 85% and with varied ratios of DMAEA:DMAEMA monomers from 100% DMAEA to 50% DMAEA. As expected, the hydrolysis was lower and slower with increasing amount of non-hydrolysable DMAEMA comonomers in the chain. Only 20% of the side chains are hydrolysed for a copolymer with 50% DMAEA while 70% is hydrolysed when the chain is composed of 100% DMAEA. This can be attributed to the hydrophobic nature of DMAEMA which is not compensated by the non-switchable cationic charge it brings.

In a second part, the influence of the architecture was studied. Star-shaped structures were synthesised using the arm-first approach by chain extending linear preformed arms with a crosslinker to bind the end of the arms covalently. The chain extension from DMAEA units showed to be challenging since only satisfactory results were obtained with acrylamide monomers (NAM and bisacrylamide crosslinker). Moreover, in order to obtain stable and soluble stars after purification and drying, a block of NAM was introduced before crosslinking to reduce the positive charge. This non-cationic part composed about 40% of the chain. Two different stars were synthesised with this non-cationic block, a star with a first block of DMAEA and DMAEMA with a DP targeted of 25 (M_n ~ 3 500 g/mol) and a smaller star with a first block with a targeted DP of 12 (M_n ~ 1 800 g/mol). A third star was synthesised with arms made by statistical copolymerisation of NAM with DMAEA and DMAEMA (M_n ~ 5 600 g/mol). All the stars were obtained with a high number of arms (N_{arm} ~ 55 – 100) and satisfactory arm incorporation (50 – 83%). Better arm incorporation was observed with smaller arms and with arms chain extended from NAM and not DMAEA. Their hydrolysis was then studied. Small differences were observed after the initial period as the hydrolysed fraction of side chains were slightly higher for the

arms compared to the stars. This can be explained by the dense and compact structure making the access for water more difficult for hydrolysis to occur.

4.5. Experimental

4.5.1. Materials

Ethanethiol (Sigma-Aldrich, 97%), sodium hydroxide (Sigma-Aldrich), carbone disulphide (Sigma-Aldrich, 99%), iodine (Acros Organics),2-(Dimethylamino)ethyl acrylate (DMAEA; Sigma-Aldrich, 98%), 2-(dimethylamino)ethyl methacrylate (DMAEMA; Sigma-Aldrich, 98%), methyl acrylate (MA; Sigma-Aldrich, 99%), methyl methacrylate (MMA; Sigma-Aldrich, 99%), *N*,*N*′-methylenbis(acrylamide) (NAM; Sigma-Aldrich, 99%), 4,4′-Azobis(4-cyanovaleric acid) (ACVA; Alfa Aesar, 98%), 1,1'-azobis(cyclohexane-1-carbonitrile) **(**V40; Sigma-Aldrich, 98%), 2,2'-azobis[*N*-(2-hydroxyethyl)-2-methylpropionamide] (VA86; Wako chemicals).

DMAEA, DMAEMA, NAM monomers were passed through alumina column prior to use.

4.5.2. Synthesis

4.5.2.1. Synthesis of the CTA, (4-cyano pentanoic acid)yl ethyl trithiocarbonate (CPAETC)

Ethanethiol (9.0 mL, 121.5 mmol, 1 equiv.) was added to diethyl ether (100 mL) under strong stirring at room temperature, to which a 27 wt % aquous solution of sodium hydroxide (about 20 g of solution containing 4.86 g of NaOH, 121.5 mmol, 1 equiv.) was added. The clear, colourless solution was stirred for 30 min. It was then treated with carbon disulphide (9.1 mL, 151.9 mmol, 1.25 equiv.) to give an orange solution. After further 30 minutes stirring, a solution of iodine (9.6 g, 76.0 mmol, 0.5 equiv.) in 30 mL diethyl ether was slowly added via a dropping funnel. After 1.5 hours, diethyl ether (60 mL) was added and the ether phase washed twice with an aqueous solution of sodium thiosulfate (100 mL) and once with water (100 mL). The ether phase was dried over magnesium sulfate, filtered and the solvent removed under reduced pressure to give the intermediate product bis-(ethylsulfanylthiocarbonyl) disulfide as an orange oil. ^{1}H NMR (400 MHz, $CDCl_3$): δ=3.3 (4H, t, -CH_2-S), 1.4 (6H, m, -CH_3).

As the intermediate product is more stable than the final product, only a part of it was used for the second step, the rest was stored in the fridge.

To a solution of bis-ethylsulfanylthiocarbonyl) disulphide (2.04 g, 7.8 mmol, 1 equiv.) in 50 mL of dioxane, 4,4′-azobis(4-cyanovaleric acid) (ACVA) (4.5 g, 16.3 mmol, 2.1 equiv.) was added and the mixture was stirred for 20 hours at 75°C. The solvent was removed under reduced pressure and chloroform (100 mL) was added, the phase was washed 3 times with water (75 mL). The organic phase was dried over magnesium sulfate, filtered and the solvent removed under reduced pressure. The product was purified by silica gel column chromatography (eluent: n-hexane/ethyl acetate, gradient from 100/0 to 20/80 over 30 min). After drying under vacuum, a yellow powder was obtained with a yield for the second step of 80%. ^{1}H NMR (400 MHz, $CDCl_3$): δ (ppm) = 3.3 (2H, q, J=7.2 Hz, -CH_2-S), 2.7 (2H, t, J=7.2 Hz, -CH_2-), 2.6 (1H, dd, -CH-H-), 2.7 (1H, dd, -H-CH-), 1.9 (3H, s, -CH_3), 1.4 (3H, t, J=7.2 Hz, -CH_3) (Figure A4.4). ^{13}C NMR (400 MHz, $CDCl_3$): δ (ppm) = 216.6, 176.9, 118.9, 46.2, 33.5, 31.5, 29.5, 24.8, 12.7 (Figure A4.5). Analysis were matching what was reported in the literature.[13, 22]

4.5.2.2. Synthesis of P(DMAEA-*co*-DMAEMA)

For a typical polymerisation in which [DMAEA]:[DMAEMA]:[CTA]:[I] = 40:10:1:0.05, CPAETC (31.6 mg , 0.12 mmol), DMAEA (687.3 mg, 4.80 mmol), DMAEMA (188.6 mg, 1.20 mmol), ACVA (1.7 mg, 0.01 mmol) and dioxane (1.07 mL) were added to a vial equipped with a magnetic stirrer and deoxygenated by bubbling with nitrogen for 25 minutes. The vial was place in an oil bath at 70°C for 24 hours. Monomer conversions are determined by ^{1}H NMR. The polymer is precipitated 3 times in n-Hexane and dried under vacuum. The material was analysed by GPC and ^{1}H NMR (400 MHz, $CDCl_3$): δ (ppm) = 4.1 (-CO-O-C**H**$_2$-CH_2-), 2.5 ((-CO-O-CH_2-C**H**$_2$-), 2.3 (-C-(C**H**$_3$)$_2$ + -CH(CH_2-)(CO-O-)), 2.0 – 1.2 (backbone) (Figure A4.3).

4.5.2.3. Chain extensions: p(DMAEA-*stat*-DMAEMA-*b*-NAM)

For the synthesis of the first block (mCTA) refer to the synthesis of p(DMAEA-*co*-DMAEMA). A typical synthesis is given here for an extension of the chain with NAM in which [NAM]:[mCTA]:[I] = 15:1:0.05. The mCTA (3 500 g.mol^{-1}) (1 223

mg, 0.35 mmol), NAM (740 mg, 5.25 mmol) and ACVA (0.22 mg, 0.001 mmol) were dissolved in dioxane (1.95 mL) in a vial equipped with a magnetic stirrer and deoxygenated by bubbling with nitrogen for 25 minutes. The vial was place in an oil bath at 70°C for 6 hours. Monomer conversions are determined by ^{1}H NMR and the final material analysed by DMF GPC and ^{1}H NMR (400 MHz, $CDCl_3$): δ (ppm) = 4.1 – 3.2 (-CO-O-C**H**$_2$-CH$_2$- from DMAEA and DMAEMA + -O-**CH$_2$-CH$_2$**-N-), 2.2 – 2.8 ((-CO-O-CH$_2$-C**H**$_2$- from DMAEA and DMAEMA + -CH$_2$-C**H**-CO- from NAM), 2.3 – 1.5 (-C-(C**H**$_3$)$_2$ + -C**H**(CH$_2$-)(CO-O-) from DMAEA and DMAEMA + -C**H**$_2$-CH- NAM backbone), 2.0 – 1.2 (backbone).

4.5.2.4. Synthesis of star polymers

For the synthesis of the arms (mCTA) refer to the synthesis of p(DMAEA-*co*-DMAEMA-*b*-NAM). For a typical synthesis, [Bisacrylamide]:[mCTA]:[I] = 3:1:0.05, the mCTA (5 500 g.mol^{-1}) (910 mg, 0.17 mmol), bisacrylamide (76.5 mg, 0.50 mmol), ACVA (2.32 mg, 0.008 mmol) in dioxane (2.50 mL) were added in a vial equipped with a magnetic stirrer and deoxygenated by bubbling with nitrogen for 15 minutes. The vial was place in an oil bath at 70°C for 5 hours. Monomer conversions are determined by ^{1}H NMR and the material analysed by DMF GPC and ^{1}H NMR (400 MHz, $CDCl_3$): δ (ppm) = 4.1 – 3.2 (-CO-O-C**H**$_2$-CH$_2$- from DMAEA and DMAEMA + -O-**CH$_2$-CH$_2$**-N-), 2.2 – 2.8 ((-CO-O-CH$_2$-C**H**$_2$- from DMAEA and DMAEMA + -CH$_2$-C**H**-CO- from NAM), 2.3 – 1.5 (-C-(C**H**$_3$)$_2$ + -C**H**(CH$_2$-)(CO-O-) from DMAEA and DMAEMA + -C**H**$_2$-CH- NAM backbone + bisacrylamide), 2.0 – 1.2 (backbone).

4.5.3. Hydrolysis study

The hydrolysis studies of the copolymers were performed in NMR tubes at 10 mg/mL in D_2O at room temperature. The reaction was followed by ^{1}H NMR spectroscopy.

4.5.4. AFM

AFM images were taken using an Asylum Research MFP-3D stand alone atomic force microscope. Samples were prepared by drop casting 5 µL of aqueous polymer solution at 0.025 mg/mL onto freshly cleaved mica, leaving to stand for 1 minute, tipping substrate and drying with filter paper, then under a stream of nitrogen.

4.6. References

1. McCool, M.; Senogles, E., The self-catalysed hydrolysis of poly (N, N-dimethylaminoethyl acrylate). *Eur. Polym. J.* **1989,** *25* (7-8), 857-860.

2. Truong, N. P.; Jia, Z.; Burges, M.; McMillan, N. A.; Monteiro, M. J., Self-catalyzed degradation of linear cationic poly (2-dimethylaminoethyl acrylate) in water. *Biomacromolecules* **2011,** *12* (5), 1876-1882.

3. Truong, N. P.; Jia, Z.; Burgess, M.; Payne, L.; McMillan, N. A.; Monteiro, M. J., Self-catalyzed degradable cationic polymer for release of DNA. *Biomacromolecules* **2011,** *12* (10), 3540-3548.

4. Whitfield, R.; Anastasaki, A.; Truong, N. P.; Wilson, P.; Kempe, K.; Burns, J. A.; Davis, T. P.; Haddleton, D. M., Well-defined PDMAEA stars via Cu (0)-mediated reversible deactivation radical polymerization. *Macromolecules* **2016,** *49* (23), 8914-8924.

5. Ros, S.; Burke, N. A.; Stöver, H. D., Synthesis and Properties of Charge-Shifting Polycations: Poly [3-aminopropylmethacrylamide-co-2-(dimethylamino) ethyl acrylate]. *Macromolecules* **2015,** *48* (24), 8958-8970.

6. Ros, S.; Kleinberger, R. M.; Burke, N. A.; Rossi, N. A.; Stöver, H. D., Charge-Shifting Polycations with Tunable Rates of Hydrolysis: Effect of Backbone Substituents on Poly [2-(dimethylamino) ethyl acrylates]. *Macromolecules* **2018**.

7. Ros, S.; Wang, J.; Burke, N. A. D.; Stöver, H. D. H., A Mechanistic Study of the Hydrolysis of Poly[N,N-(dimethylamino)ethyl acrylates] as Charge-Shifting Polycations. *Macromolecules* **2020,** *53* (9), 3514-3523.

8. Gurnani, P.; Blakney, A. K.; Terracciano, R.; Petch, J. E.; Blok, A. J.; Bouton, C. R.; McKay, P. F.; Shattock, R. J.; Alexander, C., The In Vitro, Ex Vivo, and In Vivo Effect of Polymer Hydrophobicity on Charge-Reversible Vectors for Self-Amplifying RNA. *Biomacromolecules* **2020,** *21* (8), 3242-3253.

9. Cook, A.; Peltier, R.; Hartlieb, M.; Whitfield, R.; Moriceau, G.; Burns, J.; Haddleton, D.; Perrier, S., Cationic and hydrolysable branched polymers by RAFT for complexation and controlled release of dsRNA. *Polym. Chem.* **2018**.

10. Rolph, M. S.; Pitto-Barry, A.; O'Reilly, R. K., The hydrolytic behavior of N, N′-(dimethylamino) ethyl acrylate-functionalized polymeric stars. *Polym. Chem.* **2017,** *8* (34), 5060-5070.

11. Barner-Kowollik, C., *Handbook of RAFT polymerization*. John Wiley & Sons: 2008.

12. Perrier, S. b., 50th Anniversary Perspective: RAFT Polymerization· A User Guide. *Macromolecules* **2017,** *50* (19), 7433-7447.

13. Larnaudie, S. C.; Brendel, J. C.; Jolliffe, K. A.; Perrier, S., Cyclic peptide–polymer conjugates: Grafting-to vs grafting-from. *J. Polym. Sci., Part A: Polym. Chem.* **2016,** *54* (7), 1003-1011.

14. Ho, H. T.; Bohec, M. L.; Frémaux, J.; Piogé, S.; Casse, N.; Fontaine, L.; Pascual, S., Tuning the Molar Composition of "Charge-Shifting" Cationic Copolymers Based on 2-(N, N-Dimethylamino) Ethyl Acrylate and 2-(tert-Boc-Amino) Ethyl Acrylate. *Macromol. Rapid Commun.* **2017,** *38* (5).

15. Ren, J. M.; McKenzie, T. G.; Fu, Q.; Wong, E. H. H.; Xu, J.; An, Z.; Shanmugam, S.; Davis, T. P.; Boyer, C.; Qiao, G. G., Star Polymers. *Chem. Rev.* **2016,** *116* (12), 6743-6836.

16. Rohini Anandrao, P.; Aloorkar, N. H.; Kulkarni, A. S.; Ingale, D. J., Star Polymers: An Overview. *Int. J. Pharm. Sci. Nanotech* **2012,** *5* (2).

17. Barner-Kowollik, C.; Davis, T. P.; Stenzel, M. H., Synthesis of Star Polymers using RAFT Polymerization: What is Possible? *Aust. J. Chem.* **2006,** *59* (10), 719-727.

18. Chen, Q.; Cao, X.; Xu, Y.; An, Z., Emerging Synthetic Strategies for Core Cross-Linked Star (CCS) Polymers and Applications as Interfacial Stabilizers: Bridging Linear Polymers and Nanoparticles. *Macromol. Rapid Commun.* **2013,** *34* (19), 1507-1517.

19. Whitfield, R. The controlled radical polymerisation of hydrophobic and cationic monomers via Cu(0)-RDRP. University of Warwick, 2018.

20. Ferreira, J.; Syrett, J.; Whittaker, M.; Haddleton, D.; Davis, T. P.; Boyer, C., Optimizing the generation of narrow polydispersity 'arm-first' star polymers made using RAFT polymerization. *Polym. Chem.* **2011,** *2* (8), 1671-1677.

21. Whitfield, R.; Anastasaki, A.; Truong, N. P.; Cook, A. B.; Omedes-Pujol, M.; Loczenski Rose, V.; Nguyen, T. A.; Burns, J. A.; Perrier, S. b.; Davis, T. P., Efficient Binding, Protection, and Self-Release of dsRNA in Soil by Linear and Star Cationic Polymers. *ACS Macro Lett.* **2018,** *7*, 909-915.

22. Moad, G.; Chong, Y. K.; Postma, A.; Rizzardo, E.; Thang, S. H., Advances in RAFT polymerization: the synthesis of polymers with defined end-groups. *Polymer* **2005,** *46* (19), 8458-8468.

4.7. Appendix

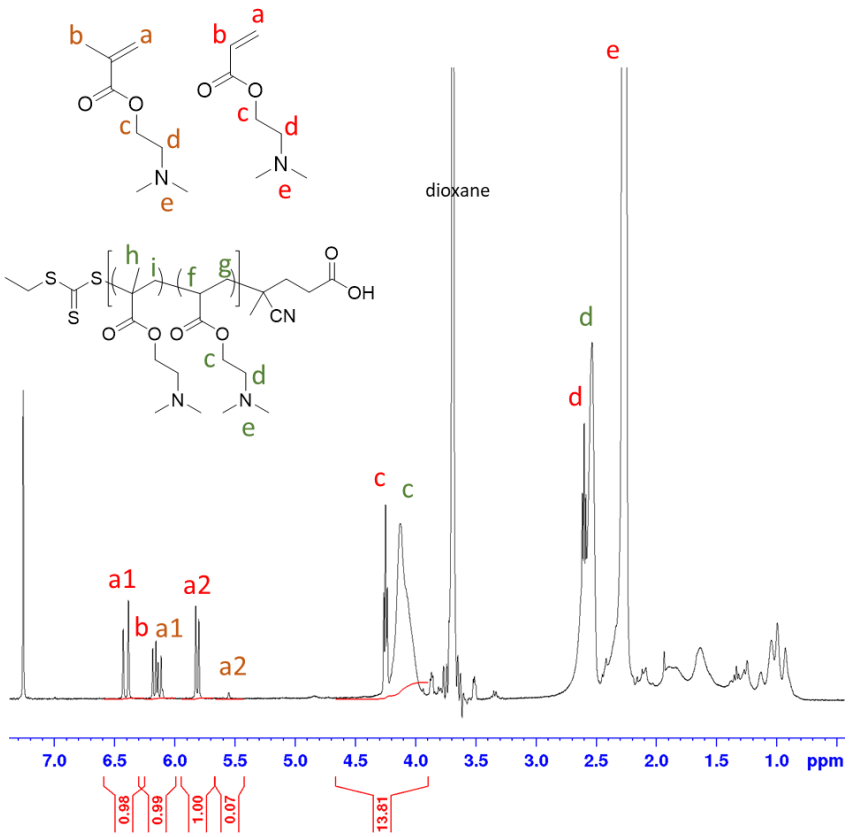

Figure A 4.1: ^{1}H NMR spectrum (400 MHz, $CDCl_3$, 128 scans) of unpurified p(DMAEA$_{70}$-co-DMAEMA$_{30}$).

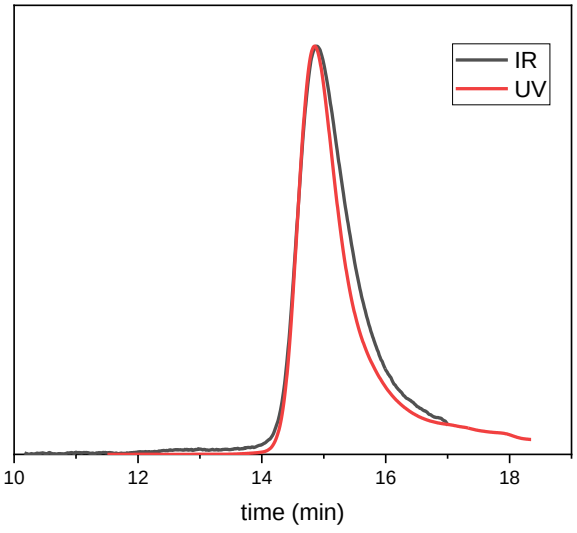

Figure A4.2: DMF-GPC traces of RI and UV signals of p(DMAEA-co-DMAEMA).

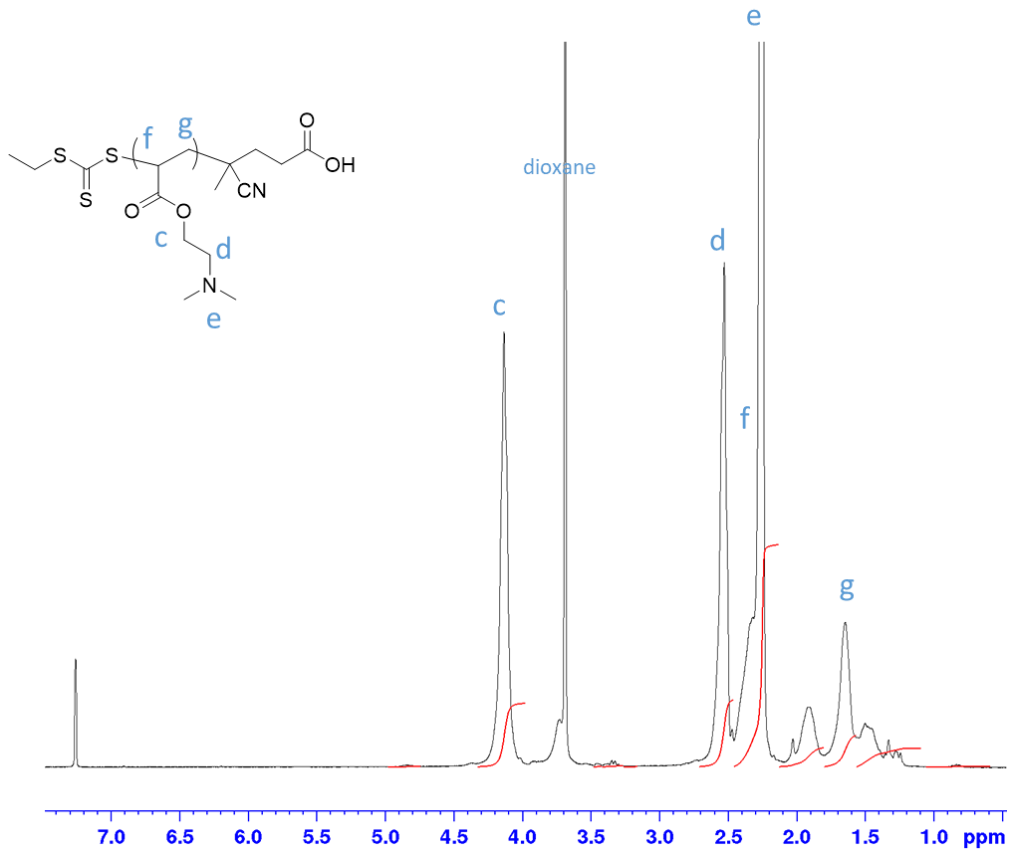

Figure A4.3: ^{1}H NMR spectrum (400 MHz, $CDCl_3$, 128 scans) of purified pDMAEA in $CDCl_3$.

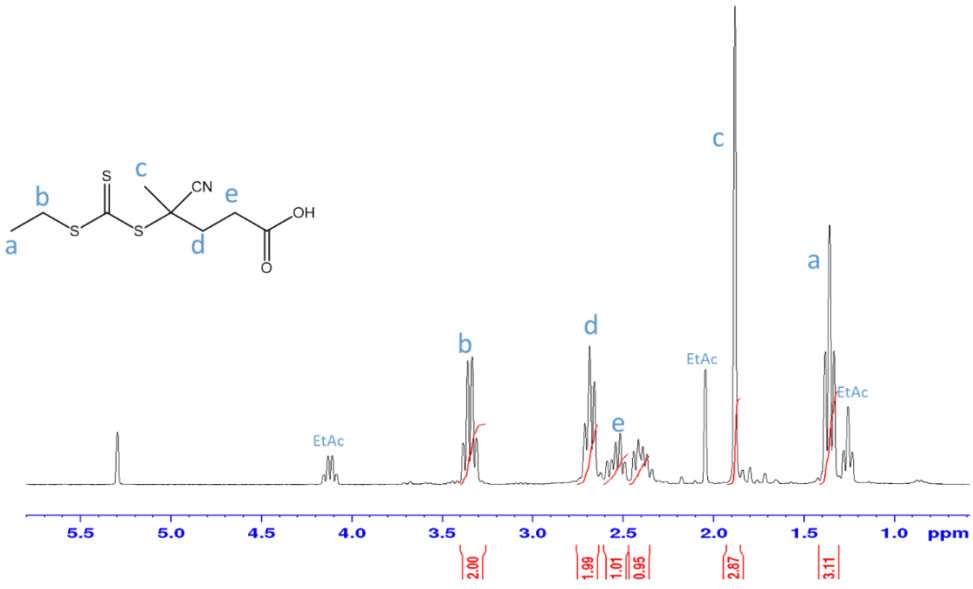

Figure A4.4: ^{1}H NMR spectrum of CPAETC (400 MHz, $CDCl_3$, 128 scans).

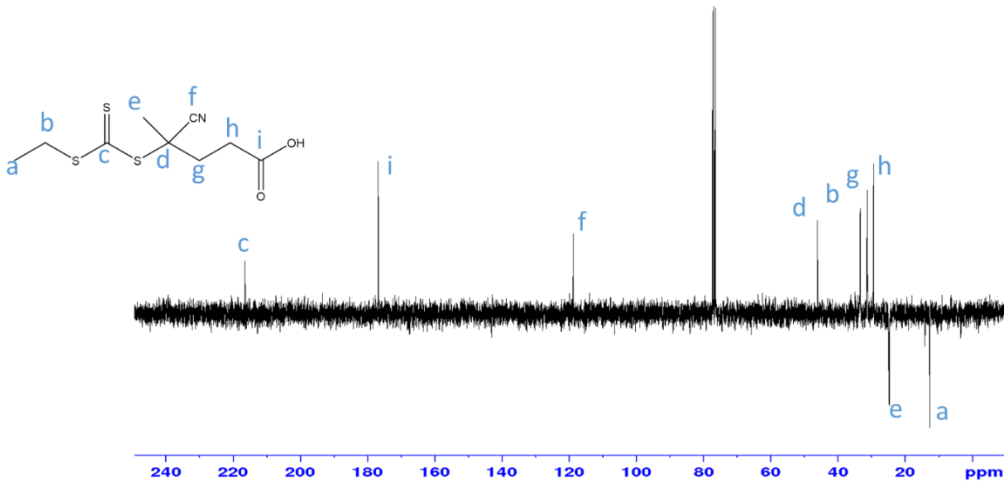

Figure A4.5: ^{13}C NMR spectrum of CPAETC (400 MHz, $CDCl_3$, 512 scans).

Chapter 5: Assessing the Ability of pDMAEA-DMAEMA Copolymers to Bind, Protect and Release Nucleic Acids.

5.1. Abstract

Here, the impact of the incorporation of DMAEMA as a non-hydrolysable comonomer on the release of dsRNA was studied. By increasing the DMAEMA content, the release was slowed down. Full release was delayed to up to 15 days for the copolymer containing 20% DMAEMA, whereas only 2 days were necessary to fully release the dsRNA in the absence of the non-hydrolysable comonomers. However, although the release could be delayed by incorporating DMAEMA statistically, limited protection in soil was obtained with the linear copolymers, including the non-hydrolysable homopolymer of DMAEMA.

Additionally, the influence of the architecture of pDMAEA-DMAEMA copolymers on the complexation with nucleic acids and soil stability was studied. Dense and compact star structure were made by the arm-first approach, with arms composed of 80:20 DMAEA:DMAEMA. Three stars were studied for complexation, Star 1 and 2 were composed of p(DMAEA-*stat*-DMAEMA)-*b*-NAM arms (M_n ~ 5 500 g/mol and 2 800 g/mol respectively) and Star 3 was composed of pDMAEA-*stat*-DMAEMA-*stat*-NAM (M_n ~ 5 600 g/mol). All stars were able to complex dsRNA at N/P ratios of 3 and higher, as well as plasmid DNA (pDNA) at N/P 2 as shown by agarose gel electrophoresis. The resulting polyplexes were positively charged (15 – 29 mV). The study of the release of dsRNA over time showed a less gradual and faster release with the stars than with the linear copolymers. Very limited protection against dsRNase and easy displacement by heparin was observed and no improvement of the stability of dsRNA in soil was observed. These results suggest the binding was weaker than with the linear copolymer because of the dsRNA interacting only at the surface of multiple dense stars, thus forming big polydisperse aggregates (200 – 500 nm) as observed by TEM and SEM. Finally, the three stars and linear copolymers composed

of 80% DMAEA were tested for transfection of pDNA encoding for green fluorescent protein (GFP) into mammalian cells. Poor transfection rates were observed, likely to be due to considerable aggregation. Nevertheless, the copolymers were not toxic to HEK293T even at high concentrations up to 1 mg/mL.

5.2. Introduction

Protection of dsRNA/DNA is necessary to avoid its degradation in the environment.[1-3] Cationic polymers such as pDMAEA or pDMAEMA have shown to efficiently complex nucleic acids through electrostatic binding, thus forming a polyplex that is positively charged.[4-6] In the case of pDMAEA, the ester bond hydrolyses over time in aqueous conditions (**Chapter 3**), releasing the group containing the positive charge and renders the polymer negatively charged. Hence, this charge-shifting leads to the release of the complexed nucleic acids as evidenced for the first time by Truong *et al*.[7, 8] The hydrolysis kinetics seems to play an important role in controlling the speed of the release and the composition seems to be the main parameter. The cationic moiety as well as the architecture seem to be affecting the binding efficiency as discussed below.

5.2.1. Influence of composition on complexation and release

Cook *et al.* reported the copolymerisation of DMAEA with non-hydrolysable DMAEMA, with ratios of DMAEA to DMAEMA of 80% and 20%. For the 80% DMAEA copolymer, full release was observed between 14 and 21 days, whereas no release was observed after 28 days for the 20% hydrolysable copolymer.[9] According to Truong *et al*., it takes less than 2 days to fully release DNA from homopolymer of DMAEA.[7] Therefore, these results are in agreement with the slower and lower hydrolysis seen for these two copolymers. As mentioned in the previous chapter, the hydrolysis of DMAEA-based polymers can be affected by the introduction of comonomers such as APM which is cationic but non-hydrolysable.[10, 11] When APM is added, the hydrolysis is stronger and faster. To slow down hydrolysis, the incorporation of AA as anionic comonomers resulted in slower and lower hydrolysis of the side chains. However, no complexation with DNA or RNA have been reported in the literature to show how it was impacted, but from hydrolysis results we can expect the release speed to be directly related to the hydrolysis rate.

The binding efficiency is also an important parameter affecting the ability of a polymer to provide good protection of the RNA or DNA during its transport into the cytoplasm as well as a good transfection efficiency. The nature of the cationic moiety was shown to have an impact on the strength of the binding, the complexation

efficiency and the transfection.[12, 13] The introduction of aminoethyl acrylate (AEA) as comonomer, a primary amine cationic moiety, with DMAEA was observed to result in high efficiency of interaction with nucleic acids, better transfection efficiency and a reduced toxicity compared to pDMAEA. PAEA presented a similar hydrolysis behaviour to pDMAEA but at a much slower rate. 5.7% hydrolysis was reached after 8 weeks at pH 7 and 37°C in D_2O. The copolymer of 50:50 DMAEA:AEA fully complexed pDNA at N/P ratio of 2 and partial release of plasmid DNA (pDNA) was obtained after 7 days.[14]

5.2.2. Influence of architecture

Polymer architecture and molecular weight were shown to have an important impact on gene delivery efficiency.[15-17] High molecular weight polymers tend to show better DNA/RNA binding, cellular uptake and transfection efficiency, whereas lower molecular weight polymers show less cytotoxicity.[16] This trend has been observed again recently by Richter *et al.* with a systematic study on different types of cationic polymers and varied molecular weights. Longer linear polymers were found to have better transfection efficiency but also higher toxicity as the density of charge was higher. The binding was also improved with higher molecular weight polymers but to a lower extent, as only the smaller polymers were binding pDNA slightly less.[12] Star-shaped structures have shown promising results, having better transfection efficiencies compared to their linear version along with lower toxicity.[18, 19] A decrease in cytotoxicity was observed with increasing number of arms for pDMAEMA polymers and a good transfection efficiency was obtained with molecular weight higher than 20kDa.[20] This can be attributed to the spherical shape of the polyplex and the better condensation of the DNA. It is important to note that to properly compare star polymers, the length of the arms as well as the number of branches have to be taken into account.[21] Liao *et al.* also reported stronger binding of DNA with star-shaped pDMAEA polymers with longer arms.[22] Increasing the size of the polymer showed increase of cytotoxicity, as expected, but the architecture did not have an impact in this study. Whitfield *et al.* reported the complexation of dsRNA with hydrolysable 4-arm pDMAEA star polymer synthesised by the core-first approach. The polymers showed better binding with dsRNA and although the stars were found to have similar hydrolysis rate than their linear equivalent, slower release of dsRNA was observed compared to the linear pDMAEA equivalent at the same molecular weight (Figure

5.1).[23] Cook *et al*. reported the complexation with branched copolymers of DMAEA and DMAEMA and observed protection in soil for more than 7 days.[24] Again, soil conditions are particularly harsh for dsRNA as it is composed of a lot of competing species, disrupting the interactions between the cationic polymer and the nucleic acids. The half-life of naked dsRNA in soil is reported to be of less than 30 hours.[25, 26] Good binding and resistance to competing species is again essential for a good protection in these conditions.

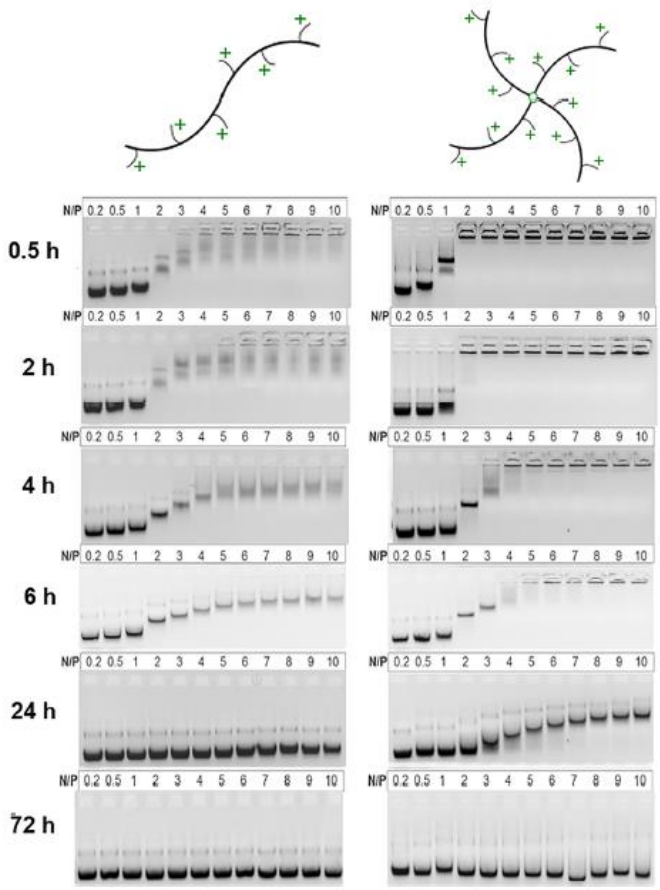

Figure 5.1: Agarose gel electrophoresis of complexes dsRNA with linear pDMAEA and 4-arm pDMAEA. Complexed were formed in sterile water at increasing N/P ratios (0.2, 0.5, 1, 2, 3, 4, 5, 6, 7, 8, 9, 10) and evaluated after 0.5, 2, 4, 6, 24, 72 hours. Samples were incubated at room temperature and loaded onto a 2% w/v agarose gel (100V, 30 min). Figure adapted from ref.[23]

As demonstrated in **chapter 2**, the 4-arm star homopolymers of DMAEA was not as efficient as reported by Whitfield *et al*. in protecting dsRNA in soil conditions. In **chapter 3**, we demonstrated that the hydrolysis of DMAEA could be controlled by incorporating DMAEMA in different proportions. The more DMAEMA in the chain the less hydrolysis was observed. In this chapter, the aim was to study the effect of the composition of linear copolymers on the binding with dsRNA and its release in ideal conditions (in sterile water) and in soil. In a second part, the influence of the dense star architecture combined with the incorporation of DMAEMA as comonomer was investigated. Branched structures with higher content of DMAEMA were showing promising results for the binding and protection of dsRNA in soil.[24] However, the controlled release of dsRNA was desired to make the dsRNA available in soil. Therefore, a higher content of DMAEA (80%) was chosen in order to guarantee its release in soil while extending its stability.

5.3. Results and discussion

5.3.1. Influence of the composition

The linear copolymers with varying ratios of DMAEA:DMAEMA synthesised and characterised in **chapter 3** were tested for complexation with dsRNA and to study the effect of the composition and their hydrolysis on the release of the nucleic acid.

5.3.1.1. Polyplex formation

To assess the binding of dsRNA with the cationic polymers agarose gel electrophoresis was used.[9, 22, 23] Complexation was performed with dsRNA in sterile water at N/P ratios ranging from 0, corresponding to dsRNA only, to 20, with increasing amount of polymers (Figure 5.2). For ratios lower than 1, traces of non-bounded dsRNA could be observed. For copolymers with higher DMAEMA content, a faint band could still be seen at N/P 2 implying a small part of the dsRNA was not incorporated in the polyplexes.

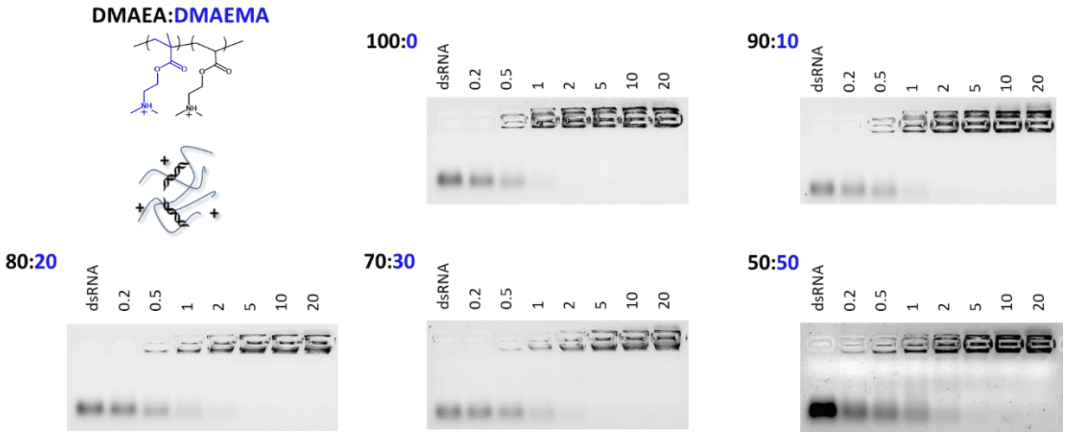

Figure 5.2: Complexation of the different copolymers at N/P ratios 0.2, 0.5, 1, 2, 5, 10, 20 in sterile water onto a 2 % w/v agarose gel (100V, 30 min).

Ethidium bromide displacement assays were performed to bring complementary information on the binding efficiency with the dsRNA. Polyplexes were prepared at N/P ratios from 0 to 10 and the decrease of fluorescence was followed to calculate the percentage of displaced dsRNA by the cationic copolymers (Figure 5.3). Four different copolymers of DMAEA and DMAEMA were tested with branched PEI (bPEI) as a reference. All of them displaced 95-96% of the dsRNA at N/P 2. Differences could be observed at N/P 1 as all copolymers displaced more nucleic acids than bPEI. And polymers with more DMAEA were seen to displace dsRNA more efficiently. This is in agreement with what could be observed with the agarose gel electrophoresis as better complexation was seen with copolymers with higher DMAEA content. However, as the N/P ratio increased, the percentage of relative bound dsRNA slowly decreased for all four copolymers, while bPEI was stable at around 95-96%. This could be explained by the concentration of cationic polymers leading to increasing pH (from around 6.9 for N/P 1 to 8.2 for N/P 10), resulting in less cationic charges as the pKa was approached.

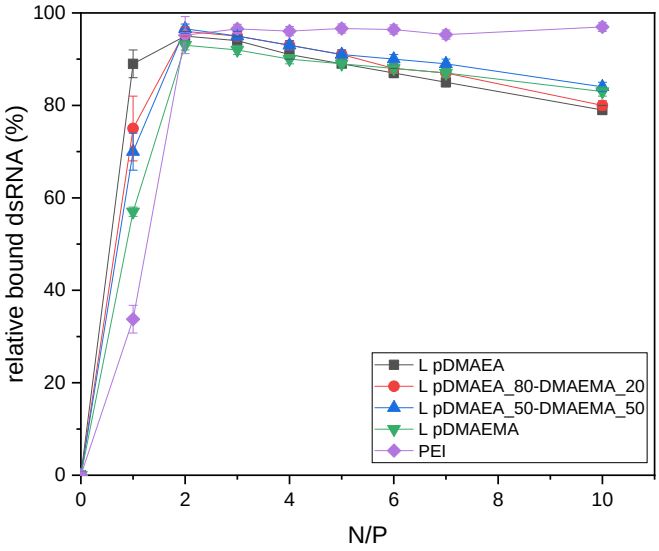

Figure 5.3: Ethidium bromide displacement assays for copolymers with 100, 80, 50 and 0 % DMAEA compared to bPEI

For the following studies, a N/P ratio of 5 was chosen to guarantee a good complexation of the dsRNA.

5.3.1.2. Release of dsRNA

In order to investigate how the composition and the hydrolysis of the polymers could influence the release of the nucleic acids, polyplexes were formed at a N/P ratio of 5 in sterile water and incubated for different amounts of time, up to 30 or 50 days. Results were analysed by agarose gel electrophoresis (Figure 5.4). For the homopolymer of DMAEA, the dsRNA was completely released in less than 2 days, as expected from previous studies,[7, 9, 23, 27] whereas the complex containing 90%, 80%, 70% and 50% DMAEA took 3, 15, 30 and more than 50 days to release, respectively. For the 50% DMAEA, the release was very slow, some changes could be noticed only after 7 days incubation and no full release was reached even after 50 days. This can be explained by the very low amount of hydrolysed side chains (25% after 20 days) that are not enough to release the nucleic acids. Finally, no release at all could be observed in these conditions with the hopolymer of DMAEMA.

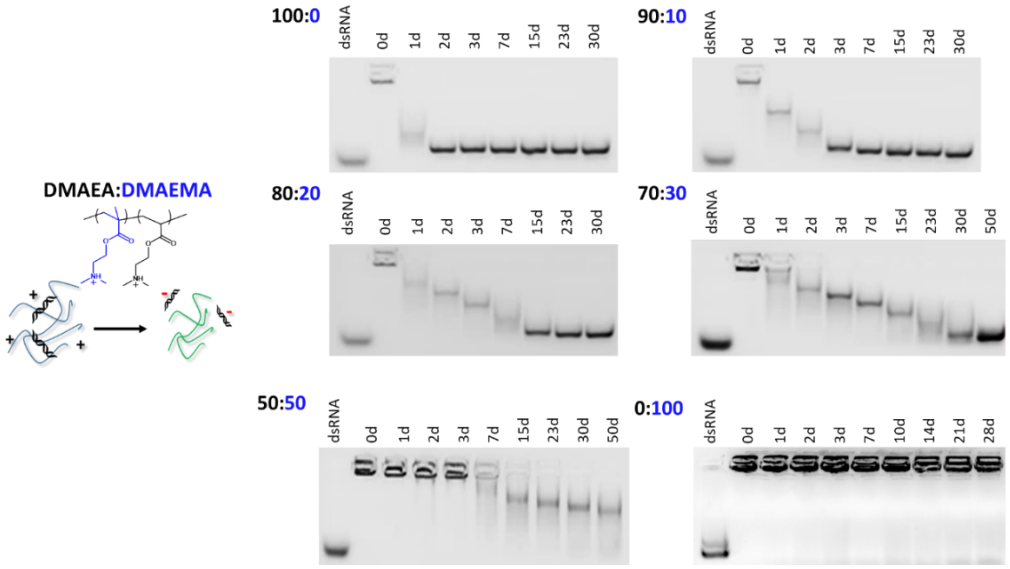

Figure 5.4: DsRNA release over 30 to 50 days (all polyplexes at N/P 5 in sterile water): Agarose gel electrophoresis (100V, 30 min) for pDMAEA, p(DMAEA$_{90}$-DMAEMA$_{10}$), p(DMAEA$_{80}$-DMAEMA$_{20}$), p(DMAEA$_{70}$-DMAEMA$_{30}$) and p(DMAEA$_{50}$-DMAEMA$_{50}$).

In conclusion, these well-defined hydrolysable copolymers of DMAEA and DMAEMA can be used to tune the speed of hydrolysis and therefore to tune the time for the full release of dsRNA. By increasing the amount of non-hydrolysable DMAEMA, the release of dsRNA can be delayed by multiple days.

5.3.1.3. Stability in soil

After showing that the release of the dsRNA can be controlled in ideal conditions (sterile water), we are looking at how this affects the protection in soil. Method 1 (refer to method chapter) was used for the extraction of the dsRNA, involving phenols and heparin instead of PVS for the decomplexation of the dsRNA (method 2, refer to method chapter) and the results were analysed by agarose gel electrophoresis. This first method was used before the fluorescence analysis was developed and used for previous work by Cook *et al.*[24] and Whitfield *et al.*[23]. Although the latter method is simpler, less time consuming and can give a better idea of the level of degradation, the former enables to investigate the soil stability of the dsRNA.

After extraction and decomplexation, agarose gel electrophoresis (Figure 5.5) showed some dsRNA for all the copolymers after 2 or 3 days since they all showed a band after 3 days. However, the bands had variable intensity (implying less dsRNA)

and eluted lower on the gel (implying smaller dsRNA), an indication of the degradation of the nucleic acids. When using a homopolymer of DMAEA, the nucleic acids was completely degraded at 7 days, whereas the use of a non-hydrolysable pDMAEMA led to degradation, despite the fact that no release was observed in sterile water. Faint bands are observed up to 14 days (repeat of missing time points in the gel presented in Figure 5.5 because of experimental error showed strong intensity at day 0 and low intensity bands at 7 and 10 days). Note that even if it was not clear how much dsRNA might still be intact, if pDMAEMA was protecting dsRNA efficiently, results would be comparable to bPEI, which exhibited strong dsRNA band even after 28 days of incubation.

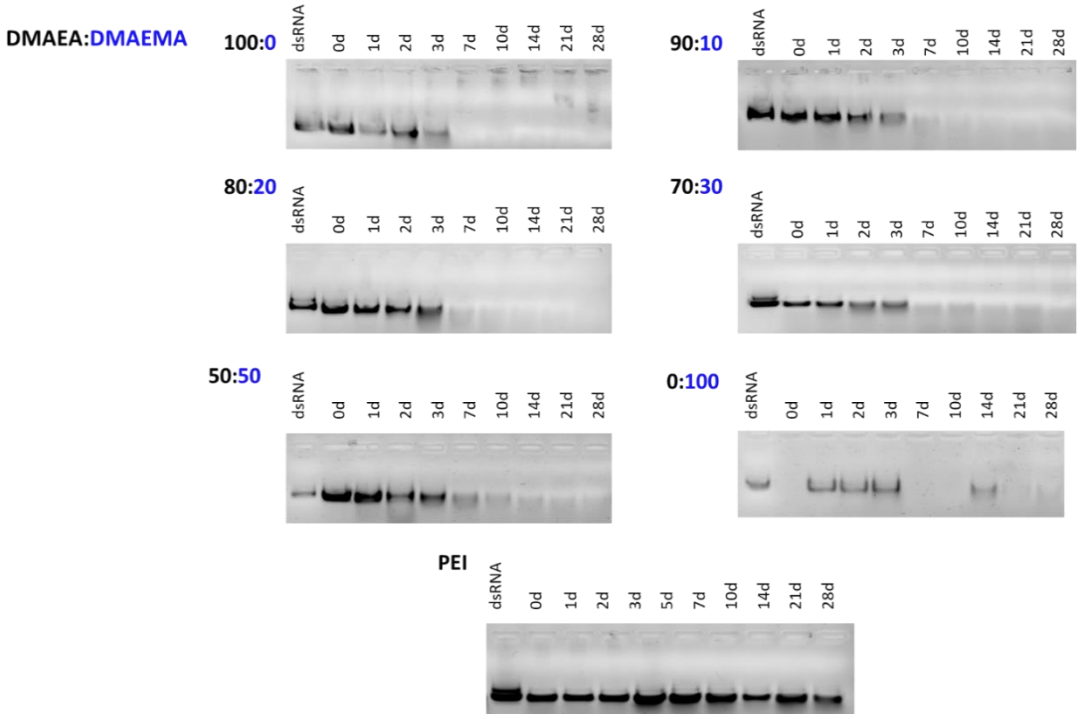

Figure 5.5: Agarose gel electrophoresis (100V, 30 min) of extracted dsRNA from soil. Soil stability assays performed with polyplexes at N/P 5 with 100, 90, 80, 70, 50 and 100% DMAEA:DMAEMA linear copolymers and bPEI and incubated in soil for 0, 1, 2, 3, 5, 7, 10, 14, 21 and 28 days and extracted from soil and decomplexed before analysis. Repeat of missing time points in the gel because of experimental error showed strong intensity at day 0 and low intensity bands at 7 and 10 days.

To confirm these results, the stability assays were repeated with method 2 (see method chapter) using the fluorescence-based analysis, for the copolymers with 70% DMAEA and the homopolymer of DMAEMA (Figure 5.6). The fluorescence results

showed less degradation of dsRNA after 2 days compared to naked dsRNA which is used as a negative control. Neither of these two copolymers were able to protect dsRNA efficiently, with results showing that *ca.* 70 to 80% of the dsRNA was degraded after 2 days. After 7 days, slightly more dsRNA could be detected when complexed to polymers, in particular pDMAEMA, when compared to naked dsRNA. However, efficiency was far poorer than that observed in the positive control based on bPEI, which showed almost no degradation of the nucleic acids even after 10 days.

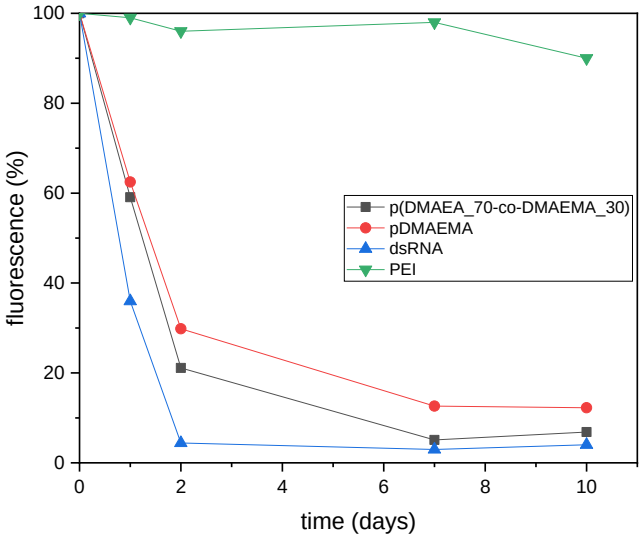

Figure 5.6: Soil stability assay, fluorescence results after incubation (for 1, 2, 3, 5,7 and 10 days) in soil with naked dsRNA (negative control) and dsRNA formulated with linear p(DMAEA$_{70}$-DMAEMA$_{30}$) and pDMAEMA and bPEI (positive control) at N/P 5 with a final concentration of dsRNA of 1 mg/mL. The dsRNA is decomplexed before analysis.

In conclusion, even if the release of the dsRNA could be tuned, none of these linear copolymers were able to give a good protection of the dsRNA in soil conditions. The strength of the binding was likely not good enough to give a sufficient protection and avoid degradation. In addition, interactions with elements in the soil could also be responsible for the displacement of dsRNA, thus releasing it without the need of the cationic polymers to hydrolyse.

5.3.2. Influence of the architecture on complexation of dsRNA.

Tuning the hydrolysis by incorporating DMAEMA was not enough to control the stability of dsRNA in soil. Therefore, in addition to introducing DMAEMA in the structure, the architecture of the polymer was investigated.[23, 24] Since, we observed that the incorporation of 20% DMAEMA delay the release of dsRNA to *ca.* 15 days instead of 2 for the DMAEA homopolymer in sterile water, we used this composition for this study. As described in **chapter 3**, dense and compact star architectures were prepared using the arm-first approach. Three stars were synthesised and are illustrated in Scheme 5.1. Star 1 is composed of longer arms (M_n ~ 5 500 g/mol) with a block of statistical DMAEA and DMAEMA and a block of NAM that corresponds to about 40% of the total DP. Star 2 has arms with the same composition but with half the size of star 1 (M_n ~ 2 800 g/mol). Finally, star 3 is based on arms made of the statistical incorporation of NAM with DMAEA and DMAEMA and comparable arms' size to star 1 (M_n ~ 5 600 g/mol). The three stars are obtained with a high number of arms (N_{arm} ~ 55 – 100) giving very dense and compact high molecular weight materials.

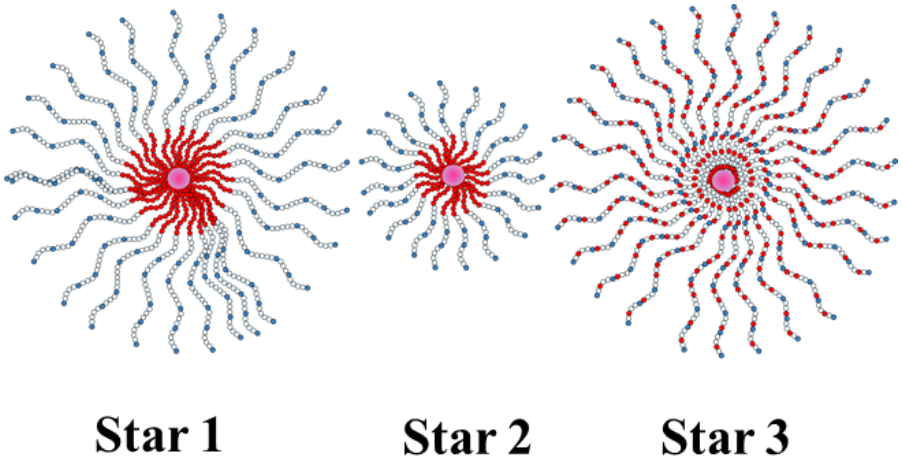

Scheme 5.1: Star representation. Light blue circles represent DMAEA, darker blue circles correspond to DMAEMA monomer, red circles corresponds to NAM and the pink center represent the crosslinked core linking the arms with the bisacrylamide difunctional monomer.

5.3.2.1. Polyplex formation

Since these stars were new materials, they were characterised for complexation with pDNA in addition to dsRNA to compare to assess the influence of nucleic acids

of variable size (10 000 base pairs (bp) in plasmid DNA versus 258 bp in dsRNA), and to test their transfection efficiency. The ability of the different star copolymers to complex pDNA and dsRNA were characterised by agarose gel electrophoresis and ethidium bromide displacement assays.

Complexation was performed with pDNA and dsRNA at N/P ratios from 0 to 10 (Figure 5.7). The three star copolymers were able to fully complex pDNA at a N/P ratio of 2 (Figure 5.7a). Smears can be observed on the gels at N/P 1, suggesting most pDNA was complexed to the polymers but some nucleic acids were still free. The same complexation process was used to complex the dsRNA (Figure 5.7b), full complexation was obtained only at N/P 3 or even 4. A higher N/P was necessary to fully complex the dsRNA for all three stars compared to the linear copolymers above or the 4-arms pDMAEA stars reported in **chapter 2**.

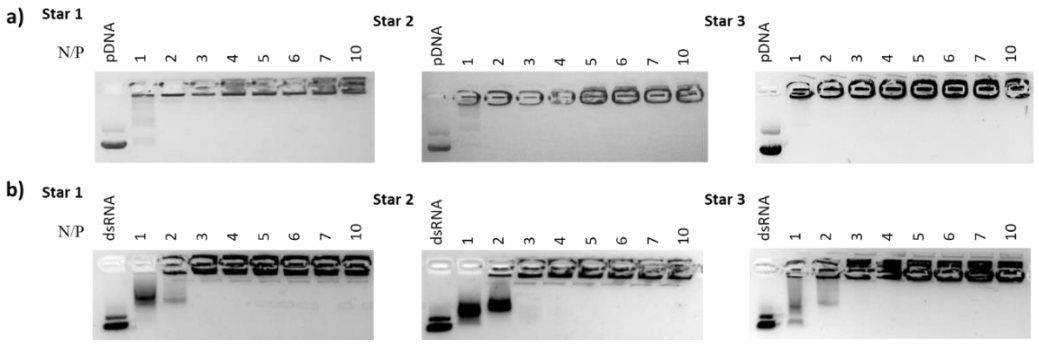

Figure 5.7: Agarose gel electrophoresis pictures of complexation of a) pDNA and b) dsRNA with Star 1, 2 and 3 at N/P ratios of 0, 1, 2, 3, 4, 5, 6, 7 and 10.

Ethidium bromide displacement assays were performed with both dsRNA and pDNA (Figure 5.8). Star 1 was able to displace the highest percentage of dsRNA (95%) at N/P 2, showing similar results to bPEI. Star 2 was able to displace 88% of the nucleic acids at N/P 3. This is in agreement with what could be observed with agarose gel electrophoresis as a stronger band was observed at N/P 2 for star 2 than for star 1 and full complexation was observed at N/P 3. Star 3 was only able to displace a maximum of 77% of dsRNA at N/P 1. This implied that the binding might be weaker for this star since full complexation can be observed on the gel at N/P 3 but the displacement was weaker. When compared to the complexation performed with the bigger pDNA, it is interesting to note the significant difference of ethidium bromide displaced. The displacement with bPEI reached 79% of pDNA at N/P 10. Higher N/P ratios (around 10) were required to complex a maximum of plasmids and displace the

ethidium bromide. The size of the nucleic acids seems to play an important role on the displacement. Even if most pDNA was still interacting with ethidium bromide at low N/P ratios, some complexation with the polymer might have happened. More polymer was required to compete with the dye. However, as observed by running agarose gel electrophoresis (Figure 5.7a), full complexation was observed at low N/P ratios. Compared to dsRNA, star 1 was still performing better than the others. However, the performance of star 2 was more comparable to the one of star 3 which even displaced slightly more pDNA.

Overall, the stars did not perform as well as the flexible linear copolymer, the 4-arms pDMAEA stars or the branched copolymer structures probably because of their dense structure. The nucleic acids probably stay mostly at the surface of the stars and more material was necessary to obtain similar displacement of ethidium bromide.

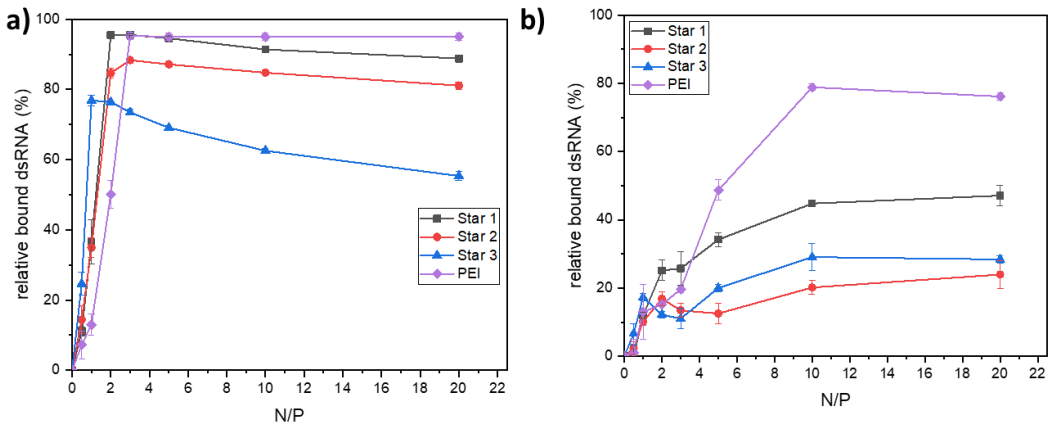

Figure 5.8: Ethidium bromide displacement of a) dsRNA b) pDNA with star 1, 2 and 3.

5.3.2.2. Polyplexes characterisations

Polyplexes were also characterised by measuring their zeta potential. The formed polyplexes at N/P 5 all appeared to be overall positively charged (15,6 mV for Star 1, 27.8 mV for Star 2 and 29 mV for Star 3). DLS did not lead to usable data as polydispersities (PDI) were very high, which is due to the non-spherical shape and high dimension of the particles. The polyplexes were imaged using different techniques. Transmission electron microscopy (TEM) was able to demonstrate the presence of big non-spherical structures of 200 to 500 nm (Figure 5.9). This was also supported by scanning electron microscopy (SEM) (Figure A 5.2), showing polydisperse particles with aggregates of similar sizes to the one observed by TEM.

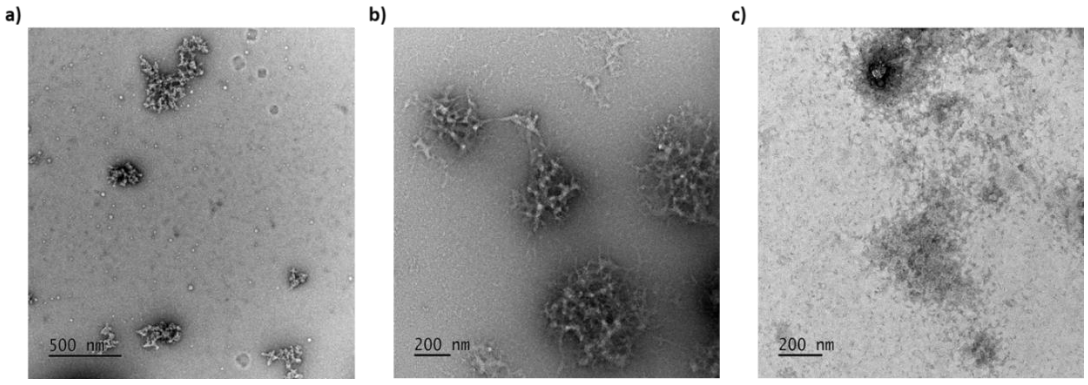

Figure 5.9: TEM pictures of polyplexes at N/P 5 of dsRNA with a) Star 1 b) Star 2 c) Star 3

5.3.2.3. dsRNA release

The release of the dsRNA over time was studied with the three stars (Figure 5.10) and compared to their equivalent linear 80% DMAEA polymers (Figure 5.4). The release of dsRNA appeared to be less gradual than with the linear chains, lower bands could be observed within 1 or 2 days. Star 1 displayed slower release than the two other stars as the dsRNA was fully released after 14 days whereas it took only 7 days for star 2 and 10 days for star 3, and some released dsRNA could be observed after only 2 days for both these stars. In comparison, with the linear equivalent, full release was obtained after 15 days and even after about 28 days for the high molecular weight linear copolymer (M_n=25 000 g/mol) (Figure A5.1). The comparison with a higher molecular weight linear copolymer showed the impact of the distribution of the charge similarly to the comparison between the linear pDMAEA and 4-arm star pDMAEA.[23] For the longer linear chain, the cationic charges are concentrated on one chain instead of multiples when the polymer is smaller for the same amount of charges, and the density of charge is higher in a star structure. However, faster release was observed when using the stars obtained from the arm-first approach, probably due to the high density of the structure. The dsRNA is likely to be mainly complexed at the surface of multiple stars, rather than wrapped within one single chain. Moreover, since the hydrolysis is likely to happen first at the surface of the stars, the dsRNA would be released faster. Complexation with star 1 gave better delay of the dsRNA which is in agreement with results with ethidium bromide. Star 3, with the same arm length released the nucleic acids slightly faster; this could be explained by the difference in hydrophobicity brought by the NAM units throughout the arm and the slightly higher

hydrolysis. The smaller size resulted in faster release which could be explained by their smaller surface of contact with the dsRNA.

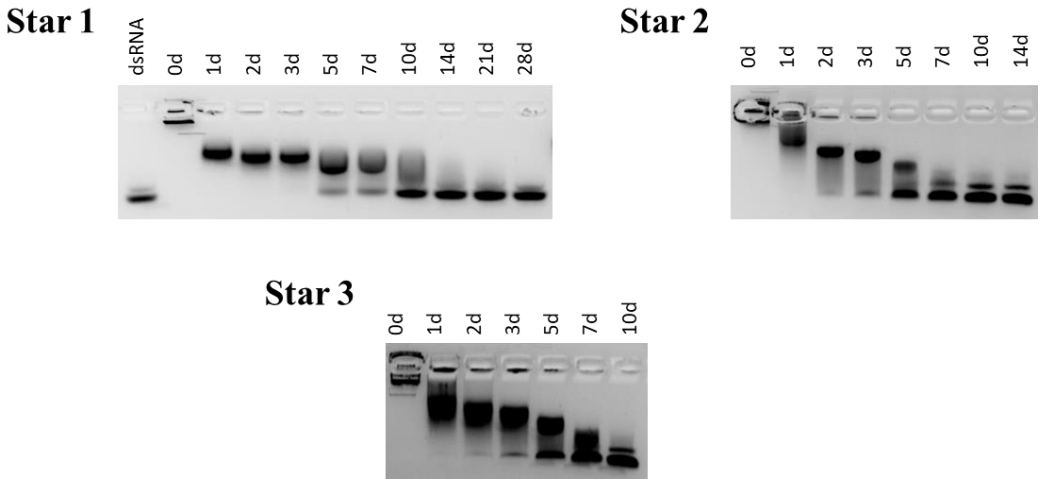

Figure 5.10: DsRNA release over 10 to 28 days (all polyplexes at N/P 5 in sterile water) : Agarose gel electrophoresis (100V, 30 min) for star 1, star 2 and star 3.

5.3.2.4. Polyplex stability in the presence of competing and/or degrading species

In order to assess the ability of these stars to give a good protection against nucleases and hydrolysis in the presence of competing or degrading species, heparin displacement assays, nuclease stability assays and soil stability assays were performed.

5.3.2.4.1. Heparin displacement assays

The stability of the polyplex in the presence of competing species can be estimated using heparin dissociation assays.[28, 12, 29] Heparin was added at increasing concentration in the polyplex solution and agarose gel electrophoresis was used to observe any decomplexation of the dsRNA after 20 minutes incubation (Figure 5.1). Results showed stability of the polyplexes at low concentrations, however as heparin concentration increased, release of the dsRNA could be observed (0.2 mg/mL for Star 1, 0.1 mg/mL for Star 2 and 0.2 for Star 3). The same experiment was performed with plasmids, where surprisingly better stability was observed overall with the three stars as release of pDNA was observed at higher concentrations (0.3 mg/mL for Star 1, 0.2 for Star 2 and more than 0.4 mg/mL for Star 3)

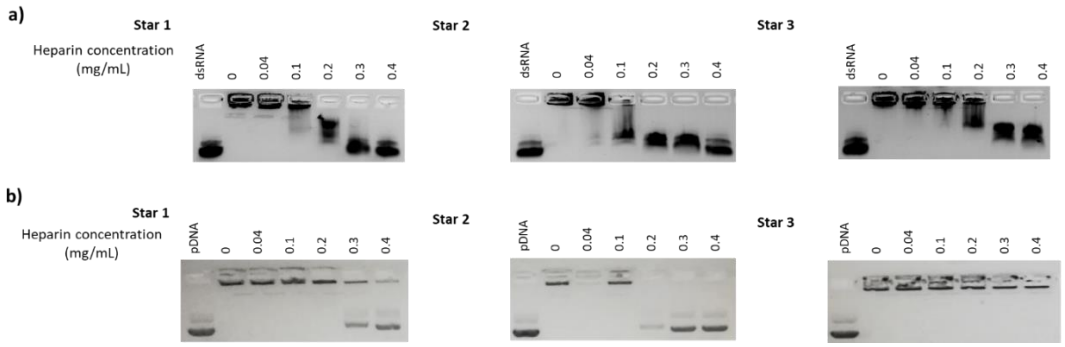

Figure 5.11: Heparin displacement assays with a) dsRNA complexes b) pDNA complexes .5 µL heparin solution of increasing concentration were added to the polyplex solution at N/P 5 and incubated for 20 minutes upon gel electrophoresis run (100V, 30 min).

5.3.2.4.2. Nuclease protection assay

The nuclease stability assay gives information on the ability of the polymer to protect the nucleic acids in the presence of dsRNases without the interactions of competing species that could cause more decomplexation.

Polyplexes were prepared at N/P 5 by mixing a solution of dsRNA with a solution of polymer and added to a solution containing dsRNase, buffer and $MgCl_2$. After incubation overnight at 37 °C, EDTA was added to stop the degradation and PVS to induce decomplexation. Controls were realised in pure water and incubated in the same conditions. Agarose gel electrophoresis was used to analyse the results (Figure 5.12). Naked dsRNA was used as control, without the presence of dsRNase. Strong bands corresponding to the dsRNA could be observed on the picture showing the dsRNA had not been degraded in the absence of nuclease. However, when nuclease was present, gels only exhibited faint bands showing the dsRNA has mostly been degraded. bPEI was used as a positive control for the protection of the nucleic acids. After incubation with nucleases, strong bands could still be seen on the gel showing that bPEI was able to protect the dsRNA efficiently. When the dsRNA was complexed with the stars, faint bands could be observed implying most of the dsRNA was degraded. Therefore, these star materials were not able to give a good protection by binding efficiently with the nucleic acids in these conditions. The linear copolymer p($DMAEA_{80}$-$DMAEMA_{20}$) and the 4-arm star 4-p$DMAEA_{38}$ were also tested (Figure A 5.3). While the linear copolymer was able to give a better protection than the dense

stars, but not as good as bPEI if intensities are compared, the 4-arm star did not give a good protection as most of the dsRNA was degraded. This supports the previous results showing weaker complexation with the dense structures compared to the linear copolymers and the faster degradation in soil for the 4-arm stars of DMAEA (**Chapter 2**). However, even though linear copolymers appear to protect from nuclease activity, this was not sufficient to provide lasting stability in soil.

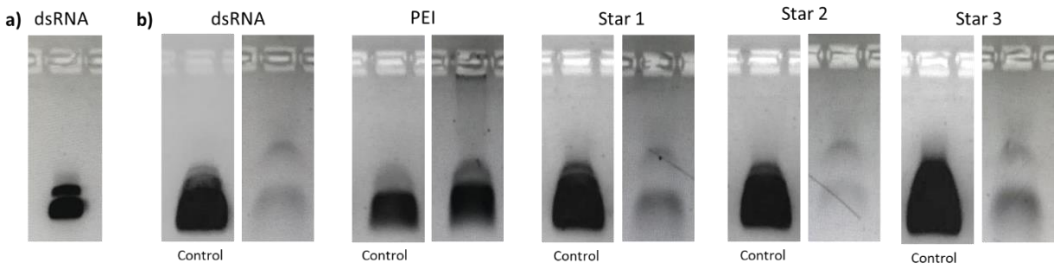

Figure 5.12: a) dsRNA in sterile water b) Nuclease protection assay gel results for naked dsRNA and complexes with bPEI, Star 1, Star 2 and Star 3. Controls on the left are incubated in water at 37°C.

This experiment only compares the materials in very specific conditions (concentrations) which can be different from real environmental conditions. The concentration of nucleases and their activity have shown to vary among insects[30] therefore tests in conditions closer to real conditions (soil environment, gut juice, hemolymph...) are necessary to assess the efficiency of one polyplex.[2, 31-33] Nonetheless, the heparin displacement assay or nuclease stability are still valuable assays in order to compare materials in simpler conditions, possibly as a screening method for libraries of materials.

5.3.2.4.3. Soil stability assay

The soil stability assay was used to test the polymers' ability to complex and protect dsRNA in environmental conditions in the presence of competing species present in the soil environment as well as dsRNases which are able to degrade the nucleic acids.[25, 26] The polyplexes (N/P 5) were added to live soil and were incubated for up to 14 days. Decomplexation was performed and fluorescence was used to determine the amount of dsRNA left (refer to soil stability method 2). Very small protection was observed with these three stars as shown in Figure 5.13. Star 1 and 3

produced similar results to bPEI and the linear copolymer after 1 day but after days 2 and 3, stability quickly dropped similarly to previous DMAEA-based polymers tested. Star 2 seemed to give less protection than the others. This is in agreement with what was observed with ethidium bromide displacement assays and dsRNA release in sterile water. bPEI was used as a positive control and even if the fluorescence dropped to about 60% within 3 days it stayed stable up to 14 days contrary to the stars and linear copolymers. Therefore, these complex architectures do not result to better outcomes than the linear polymer.

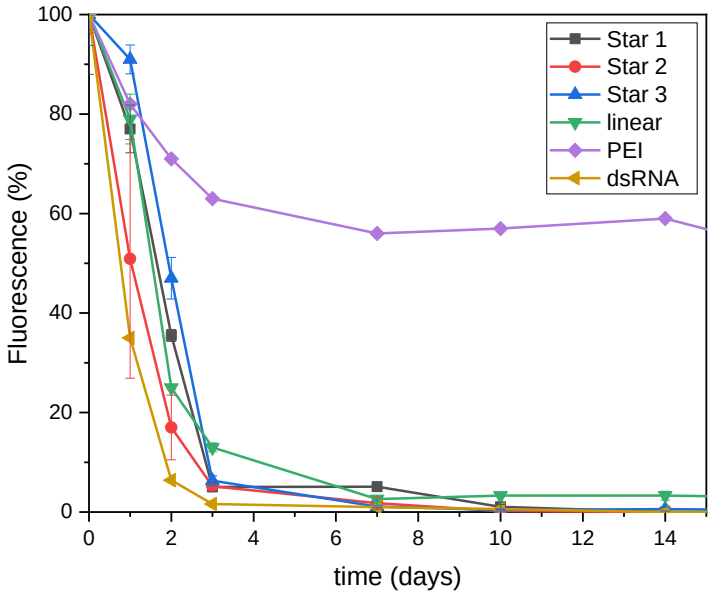

Figure 5.13: Soil stability assay, fluorescence results after incubation (for 1, 2, 3, 5,7 and 10 days) in soil with naked dsRNA (negative control) and dsRNA formulated with Star 1, star 2, star 3, linear p(DMAEA$_{80}$-DMAEMA$_{20}$) and bPEI (positive control) at N/P 5 with a final concentration of dsRNA of 1 mg/mL. The dsRNA is decomplexed before analysis.

5.3.2.5. Toxicity and Transfection efficiency in vitro

Since the polymers were able to complex pDNA, cytotoxicity and their ability for transfection was investigated. The complexes need to penetrate the cell barriers to be able to induce transcription of the green fluorescent protein (GFP) by crossing the cell membrane.[17] As this membrane is negatively charged, the interaction and internalisation is enhanced by the positive charge of the complexes. Internalisation mainly happens by endocytosis.[34, 35] However, this cationic charge can also induce cytotoxicity; this is why finding a good balance between high transfection efficiency and low cytotoxicity can be often challenging.[15, 36, 37] The complex then needs to be

released to be able to gain access to the cell machinery so the pDNA can be transcribed after dissociation from the cationic polymer.[38] To improve transfection efficiency and balance toxicity, polymer composition, molecular weight and architecture are important parameters that can be manipulated.[13, 17, 39] In particular star-shaped polymers were investigated with regards to pDNA transfection efficiency, as these types of structures often display high flexibility, which may allow for better complexation as well as usually having reduced cytotoxicity.[17, 40, 41]

Cytotoxicity of the polymers was first established. This was evaluated using the XTT assay on HEK293T cells as a model (Figure 5.14). The XTT assay measures cellular metabolic activity, which is then used as an indicator for viability.[42] Linear bPEI was used as a reference and showed toxicity even at low concentrations (0.125 mg/mL) confirming what is reported in the literature.[5] However, cells treated with the stars or the linear copolymer showed high viability of HEK293T cells at concentration up to 1 mg/mL. These results are promising for potential other applications especially for their high molecular weight since toxicity is usually an issue.[43]

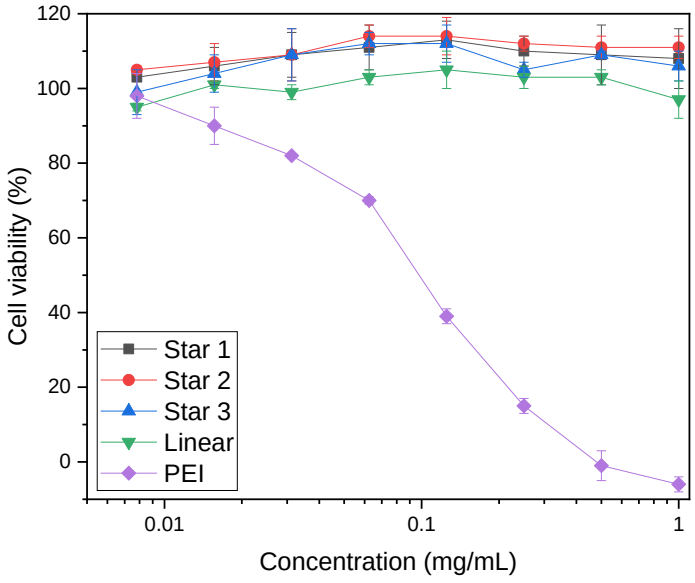

Figure 5.14: Toxicity of stars and linear copolymer of DMAEA and DMAEMA. Viability of HEK293T cells using XTT assay.

Complexes of pDNA expressing GFP with Star 1, Star 2, Star 3 and p(DMAEA$_{80}$-DMAEMA$_{20}$) linear chain at N/P 20 were incubated with HEK293T cells. Cells were then incubated for 5 hours. After replacing the media the cells were incubated for a further 48 hours to measure the transfection efficiency with these

polymers compared to linear bPEI (Figure 5.15). Transfection efficiency is expressed as the percentage of cells expressing GFP, as measured by flow cytometry. Poor transfection rates were obtained for the stars compared to linear PEI (lPEI), as a maximum of 7.6 % transfection was measured for Star 1 and only 1.6% for Star 3 while 31.8% was reached with linear lPEI. The linear copolymer of DMAEA and DMAEMA did not perform well either as only 1.8 % transfection was achieved. Imaging using optical microscopy (Figure A5.4) showed big non-spherical aggregates (size of about 2 to 40 µm) corresponding to the polyplexes in these conditions and aggregation with the cells. In comparison complexes with lPEI formed much smaller particles and caused less aggregation of the cells. Size is an important factor to obtain good transfection efficiency; usually particles under 500 nm result in efficient endocytosis mechanism.[44, 45] It is therefore possible that the size of the polyplexes, or polyplex aggregates, was responsible for the low transfection rates, with only small polyplexes being taken up by the cells.

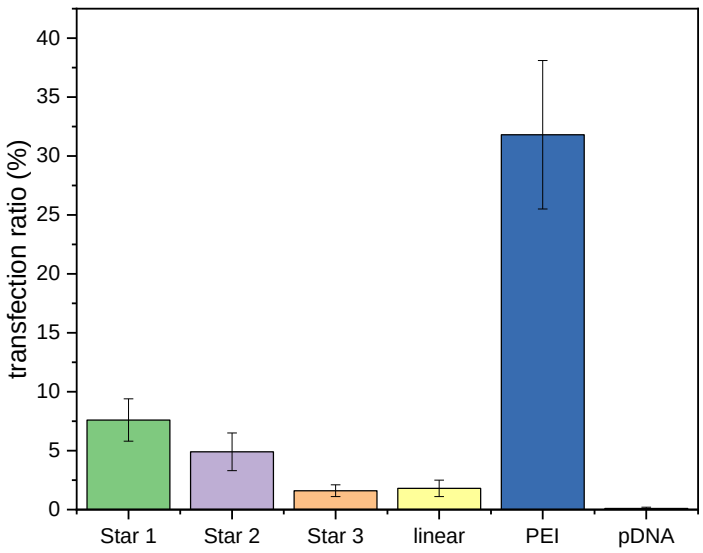

Figure 5.15: GFP pDNA transfection inHEK293T cell-line with polyplex (N/P 20) incubated for 48 hours growth. Samples were analysed by flow cytometry to determine fluorescence.

5.4. Conclusion

In this chapter, the influence of the composition of the copolymer and its hydrolysis rate on the release of nucleic acids was first established. By copolymerising DMAEA with its methacrylate version, DMAEMA, which is non-hydrolysable, the time for the full release of dsRNA could be tuned. With 100% DMAEA, 2 days were enough to lead to complete release while with only 20% of DMAEMA, this full release was delayed to approximately 15 days. Although these copolymers were able to complex the dsRNA efficiently as shown with agarose gel electrophoresis and ethidium bromide displacement assays, they were not enough to protect it efficiently in soil and delay its degradation by more than a couple of days. Even the non-hydrolysable homopolymer of DMAEMA was not able to give a good protection for the dsRNA in soil. This implies that the strength of the binding was not strong enough to preserve it against competing species present in soil.

In a second part of this chapter, the incorporation of DMAEMA to delay the hydrolysis was combined with a more complex architecture in order to try to improve the binding strength and protection in soil. Even if this type of architecture is better controlled compared to the branched copolymers previously studied for this application,[9] since we have a control over the arms' length and composition, there are still a lot of parameters to take into account when comparing these polymers: the molecular weight and arm length but also the number of arms per star, their density as well as their composition. The three stars were able to complex both dsRNA and pDNA at N/P 3 and higher. The size of the complexes was characterised using different microscopy techniques (SEM, TEM), with images showing some big complexes, probably aggregates (200 – 500 nm) but also small particles in the background. The release of dsRNA was faster and less gradual than with the equivalent linear chain with the same composition of DMAEA (DMAEA:DMAEMA 80:20). This could be explained by the nucleic acids being at the surface of the stars because of their very dense structure, therefore the dsRNA was not well wrapped inside and hydrolysis of the end of the arms was enough to release it. Heparin and nuclease assays also supported a non-efficient binding and a very limited protection against nucleases. Thus, soil stability assays showed the stars did not perform better than the linear copolymers. The binding strength was not good enough to face

nucleases and competitive species present in soil. Previous results obtained with branched structures[9] suggest a highly branched system can improve protection as it may act like a net. However, the present stars studied in this work were too dense and not flexible enough to shield the nucleic acids and bind to it efficiently. Another drawback with these structures was their stability in dry state over time even when stored at 4°C, as after some time, their solubility decreases.

Finally, the stars were tested for transfection of pDNA encoding for GFP. Even though XTT assays displayed very low toxicity, the materials showed poor transfection efficiency compared to linear lPEI used as a reference.

Flexibility and charge density seem to be key to improve the stability of dsRNA in more complex conditions. An interesting parameter to work on might be the stability of the polyplexes in water (size, size distribution) as in it was shown in this chapter that polyplexes were big and disperse in size. The cationic moiety might also play an important role to increase the binding efficiency.

5.5. Experimental

5.5.1. Materials

Agarose (Sigma-Aldrich), GelRed (Biotium, 2000X), Tris-Borate-EDTA buffer (TBE), Orange G/blue loading dye (6X) (Alfa Aesar), sterile water (Sigma-Aldrich), ethidium bromide (Sigma-Aldrich, 500 mg/mL), PVS solution (Sigma-Aldrich, 30 wt. % in water, technical grade), EGTA (Sigma-Aldrich, 97%), Optimem® cell culture media (Thermo Fisher Scientific). dsRNA was provided by Syngenta.

5.5.2. Characterisation

5.5.2.1. Zeta-potential measurements

Polyplexes (N/P 5) were prepared by mixing 5 µL of dsRNA solution of appropriate concentration to 795 µL of a solution of polymer at 0.1 mg/mL in water and incubated for 30 minutes at room temperature. The samples were analysed at 25°C using a Antoon-Paar Litesizer 500 DLS in an Omega cuvettes.

5.5.2.2. Transmission electron microscopy (TEM)

Polyplex samples were prepared at a N/P ratio of 5 by mixing a polymer stock solution with a solution of dsRNA to obtain a final solution of 0.1 mg/mL polymer. Samples were vortexed and incubated for 30 minutes at room temperature. Before adding the sample, the grid formvar/carbon coated copper was treated by glow discharge to make the surface hydrophilic. 5 µl of sample was added to a grid for 1 min. Then the sample was stained with 2 % uranyl acetate for a total of 3 minutes (3 drops for 1 minute each). Imaging was done on a Jeol 2100Plus TEM fitted with a Gatan OneView IS camera.

5.5.2.3. Scanning electron microscopy (SEM)

Polyplex samples were prepared at a N/P ratio of 5 by mixing a polymer stock solution with a solution of dsRNA to obtain a final solution of 0.1 mg/mL polymer. Samples were vortexed and incubated for 30 minutes at room temperature. A drop of sample (40 µL) was added at the surface of the borosilicate glass coverslip and was left to dry for 2 hours in laminar flow cabinet. Imaging was performed on a Zeiss Gemini Scanning Electron Microscope equipped with a InLens detector at a voltage of 2 kV.

5.5.2.4. Agarose gel electrophoresis

Refer to method.

5.5.2.5. Ethidium bromide displacement assays

Refer to method.

5.5.2.6. Nuclease stability assays

Polyplexes were prepared at a N/P ratio of 5 by mixing the correct amount of polymer stock solution with a stock solution containing 10 µg of dsRNA. 10 µL of polyplex was added to a solution containing 87 µL of sterile water, 1 µL of 10X Shortcut reaction buffer, 1 µL Shortcut RNase III and 1 µL of $MnCl_2$. The resulted solution was then incubated overnight at 37 °C. 1 µL of 10X EDTA was added to stop

the reaction and 4 µL of PVS solution to decomplex the dsRNA. The solution was loaded on the agarose gel and run for 45 min with 100V.

5.5.2.7. Heparin displacement assays

Refer to method.

5.5.2.8. Soil stability assays

Refer to method.

5.5.3. In vitro transfection

HEK293T cells were seeded in a 24 well plate at a density of 1 x 10^5 cells in 1 mL per well and left overnight. The culture medium was replaced by 300 µL Optimem® cell culture media (Thermo Fisher Scientific) without foetal bovine serum (FBS). Polyplexes were prepared by mixing pDNA solution and polymer solution. The solution was then incubated at room temperature for 60 minutes. After 60 minutes the media was replaced by fresh Optimem® plus polyplex solution (350 µL Optimem® and polyplex with final concentration of pDNA of 10 µg/mL). The cells were incubated for 5 hours under 5% CO_2 humidified atmosphere, then the wells were washed with warm medium. Media was replaced with fresh DMEM containing FBS. After 48 hours incubation (including 5 hours incubation with the polyplex), the cells were washed with PBS (0.5 mL). The cells were harvested using 150 µL of trypsin/EDTA. 300 µL of DMEM containing FBS was then added and the cell suspension was centrifuged. The cell pellet was resuspended in 100 µl PBS and 100 µL of 8% formaldehyde was added. The samples were left for 15 min at room temperature to fix cells and centrifuged. The cell pellets were washed with cold PBS (200 µL) twice. Cells were analysed using LSRIII flow cytometer (using a 488 nm laser with a 530/30 filter and a 561 nm laser with a 585/15 filter).

5.5.4. Polymer toxicity

HEK293T cells were seeded in a 96-well plate at 10 000 cells/well and left to incubate for 24 hours at 37°C in DMEM. Polymers were dissolved in serum free DMEM at 1.1 mg/mL and filtered through 0.22 µm filter. FBS was added and the concentration of polymer adjusted to 1 mg/mL. The media was replaced by the media

containing the polymer, serial dilution was used to incubate the cells with polymers of different concentrations and incubated for 18 hours at 37°C. After dry exposure, cell viability was measured by using XTT assay. Cell viability was determined in triplicate in three independent sets of experiments and their standard deviation was calculated.

5.6. References

1. Whitehead, K. A.; Langer, R.; Anderson, D. G., Knocking down barriers: advances in siRNA delivery. *Nature Reviews Drug discovery* **2009,** *8* (2), 129-138.

2. Spit, J.; Philips, A.; Wynant, N.; Santos, D.; Plaetinck, G.; Broeck, J. V. J. I. b.; biology, m., Knockdown of nuclease activity in the gut enhances RNAi efficiency in the Colorado potato beetle, Leptinotarsa decemlineata, but not in the desert locust, Schistocerca gregaria. *Insect Biochem. Mol. Biol.* **2017,** *81*, 103-116.

3. Thomas, C. E.; Ehrhardt, A.; Kay, M. A., Progress and problems with the use of viral vectors for gene therapy. *Nat. Rev. Genet* **2003,** *4* (5), 346-358.

4. Pack, D. W.; Hoffman, A. S.; Pun, S.; Stayton, Design and development of polymers for gene delivery. **2005,** *4* (7), 581.

5. Yin, H.; Kanasty, R. L.; Eltoukhy, A. A.; Vegas, A. J.; Dorkin, J. R.; Anderson, D. G., Non-viral vectors for gene-based therapy. *Nat. Rev. Genet* **2014,** *15* (8), 541-555.

6. Kaczmarek, J. C.; Kowalski, P. S.; Anderson, D. G., Advances in the delivery of RNA therapeutics: from concept to clinical reality. *Genome Med.* **2017,** *9* (1), 60.

7. Truong, N. P.; Jia, Z.; Burgess, M.; Payne, L.; McMillan, N. A.; Monteiro, M. J., Self-catalyzed degradable cationic polymer for release of DNA. *Biomacromolecules* **2011,** *12* (10), 3540-3548.

8. Ros, S.; Burke, N. A.; Stöver, H. D., Synthesis and Properties of Charge-Shifting Polycations: Poly [3-aminopropylmethacrylamide-co-2-(dimethylamino) ethyl acrylate]. *Macromolecules* **2015,** *48* (24), 8958-8970.

9. Cook, A.; Peltier, R.; Hartlieb, M.; Whitfield, R.; Moriceau, G.; Burns, J.; Haddleton, D.; Perrier, S., Cationic and hydrolysable branched polymers by RAFT for complexation and controlled release of dsRNA. *Polym. Chem.* **2018**.

10. Ros, S.; Kleinberger, R. M.; Burke, N. A.; Rossi, N. A.; Stöver, H. D., Charge-Shifting Polycations with Tunable Rates of Hydrolysis: Effect of Backbone Substituents on Poly [2-(dimethylamino) ethyl acrylates]. *Macromolecules* **2018**.

11. Ros, S.; Wang, J.; Burke, N. A. D.; Stöver, H. D. H., A Mechanistic Study of the Hydrolysis of Poly[N,N-(dimethylamino)ethyl acrylates] as Charge-Shifting Polycations. *Macromolecules* **2020,** *53* (9), 3514-3523.

12. Richter, F.; Martin, L.; Leer, K.; Moek, E.; Hausig, F.; Brendel, J. C.; Traeger, A., Tuning of endosomal escape and gene expression by functional groups, molecular weight and transfection medium: a structure–activity relationship study. *J. Mater. Chem. B* **2020,** *8* (23), 5026-5041.

13. Zhu, C.; Jung, S.; Si, G.; Cheng, R.; Meng, F.; Zhu, X.; Park, T. G.; Zhong, Z., Cationic methacrylate copolymers containing primary and tertiary amino side groups: Controlled synthesis via RAFT polymerization, DNA condensation, and in vitro gene transfection. *J. Polym. Sci., Part A: Polym. Chem.* **2010,** *48* (13), 2869-2877.

14. Pascual, S.; Montembault, V.; Casse, N.; Fontaine, L., Innovative well-defined primary amine-based polyacrylates for plasmid DNA complexation. *Polym. Chem.* **2014,** *5* (19), 5542-5545.

15. Cai, J.; Yue, Y.; Rui, D.; Zhang, Y.; Liu, S.; Wu, C., Effect of Chain Length on Cytotoxicity and Endocytosis of Cationic Polymers. *Macromolecules* **2011,** *44* (7), 2050-2057.

16. Aied, A.; Greiser, U.; Pandit, A.; Wang, W., Polymer gene delivery: overcoming the obstacles. *Drug Discovery Today* **2013,** *18* (21), 1090-1098.

17. Rinkenauer, A. C.; Schubert, S.; Traeger, A.; Schubert, U. S. J. J. o. M. C. B., The influence of polymer architecture on in vitro pDNA transfection. **2015,** *3* (38), 7477-7493.

18. Xu, F.; Zhang, Z.; Ping, Y.; Li, J.; Kang, E.; Neoh, K., Star-shaped cationic polymers by atom transfer radical polymerization from β-cyclodextrin cores for nonviral gene delivery. *Biomacromolecules* **2009,** *10* (2), 285-293.

19. Alhoranta, A. M.; Lehtinen, J. K.; Urtti, A. O.; Butcher, S. J.; Aseyev, V. O.; Tenhu, H. J., Cationic amphiphilic star and linear block copolymers: synthesis, self-assembly, and in vitro gene transfection. *Biomacromolecules* **2011,** *12* (9), 3213-3222.

20. Synatschke, C. V.; Schallon, A.; Jérôme, V.; Freitag, R.; Müller, A. H. E., Influence of Polymer Architecture and Molecular Weight of Poly(2-(dimethylamino)ethyl methacrylate) Polycations on Transfection Efficiency and Cell Viability in Gene Delivery. *Biomacromolecules* **2011,** *12* (12), 4247-4255.

21. Georgiou, T. K., Star polymers for gene delivery. *Polym. Int.* **2014,** *63* (7), 1130-1133.

22. Liao, X.; Walden, G.; Falcon, N. D.; Donell, S.; Raxworthy, M. J.; Wormstone, M.; Riley, G. P.; Saeed, A., A direct comparison of linear and star-shaped poly (dimethylaminoethyl acrylate) polymers for polyplexation with DNA and cytotoxicity in cultured cell lines. *Eur. Polym. J.* **2017,** *87*, 458-467.

23. Whitfield, R.; Anastasaki, A.; Truong, N. P.; Cook, A. B.; Omedes-Pujol, M.; Loczenski Rose, V.; Nguyen, T. A.; Burns, J. A.; Perrier, S. b.; Davis, T. P., Efficient Binding, Protection, and Self-Release of dsRNA in Soil by Linear and Star Cationic Polymers. *ACS Macro Lett.* **2018,** *7*, 909-915.

24. Cook, A. Highly branched and hyperbranched polymers : synthesis, characterisation, and application in nucleic acid delivery. University of Warwick, 2018.

25. Dubelman, S.; Fischer, J.; Zapata, F.; Huizinga, K.; Jiang, C.; Uffman, J.; Levine, S.; Carson, D., Environmental fate of double-stranded RNA in agricultural soils. *PLoS One* **2014,** *9* (3), e93155-e93155.

26. Fischer, J. R.; Zapata, F.; Dubelman, S.; Mueller, G. M.; Jensen, P. D.; Levine, S. L., Characterizing a novel and sensitive method to measure dsRNA in soil. *Chemosphere* **2016,** *161*, 319-324.

27. Truong, N. P.; Jia, Z.; Burges, M.; McMillan, N. A.; Monteiro, M. J., Self-catalyzed degradation of linear cationic poly (2-dimethylaminoethyl acrylate) in water. *Biomacromolecules* **2011,** *12* (5), 1876-1882.

28. Kwok, A.; Hart, S. L., Comparative structural and functional studies of nanoparticle formulations for DNA and siRNA delivery. *Nanomed. Nanotechnol. Biol. Med.* **2011,** *7* (2), 210-219.

29. Wagner, M.; Rinkenauer, A. C.; Schallon, A.; Schubert, U. S., Opposites attract: influence of the molar mass of branched poly(ethylene imine) on biophysical characteristics of siRNA-based polyplexese. *RSC Advances* **2013,** *3* (31), 12774-12785.

30. Kunte, N.; McGraw, E.; Bell, S.; Held, D.; Avila, L.-A., Prospects, challenges and current status of RNAi through insect feeding. *Pest. Manag. Sci* **2020,** *76* (1), 26-41.

31. Christiaens, O.; Tardajos, M. G.; Martinez Reyna, Z. L.; Dash, M.; Dubruel, P.; Smagghe, G., Increased RNAi Efficacy in Spodoptera exigua via the Formulation of dsRNA With Guanylated Polymers. *Front. Physiol.* **2018,** *9*, 316.

32. Gillet, F.-X.; Garcia, R. A.; Macedo, L. L. P.; Albuquerque, E. V. S.; Silva, M. C. M.; Grossi-de-Sa, M. F., Investigating Engineered Ribonucleoprotein Particles to Improve Oral RNAi Delivery in Crop Insect Pests. *Front. Physiol.* **2017,** *8*, 256.

33. Shukla, J. N.; Kalsi, M.; Sethi, A.; Narva, K. E.; Fishilevich, E.; Singh, S.; Mogilicherla, K.; Palli, S. R., Reduced stability and intracellular transport of dsRNA contribute to poor RNAi response in lepidopteran insects. *RNA Biology* **2016,** *13* (7), 656-669.

34. van der Aa, M. A. E. M.; Mastrobattista, E.; Oosting, R. S.; Hennink, W. E.; Koning, G. A.; Crommelin, D. J. A., The Nuclear Pore Complex: The Gateway to Successful Nonviral Gene Delivery. *Pharmaceutical Research* **2006,** *23* (3), 447-459.

35. Xiang, S.; Tong, H.; Shi, Q.; Fernandes, J. C.; Jin, T.; Dai, K.; Zhang, X., Uptake mechanisms of non-viral gene delivery. *J. Controlled Release* **2012,** *158* (3), 371-378.

36. Fischer, D.; Li, Y.; Ahlemeyer, B.; Krieglstein, J.; Kissel, T., In vitro cytotoxicity testing of polycations: influence of polymer structure on cell viability and hemolysis. *Biomaterials* **2003,** *24* (7), 1121-1131.

37. Rinkenauer, A. C.; Vollrath, A.; Schallon, A.; Tauhardt, L.; Kempe, K.; Schubert, S.; Fischer, D.; Schubert, U. S., Parallel High-Throughput Screening of Polymer Vectors for Nonviral Gene Delivery: Evaluation of Structure–Property Relationships of Transfection. *ACS Combinatorial Science* **2013,** *15* (9), 475-482.

38. Cho, Y. W.; Kim, J.-D.; Park, K., Polycation gene delivery systems: escape from endosomes to cytosol. *Journal of Pharmacy and Pharmacology* **2003,** *55* (6), 721-734.

39. Han, S.; Wan, H.; Lin, D.; Guo, S.; Dong, H.; Zhang, J.; Deng, L.; Liu, R.; Tang, H.; Dong, A., Contribution of hydrophobic/hydrophilic modification on cationic chains of poly(ε-caprolactone)-graft-poly(dimethylamino ethylmethacrylate) amphiphilic co-polymer in gene delivery. *Acta Biomater.* **2014,** *10* (2), 670-679.

40. Xu, F. J.; Yang, W. T., Polymer vectors via controlled/living radical polymerization for gene delivery. *Prog. Polym. Sci.* **2011,** *36* (9), 1099-1131.

41. Yang, Y.-Y.; Wang, X.; Hu, Y.; Hu, H.; Wu, D.-C.; Xu, F.-J., Bioreducible POSS-Cored Star-Shaped Polycation for Efficient Gene Delivery. *ACS Appl. Mater. Interfaces* **2014,** *6* (2), 1044-1052.

42. Alonso, B.; Cruces, R.; Pérez, A.; Sánchez-Carrillo, C.; Guembe, M., Comparison of the XTT and resazurin assays for quantification of the metabolic activity of Staphylococcus aureus biofilm. *Journal of Microbiological Methods* **2017,** *139*, 135-137.

43. Bauer, M.; Tauhardt, L.; Lambermont-Thijs, H. M. L.; Kempe, K.; Hoogenboom, R.; Schubert, U. S.; Fischer, D., Rethinking the impact of the protonable amine density on cationic polymers for gene delivery: A comparative study of partially hydrolyzed poly(2-ethyl-2-oxazoline)s and linear poly(ethylene imine)s. *Eur. J. Pharm. Biopharm.* **2018,** *133*, 112-121.

44. Morachis, J. M.; Mahmoud, E. A.; Almutairi, A., Physical and Chemical Strategies for Therapeutic Delivery by Using Polymeric Nanoparticles. *Pharmacological Reviews* **2012,** *64* (3), 505.

45. Gutjahr, A.; Phelip, C.; Coolen, A.-L.; Monge, C.; Boisgard, A.-S.; Paul, S.; Verrier, B., Biodegradable Polymeric Nanoparticles-Based Vaccine Adjuvants for Lymph Nodes Targeting. *Vaccines* **2016,** *4* (4).

5.7. Appendix

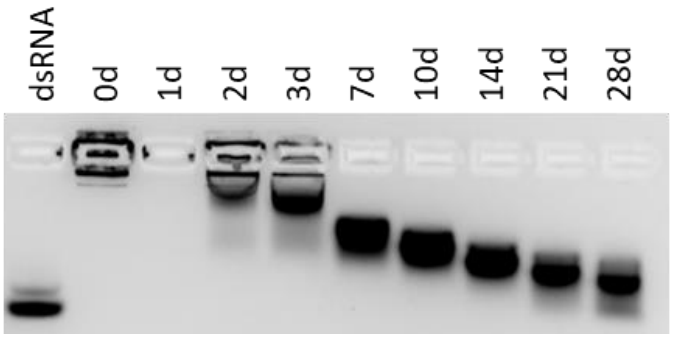

Figure A5.1: DsRNA release over 10 to 28 days (all polyplexes at N/P 5 in sterile water) : Agarose gel electrophoresis (100V, 30 min) with linear 80% DMAEA copolymer of 25 000 g/mol.

a)

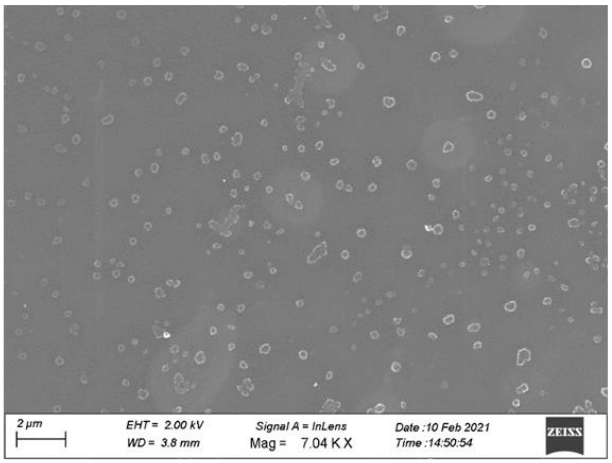

b)

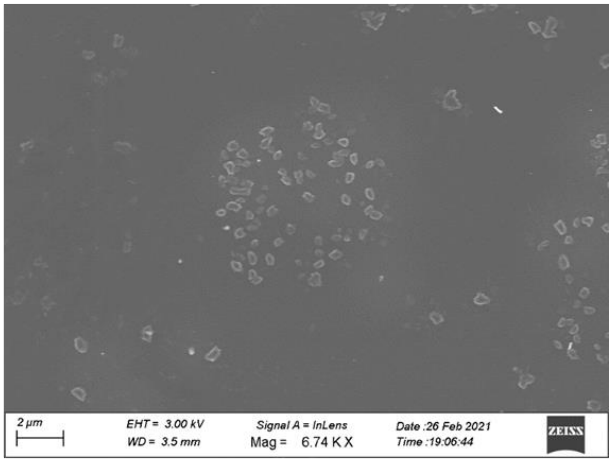

c)

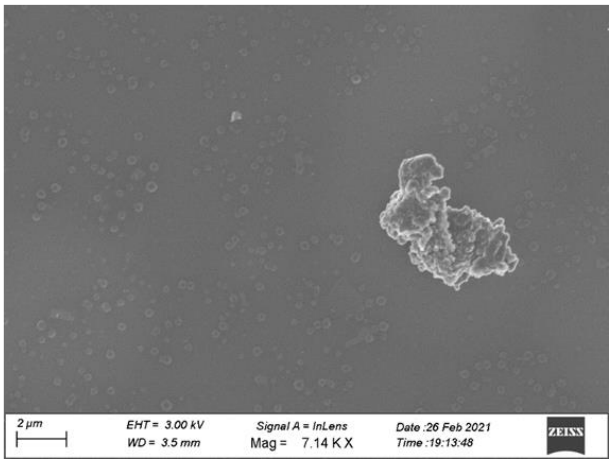

Figure A 5.2: SEM pictures of polyplexes at N/P 5 of dsRNA with a) Star 1, b) Star 2, c) Star 3

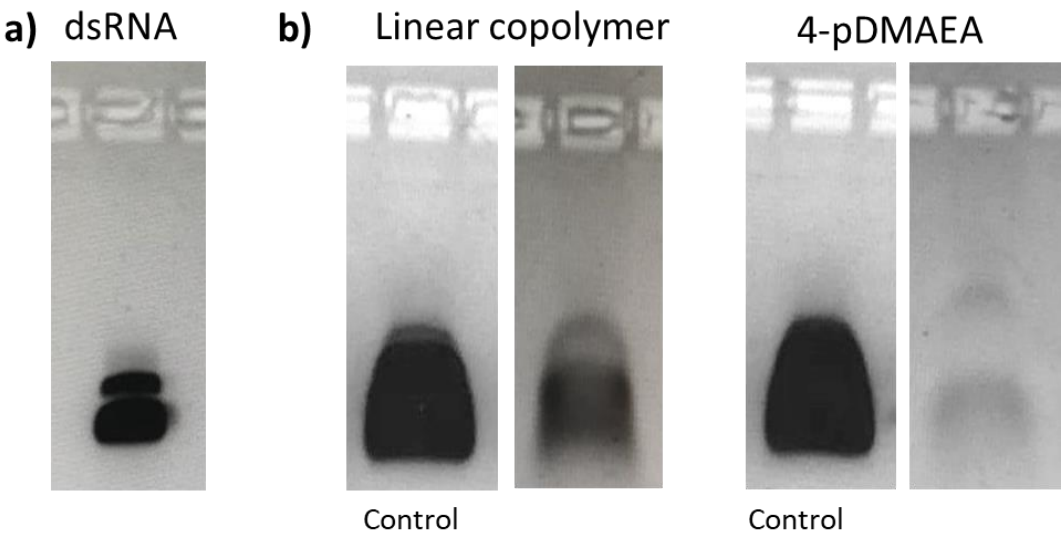

Figure A 5.3: a) dsRNA in sterile water b) Nuclease protection assay gel results for naked dsRNA and complexes with linear p(DMAEA$_{80}$-DMAEMA$_{20}$) and 4-pDMAEA$_{38}$ after overnight incubation at 37°C. Controls on the left are incubated in water at 37°C.

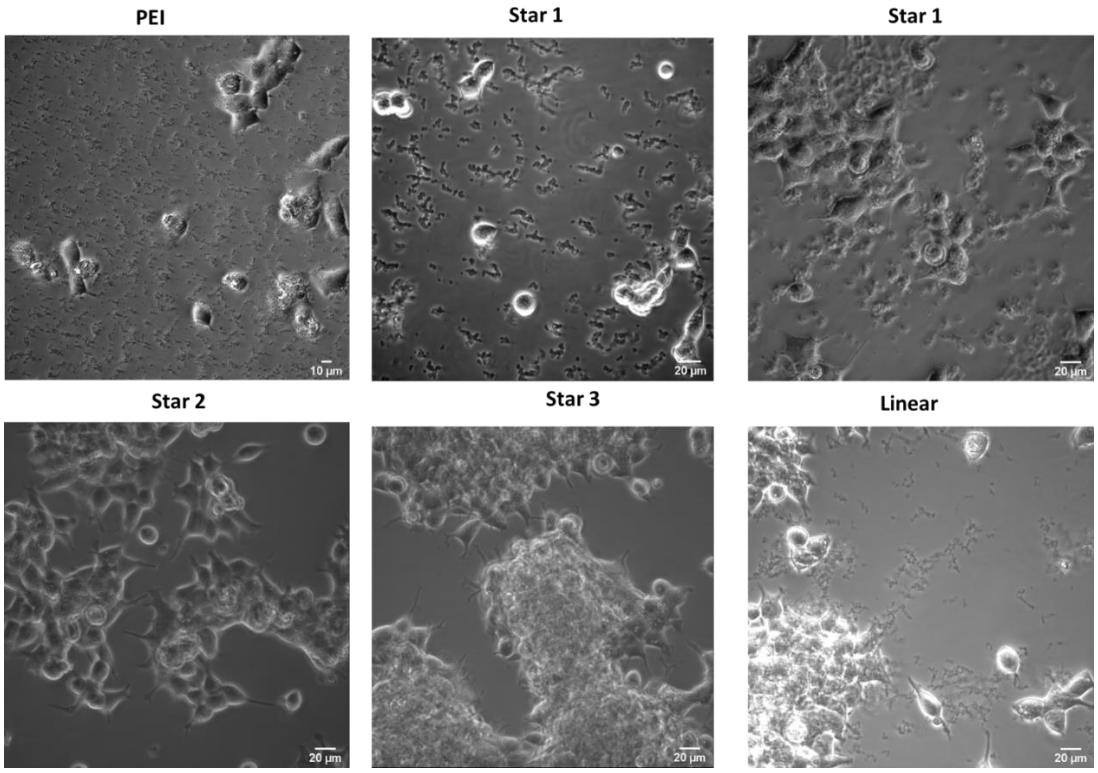

Figure A5.4: Images of cell media containing polyplexes with lPEI, Star 1, Star 2, Star 3 and linear copolymer of DMAEA and DMAEMA before wash.

Chapter 6: Conclusions and perspectives

The objective of this thesis was to synthesise new well-defined cationic DMAEA-based copolymers for the protection and controlled release of dsRNA in soil. RAFT polymerisation enabled the successful synthesis of polymers with specific molecular weight and architectures. Focus was made on stars with a high number of arms, as more defined branched structures, to improve the stability in soil and on the incorporation of DMAEMA to control the release of the dsRNA.

In **chapter 3**, 4-arm stars of DMAEA of four different molecular weights were synthesised using the core-first approach as control. Studies of the influence of the molecular weight showed only little effect on the complexation, as the lowest molecular weight star was binding slightly less efficiently than the dsRNA at low N/P ratio than the other molecular weights. However, the release of the dsRNA initiated by the hydrolysis of pDMAEA was happening too fast to obtain a prolonged protection of the dsRNA in soil.

The incorporation of DMAEMA as a non-hydrolysable monomer to control the hydrolysis and the release of the dsRNA was investigated in **chapter 4 and 5**. The composition of DMAEA and DMAEMA copolymers was varied from 100% DMAEA to 50 % DMAEA to tune the hydrolysis. With increasing amount of DMAEMA, the hydrolysis was lower and slower, going from 70% side chains hydrolysed after 29 days for the copolymer with 100% DMAEA to 20% for the copolymer with 50% DMAEA. This difference in hydrolysis impacted the time for the dsRNA release in water. The full release could be tuned as it was delayed by about 15 days by incorporating only 20% DMAEMA compared to 2 days with the homopolymer of DMAEA. Therefore, it has been demonstrated that the hydrolysis and release can be tuned by simply incorporating DMAEMA as non-hydrolysable comonomers. However, even though these linear copolymers were able to complex the dsRNA, limited protection was observed in the presence of nucleases and the binding was not strong enough to protect the dsRNA efficiently and extend its stability in soil.

To combine the controlled hydrolysis and release with the architecture, three dense and compact star copolymer with 80:20 DMAEA:DMAEMA were prepared by

the arm-first approach as presented in **chapter 4**. A diacrylamide crosslinker was used for the chain extension in order to bind efficiently the end of the arms together in a central core. A block of NAM (corresponding to 40% of the final DP of the arm) was added before the crosslinking step for Star 1 and 2, to obtain soluble stars after purification and drying. Star 3 was made by statistically incorporating NAM with DMAEA and DMAEMA in one-step. The arm length was kept constant for Star 1 and 3, and Star 2 had an arm size corresponding to half of the others. Even if good control over the arms could be obtained, the number of arms per star varied greatly between the three different stars (N_{arm} ~ 55 – 100) and high dispersities ($Đ$=1.7 – 2.3) were obtained. The hydrolysis was slightly impacted by the dense architecture of the stars compared to their corresponding arms. The hydrolysis was lower for the stars due to the possible difficulty of the water to access the side chains closer to the core of the star. The ability of these stars to complex dsRNA and pDNA was reported in **chapter 5**. The three stars were able to complex dsRNA but a higher N/P ratio (N/P 3) was necessary to obtain the full complexation of dsRNA compared to the linear copolymer. Images of the polyplexes showed polydisperse particles in sizes with aggregates of about 200 to 500 nm. As dsRNA was probably complexed by multiple stars at their surfaces, the release happened less gradually and faster than for the linear chains with the same composition, thus implying less strong binding. This was supported by the heparin and nucleases assays, the poor binding resulted in very limited protection against nucleases and easy displacement by the heparin. Finally, these materials were not able to extend the stability of the dsRNA in soil. Moreover, when tested for transfection of pDNA encoding for GFP, poor transfection efficiency was observed compared to lPEI. This was probably due to the tendency of the complexes to aggregate creating too big particles to enter the cells. However, low toxicity was measured by XTT.

A good balance must be found between the hydrolysis rate, by varying the composition, and the architecture to obtain an extended protection in soil. The flexibility and the ability of the cationic polymers to bind efficiently the nucleic acids are key parameters. The release of the dsRNA was seen as a key parameter at the beginning of this project in order to make the nucleic acids available for the pest before ingestion, yet, results have shown a release mechanism was not required to obtain good RNAi (results not shown). Good results were obtained with PEI for instance.

This is also supported by the literature (**Chapter 1**).[1-3] However, one drawback of PEI is its poor mobility in soil (Figure A6.1), as the polyplex stays at the surface of the soil, instead of spreading, thus enabling the protection of the roots of the plant from the worms. Moreover, PEI is potentially toxic on its own to the pest and other organisms. Promising results have been obtained for soil stability assays with branched copolymers with a high DMAEMA content (80%) (Figure A6.2) as about 60% of dsRNA could still be observed after 28 days of incubation in soil. Other non-hydrolysable polymer such as 4-arms pAEA and poly(2-(dimethylamino)propyl acrylate) (pDMAPA) or quaternised linear homopolymer of DMAEA (pDMAEAq) have been tested for dsRNA soil stability and have not shown significant improvement compared to the negative control (Figure A6.3). This implies that the 4-arm structures are not more efficient in soil conditions even with non-hydrolysable monomers but it supports the superiority of the branched structures over the low and high density stars. Nevertheless, pAEA and particularly pDMAEAq were able to give a better protection against nucleases than the DMAEA-based copolymers (Figure A6.4). The branched pDMAEMA polymer was also able to give some protection against the dsRNase. It is difficult to really compare the materials with these results as this nuclease assay needs to be optimised to give more information and differentiate more accurately the polymers in terms of protection efficiency. This could be done by optimising the concentration of the samples, the volume loaded or the gel content. Using fluorescence to detect the dsRNA could be also investigated to enable the quantification of dsRNA left after incubation overnight with the dsRNase.

More investigation could be carried to further study the influence of the architecture on the binding and soil stability. The star material presented in this thesis did not show good potential due to their high density and maybe their hydrolysable nature. Whereas branched structures with high content of DMAEMA showed higher potential. But the poorly defined structure of the branched polymers makes it difficult to really understand the structure-property relationship. Studying brush polymers could enable a control over the density of the structure by varying the side chain density, the backbone length or the side chain length and help understanding the parameters influencing the binding and protection of the dsRNA. Polyplexes with PAEA and pDMAEAq showed some promising results for stability in presence of nucleases, showing the importance of the cationic moiety. However, their soil mobility

was comparable to bPEI (Figure A6.5) and no efficient protection was observed in soil. Adding an outside hydrophilic block, such as poly(ethylene glycol) methacrylate for instance, able to help improving the mobility of the complex and reduce interaction with other species or soil particles, could also be an interesting future direction for this project. This could help as well with the stability of the complex and obtain a better control over their size, which is an important parameter to efficiently deliver the nucleic acid material.

References

1. Au - Zhang, X.; Au - Mysore, K.; Au - Flannery, E.; Au - Michel, K.; Au - Severson, D. W.; Au - Zhu, K. Y.; Au - Duman-Scheel, M., Chitosan/Interfering RNA Nanoparticle Mediated Gene Silencing in Disease Vector Mosquito Larvae. *JoVE* **2015,** (97), e52523.

2. Zhang, X.; Zhang, J.; Zhu, K. Y., Chitosan/double-stranded RNA nanoparticle-mediated RNA interference to silence chitin synthase genes through larval feeding in the African malaria mosquito (Anopheles gambiae). *Insect Mol. Biol.* **2010,** *19* (5), 683-693.

3. Yan, S.; Qian, J.; Cai, C.; Ma, Z.; Li, J.; Yin, M.; Ren, B.; Shen, J., Spray method application of transdermal dsRNA delivery system for efficient gene silencing and pest control on soybean aphid Aphis glycines. *J. Pest Sci.* **2020,** *93* (1), 449-459.

Appendix

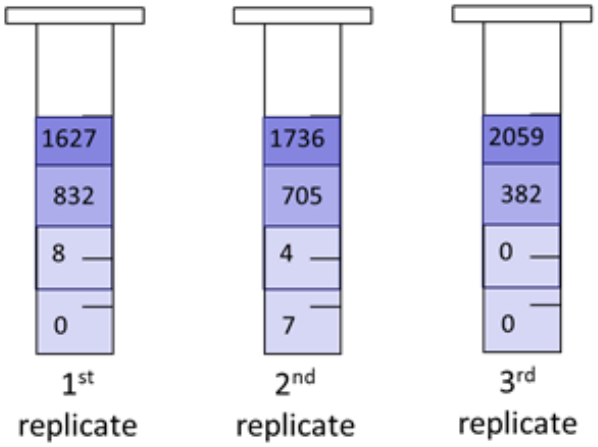

Figure A6.1: Soil mobility assay results for dsRNA/bPEI complexes. In 5 mL syringes, pre-wet soil was loaded and 500 µL of complex was added at the top. 1 mL of water was added to irrigate the soil. The syringes were left for 1 hour before slices of soil were collected for dsRNA extraction from the soil according to method 2 (see method chapter). Fluorescence was used to measure the quantity of dsRNA in each slices. Results are reported in relative

fluorescence intensity. Most of the dsRNA could be found in the top layer or in the second one indicating the polyplexes were not moving down with the water.

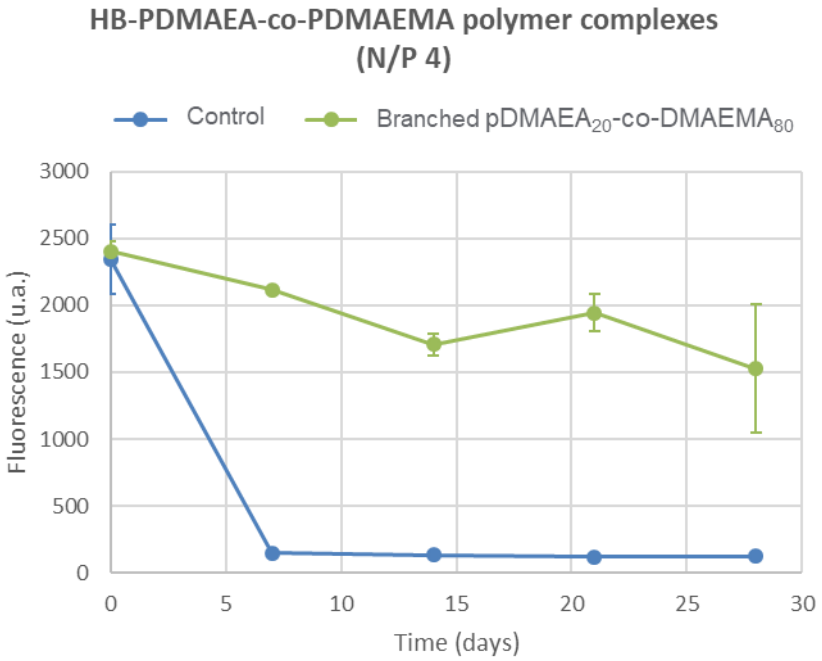

Figure A6.2: Soil stability assay results for dsRNA complexed with branched $pDMAEA_{20}$-*co*-$DMAEMA_{80}$ and naked dsRNA is used as negative control. After incubation method 2 was used for the extraction and analysis of the results (see method chapter).

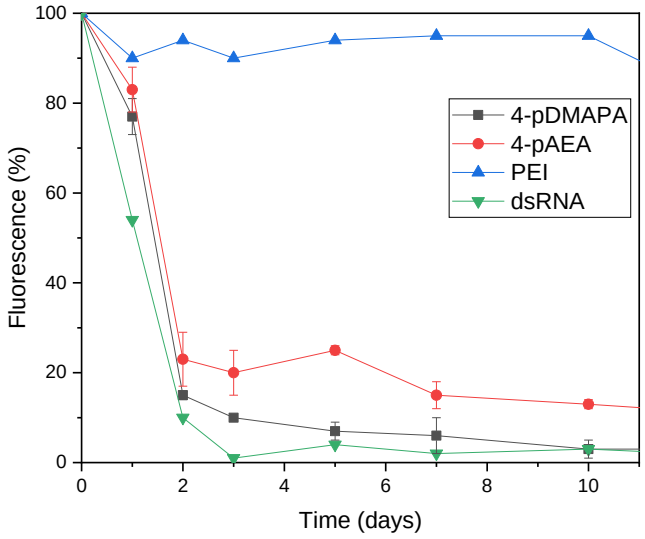

Figure A6.3: Soil stability assay results for dsRNA complexed with 4-arm stars of AEA and DMAPA and bPEI was used as a positive control and naked dsRNA as negative control. After incubation method 2 was used for the extraction of dsRNA and analysis of the results (see method chapter).

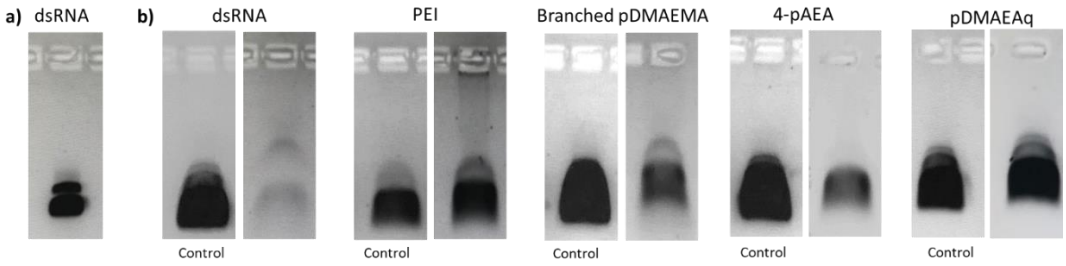

Figure A6.4: a) dsRNA in sterile water b) Nuclease protection assay gel results for naked dsRNA and complexes with bPEI, Star 1, Star 2 and Star 3. Gels were run after decomplexation with PVS. Controls on the left are incubated in water at 37°C.

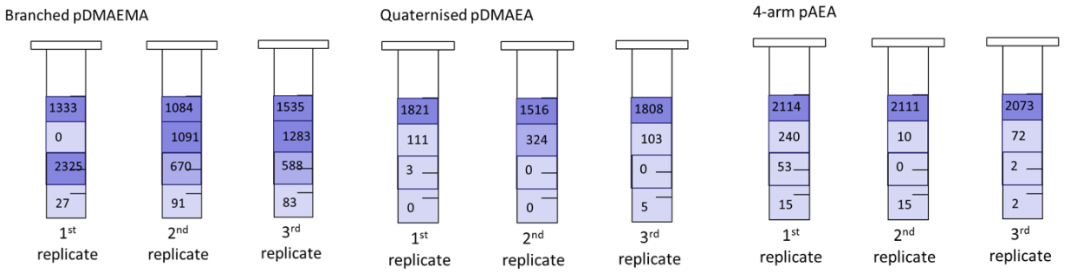

Figure A6.5: Soil mobility assay results for dsRNA complexes with branched pDMAEA, linear pDMAEAq and 4-arm pAEA. In 5 mL syringes pre-wet soil was loaded and 500 µL of complex was added at the top. 1 mL of water was added to irrigate the soil. The syringes were left for 1 hour before slices of soil were collected for dsRNA extraction from the soil according to method 2 (see method chapter). Fluorescence was used to measure the quantity of dsRNA in each slices. Results are reported in relative fluorescence intensity. Except for branched pDMAEMA, most of the dsRNA could be found in the top layer or in the second one indicating the polyplexes were not moving down with the water.